UNIVERSITY OF CALIFORNIA SAN DIEGO

SAN DIEGO STATE UNIVERSITY

Structural and biochemical characterization of the *Drosophila* IKK complex: a key component of the IMD innate immune signaling pathway in flies

A dissertation submitted in partial satisfaction
of the requirements for the degree Doctor of Philosophy

in

Chemistry

by

Samantha-Joy Natividad Cohen

Committee in charge:

University of California San Diego

Professor Dionicio Siegel
Professor Emily Troemel
Professor Wei Wang

San Diego State University

Professor Tom Huxford, chair
Professor Christal Sohl

2021

The dissertation of Samantha-Joy Natividad Cohen is approved, and it is acceptable in quality and form for publication on microfilm and electronically.

_____

_____

_____

_____

_____
Chair

University of California San Diego

San Diego State University

2021

DEDICATION

To my husband David who inspires me to work hard and has been my greatest source of support and encouragement in my years as a graduate student and in anything that I strive to accomplish. I also dedicate this to my daughter Emma who brightens my day. My dog Pipi has also been a wonderful source of support and has been invaluable as part of my audience for practicing the many scientific presentations throughout the years and, importantly, while practicing my dissertation presentation. For all their support, I dedicate this dissertation to them.

TABLE OF CONTENTS

LIST OF FIGURES

LIST OF TABLES

ACKNOWLEDGEMENTS

As my graduate school journey comes to an end, I am truly thankful to those who have helped me learn and grow as a scientist and have contributed to my professional development.

First and foremost, I would like to express my gratitude to Professor Tom Huxford as my mentor and chair of my committee. I am thankful for his guidance, advice, encouragement and for helping me hone my skills in experimental design and performing research independently.

I am grateful to Dr. Gourisankar Ghosh who also served as a mentor and I am thankful for the advice, guidance, and for the opportunity to work in his laboratory on a really interesting project. I am thankful for the experience and it has truly helped me in developing my skills as a scientist.

I would like to thank my committee: Dr. Dio Siegel, Dr. Christal Sohl, Dr. Emily Troemel, and Dr. Wei Wang for working with me on my dissertation and for the invaluable advice that has helped me succeed as a graduate student and in career planning.

I would like to thank Jacob Shaul, Michaela Norrbom, and Eric Rogers for work on Drosophila IKK and starting the project. The interesting results from their work inspired me to take on the project.

I am thankful to Sheri Wu, who helped me learn Baculovirus expression and Sf9 insect cell maintenance. Her advice has helped me tremendously and learning these techniques with her guidance helped give me confidence to tackle on any construct using Baculovirus expression.

I thank Tapan Biswas for teaching me valuable protein purification techniques and collaboration on *Drosophila* IKK. I am appreciative for the helpful advice and critiques to improve experiments.

Thank you to Ingrid Niesman, the director of the SDSU Microscopy Facility for training in TEM and technical support for negative stain EM studies.

I would like to acknowledge Andrey Bobkov at the Sanford Burnham Prebys Medical Discovery Institute for AUC studies and John Love for SEC-MALS instrumentation for our biophysical characterization.

I am truly thankful for all my lab mates in the Huxford lab and in the Ghosh lab for their technical support and for the comradery. It has been an enjoyable journey working alongside you all.

Chapter 3, in part is currently being prepared for submission for publication of the material. Cohen, Samantha-Joy; Shaul, Jacob D.; and Huxford, Tom. The dissertation author was the primary investigator and author of this material.

Chapter 4, in part is currently being prepared for submission for publication of the material. Cohen, Samantha-Joy; Shaul, Jacob D.; and Huxford, Tom. The dissertation author was the primary investigator and author of this material.

VITA

2008	Bachelor of Science, University of California, Riverside
2008-2010	Master of Science, University of California, Riverside
2013-2014	Research Assistant, University of California San Diego
2014-2018, 2019-2020	Teaching Assistant, San Diego State University
2021	Doctor of Philosophy, University of California San Diego San Diego State University

ABSTRACT OF THE DISSERTATION

Structural and biochemical characterization of the *Drosophila* IKK complex: a key component of the IMD innate immune signaling pathway in flies

by

Samantha-Joy Natividad Cohen

Doctor of Philosophy in Chemistry

University of California San Diego, 2021
San Diego State University, 2021

Professor Tom Huxford, Chair

In *Drosophila*, the Immune Deficiency (IMD) pathway is indispensable for proper innate immune responses. In this pathway, infection by gram-negative bacteria elicits a signaling cascade culminating in the rapid induction of antimicrobial peptide gene expression by the NF-κB transcription factor Relish. Signal-dependent activation of Relish is an essential component

of the IMD pathway and is regulated by the *Drosophila melanogaster* IκB Kinase (DmIKK) complex. DmIKK is composed of two subunits: the catalytic subunit DmIKKβ (homologous to mammalian IKKβ) and non-catalytic subunit DmIKKγ (homologous to mammalian NEMO/IKKγ). Since the discovery of the IMD pathway in 1996, much of the molecular components of this pathway have been identified. However, the molecular details of regulation have remained equivocal. This dissertation investigates the biochemistry, substrate specificity and activation mechanism of this kinase complex using recombinant DmIKKβ:γ complex co-expressed using the Baculovirus system. In chapter III, phylogenetic analysis of extant metazoan taxa reveals that DmIKK has diverged significantly in sequence. Primary sequence comparison with mammalian IKK subunits and other metazoan taxa identified conserved as well as unique regions that may be important for its regulation and/or activity. Chapter IV is an *in* vitro study on the nature and assembly of the complex in solution using biophysical methods such as analytical scale size-exclusion chromatography (SEC), multi-angle laser light scattering (MALLS) and analytical ultracentrifugation (AUC). We show that our recombinant DmIKKβ:γ complex can non-covalently interact with poly-ubiquitin via its DmIKKγ subunit. This interaction may be a component of its signal-dependent regulatory mechanism. In chapter V, structural studies using negative stain transmission electron microscopy (TEM) examine the three-dimensional structure of this critical enzyme complex.

Chapter I

Introduction

A. Significance of innate immunity

All organisms must be able to cope with and combat everyday environmental challenges and potential threats to survive. To fight against pathogens seeking to exploit host resources, multicellular organisms have evolved complex defense mechanisms to quickly eradicate and clear infections. Innate immunity, known as the “first line of defense” against microbial attack, is the most universal type of immune defense system, present in plants, fungi, and animals. Over 95% of all extant metazoans are invertebrates that rely exclusively on innate immunity without mechanisms that result in the specific memory of aggressors (Hoffmann, 2011; Wilson, 1987). For all multicellular organisms, immune mechanisms involving early microbial recognition and rapid counter-attack is critical.

In 1989, Charles Janeway first theorized the concept of pattern recognition in the discrimination of non-infectious self vs. infectious non-self. Janeway’s pattern recognition theory postulated that conserved molecules unique to the pathogen called pathogen-associated molecular patterns (PAMPs) or microbe-associated molecular patterns (MAMPs) are detected by host-derived pattern recognition receptors (PRRs) (Janeway, 1989). Pathogen detection via PAMP recognition by PRRs rapidly and robustly evokes signaling cascades that result in antimicrobial responses that include production of antimicrobial peptides, production of cytokine or chemokines, or the induction of cell death programs. In particular, cytokine responses perform critical immune functions such as the recruitment of effector cells to the site of infection, protection of neighboring cells, inflammatory responses to eliminate infection, and also plays a role in the induction of adaptive immunity. Janeway’s PRR theory also pointed out that mechanisms of microbial recognition by PRRs are ancient and must be evolutionarily related to the system of sensing and responding to microbes in invertebrates which lack adaptive immunity (Janeway, 1989).

In the late 1990s-2000, a vibrant research community studying vertebrate and invertebrate innate immunity resulted in spectacular progress in the characterization of immune receptors and intracytoplasmic factors, revealing extraordinary evolutionary conservation between flies and mammals (Imler, 2014). The discovery of the IMD and Toll pathways in *Drosophila* catalyzed the discovery of signaling cascades and mechanistic organization of essential factors in innate immunity in mammals and in other metazoans. Biochemical and functional genetic studies uncovering these signaling pathways in *Drosophila* has revolutionized our understanding of immunity and gave substance to Janeway's PRR theory which has become a conceptual framework for the mechanisms underlying innate immunity.

Originally, the *Drosophila* Toll pathway was identified to control early embryonic patterning (Anderson, Bokla, et al., 1985). In 1996, Lemaitre *et al.*, in J. Hoffmann group showed a direct role of the Toll pathway in modulating antimicrobial peptide expression in innate immunity (Lemaitre et al., 1996). This critical result led to the rapid discovery and isolation of mammalian Toll-like receptors (TLRs) by the Janeway and B. Beutler laboratories (Medzhitov et al., 1997; Poltorak et al., 1998). Currently, there are 13 known TLRs in mammals with 10 present in humans. Mammalian TLRs are responsible for pattern recognition by scanning for a variety of microbial patterns found in bacteria and viruses such as cell wall determinants, flagellin, and nucleic acids species which serve as signals to alert the cell of a potential threat. Ground-breaking work by the S. Akira group utilized the mice knockout system to determine specificity of the mammalian TLRs (Takeda et al., 2003, 2005; Yamamoto et al., 2004).

Land-mark discoveries of the critical signaling pathways and factors in innate immunity were awarded the 2011 Nobel Prize in physiology or medicine to Jules Hoffmann and Bruce Beutler. A major discovery was that in these conserved signaling pathways, NF-κB transcription factors and its chief regulator, the IκB Kinase (IKK) complex, play a primary role in coordinating the expression of innate immune genes. Thus, a conserved NF-κB-IKK signaling axis is critical

for cells to be able to respond to stimuli and uphold cellular integrity in the maintenance of cellular homeostasis.

B. *Drosophila* immune responses

Insects, including Drosophila, live in diverse habitats that exposes them to a constant barrage of bacteria, viruses, and fungi, but they are very resistant to microbes and rarely fall ill. Despite relying completely on innate immunity, fruit flies possess powerful multi-layered immune responses to combat microbial insults. The repertoire of Drosophila innate immune mechanisms includes physical barriers, cellular responses, and humoral responses that are driven by several types of immune cells and tissues. In order to reduce the probability of infection, insects have evolved nonspecific physical barriers to prevent microbes from entering the hemocoel, which is the body cavity in the insect open circulatory system.

The major physical barrier in insects is the tough, chitin-based cuticle that forms the exoskeleton, protects the soft tissues, and lines the foregut, hindgut, and the tracheal system. When this physical barrier is breached through wounds that often form naturally in insects or by microbial enzymatic digestion, pathogens can invade the hemocoel where they encounter various host cellular and humoral immune responses.

1. Cellular responses in *Drosophila* immunity

Cellular immune responses in *Drosophila* are carried out by specialized cells analogous to vertebrate blood cells called hemocytes that engage in phagocytosis, nodulation, and encapsulation. In *Drosophila*, there are several thousand hemocytes that are classified into three types: plasmatocytes, crystal cells, and lamellocytes (Lemaitre et al., 2007).

1.1 Phagocytosis

A macrophage-like type of hemocyte known as plasmatocytes are responsible for consumption of microbes and apoptotic cells through phagocytosis. Phagocytic plasmatocytes are the most numerous type of hemocyte, comprising ~95% of mature larval hemocytes (Chamy

et al., 2010; Lemaitre et al., 2007). The numerous plasmatocytes “lie in waiting,” ready to defend cellular integrity as phagocytosis can occur instantly upon microbial attack. In addition to the phagocytosis of bacteria, yeast and other microbes, plasmatocytes are also capable of phagocytosing other foreign matter such as Sephadex beads, double-stranded RNA, and ink in a matter of minutes (Lemaitre et al., 2007).

1.2 Nodulation

Nodulation is another cellular process aimed at capturing large numbers of microbes through the coordinated formation of multicellular aggregates or nodules composed of hemocytes. This process is functionally similar to vertebrate granuloma formation by macrophages. These nodules entrap large bacterial aggregates by encasing them in a type of flocculent material (Hillyer, 2016). The end process of nodulation is characterized by the recruitment of plasmatocytes to the surface of the nodules, forming another layer of aggregated cells that immobilizes and kills microbes. Melanization of the nodules which produces toxic byproducts also occurs simultaneously and may assist in pathogen destruction. The molecular mechanism of nodulation is not well understood and much of the current knowledge of nodulation has been studied in insects other than *Drosophila*. Studies of other insect groups reveal that the mechanism of nodulation involves eicosanoid signaling, prophenoloxidase, and dopa decarboxylase cascades (Carton et al., 2002; Shrestha et al., 2010; Stanley et al., 2009). One key protein factor called Noduler has been shown to play a role in nodule formation of mosquitos (Gandhe et al., 2007). Four homologs of Noduler exist in *Drosophila* that have yet to be functionally characterized (Gandhe et al., 2007).

1.3 Encapsulation

In larvae, lamellocytes are large, flat cells that encapsulate foreign invaders that are too large to be phagocytosed (>10 microns) such as parasitic wasp eggs that are injected into the larval hemocoel. The wasp egg is recognized by plasmatocytes which transduces this signal to

induce the massive differentiation and proliferation of lamellocytes within hours (Jung et al., 2005; Russo et al., 1996). The molecular mechanism of signal-induced lamellocyte maturation and mobilization is not yet clear. It is thought that encapsulation is triggered by damage to the basement membrane of the tissue as early experiments of transplanted *D. melanogaster* tissue fragments that were damaged were encapsulated whereas fragments with an intact basement membrane remained in circulation (Rizki et al., 1980). Nevertheless, lamellocytes form a multi-layered capsule around the invader which can be killed by asphyxiation and/or the local production of cytotoxic free radicals from the phenoloxidase cascade (Nappi et al., 1995).

2. Humoral responses in *Drosophila* immunity

The humoral response can be divided into an "early" step involving three proteolytic cascades: phenoloxidase/melanization, coagulation, and complement cascades. These cascades primarily function in sealing the damaged tissue and is followed by the main systemic response involving rapid and massive synthesis of antimicrobial peptides in the fat body.

2.1 Phenoloxidase cascade

Circulating specialized hemocytes called crystal cells execute the phenoloxidase-activating or melanization cascade which is an immediate response that generates reactive oxygen species (ROS) and quinones that are toxic to the pathogen. This process results in the production of melanin at the site of wounds or on the surface of pathogens. The *de novo* synthesis of melanin is an important component of the *Drosophila* immune response playing roles in promoting wound healing and scab formation, enscapsulation, coagulation, and the sequestration of foreign invaders. Melanization involves signaling via pattern recognition receptors and a serine protease cascade in the activation of the key redox enzyme in this process, prophenoloxidase (Eleftherianos et al., 2011). After becoming proteolytically activated, a serine protease known as phenoloxidase activating enzyme cleaves prophenoloxidase into active phenoloxidase which catalyzes the oxidation of phenols into quinones that then

polymerizes into melanin. A precursor of melanin is the amino acid tyrosine. Thus, melanin production is dependent upon tyrosine metabolism. Activated phenoloxidase catalyzes the hydroxylation of tyrosine to form dopa, which is then oxidized to dopaquinone and can be converted to dopachrome. Subsequent enzymatic steps involving phenoloxidase culminate in the production of eumelanin, a black to brown colored type of melanin pigment. Dopamine can also be used as a precursor for eumelanin which is catalyzed by phenoloxidase and several other enzymes (Hillyer, 2016).

Three different phenoloxidase genes are encoded in the *Drosophila* genome: PPO1, and PPO2 are expressed in crystal cells (Binggeli et al., 2014), while PPO3 is exclusively expressed in lamellocytes (Irving et al., 2001; Nam et al., 2008). PPO3 may be involved in the melanization that often accompanies encapsulation by larval lamellocytes (Dudzic et al., 2015). Apart from its importance in immune function, melanization is also vital for exoskeleton coloration, sclerotization, and wound healing.

2.2 Coagulation cascade

Coagulation of hemolymph components or clotting is another important immediate humoral defense strategy that promotes hemostasis and the prevention of pathogen entry. A fibrous, gelatinous clot is formed by soluble hemocyte-derived factors which traps hemocytes that are rapidly produced at the lesion. Plasmatocytes and crystal cells are recruited to further seal the clot and produce clotting factors such as hemolectin and prophenoloxidase, respectively (Scherfer et al., 2004). Two enzymes, transglutaminase as well as prophenoloxidase perform covalent cross-linking activities for structural support and to solidify the fibrous network of the clot (Eleftherianos et al., 2011; Lorand et al., 2003). *Drosophila* transglutaminases and clotting factors such as hemolectin have been shown to be homologous with mammalian clotting factors, though the coagulation processes in both systems are distinct (Goto et al., 2001; Loof et al., 2011; Theopold et al., 2014; Wang et al., 2010). Melanization,

mediated by crystal cells, also often occurs with coagulation. Thus, coagulation and phenoloxidase/melanization cascade are intricately linked, though these processes occur independently in vertebrates (Sheehan et al., 2018). Due to the nature of the insect open circulatory system, hemolymph coagulation plays a vital role in the humoral immune response to prevent excessive bleeding of the hemolymph, prevent the spread of infection, and also provides a substrate for further wound healing (Galko et al., 2004).

2.3 Complement cascade

A complement-like system has been identified in insects primarily studied in mosquitoes, though there have been a few studies in *Drosophila*. The mammalian complement system involves ~50 pattern recognition receptors, circulating protein factors, and membrane bound proteins (Shokal et al., 2017). Activation of the complement system leads to a proteolytic cascade that marks a pathogen for destruction via opsonization and leads to phagocytosis or lysis. Thio-ester containing proteins (TEPs) are a family of proteins that have been conserved throughout evolution and are present in protostomes and deuterostomes. In vertebrates, they are known to be key mediators of this response (Shokal et al., 2017). TEPs contain a thioester motif (GCGEQ) with an unstable covalent bond between the cysteine and glutamic acid side chains. The thioester motif becomes reactive upon elevated temperature, proteolytic cleavage, and changes in solution media (Shokal et al., 2017). This active moiety allows for the covalent binding of pathogens to the TEPs thereby marking the pathogen for destruction via opsonization. The *Drosophila* genome encodes six TEP homologs (Adams et al., 2000). The TEP homologs exhibit different expression patterns upon bacterial, fungal, and parasitoid infection in larvae and adults (Shokal et al., 2017). TEPs 2, 4, and 6 have been shown to promote phagocytosis upon infection of Gram-negative bacteria and *C. albicans in vitro* (Stroschein-Stevenson et al., 2006). Furthermore, expression of TEPs have been shown to involve the JAK-STAT and Toll pathways (Lagueux et al., 2000). It remains to be seen whether

Drosophila TEPs directly act as opsonins in a complement-like system and the precise regulatory mechanisms controlling their action.

2.4 Systemic response: production of antimicrobial peptides

A hallmark of *Drosophila* host defense is the inducible systemic response involving the secretion of potent antimicrobial peptides in the open circulatory system. It is the best understood aspect of the humoral innate immune response in insects. Although they do not have adaptive immune responses and lack antibodies for the immunological memory of microbial attack, several groups in the 1920s demonstrated that insects exhibit “immunological priming” as a consequence of prior infection and can withstand otherwise lethal doses of bacteria if previously “vaccinated” using heat-attenuated or small doses of live cultures (Cantacuzène ,1923; Metalnikov 1927, Porchet 1928). Once “vaccinated,” the insect mounts an antibacterial defense against a broad spectrum of microbes as evident even 3 hours post infection in the hemolymph (Metalnikov 1927; Porchet 1928).

After these pioneering studies in the 1920s, it was not until 1970s that the study of insect immunity gained more traction with work from H. Boman laboratory in Stockholm. The Boman group revealed that when *D. melanogaster* were infected with the Gram-negative bacteria *A. cloacae*, they were protected by subsequent infection by the same bacterial strain or by a different strain (*E. coli* or *P. aeruginosa*) (Boman et al., 1972). This bactericidal activity was inhibited by treatment with protein translation inhibitor cycloheximide, but was not inhibited by cell division inhibitor colchicine, suggesting that the antimicrobial activity involved a humoral defense mechanism possibly mediated by protein factors instead of a cellular defense mechanism (Boman et al., 1972).

The Boman group results on the possible “immunological priming” of insects were corroborated by results from the J. Hoffmann group working with the grasshopper *L. migratoria.* The J. Hoffmann group in Strasbourg, France showed that infection of a non-lethal dose of *B.*

thuringensis protects against subsequent lethal bacterial challenge and that infection triggers strong proliferation of hemocytes (D. Hoffmann et al., 1974).

In 1981, the Boman group reported another important discovery in the isolation and characterization of the first inducible antimicrobial immune peptide in the pupae of the giant silkworm moth (*Hyalophora cecropia*). The antimicrobial activity was revealed to be due to small peptides termed antimicrobial peptides (AMPs) (Steiner et al., 1980, Steiner et al.., 1981). These first AMPs were called cecropins and attacins (Hultmark et al., 1983; Steiner et al., 1980; Steiner et al., 1981). At the time, the advantage of using larger insects was that larger amounts of protein yields could support these early biochemical and functional studies on AMPs. The Boman group's discovery of antibacterial proteins led to the discovery of many more (~150) antimicrobial peptides in different insect groups such as Lepidoptera and eventually in smaller Dipteran species including *Drosophila* (Bulet et al., 1993; Kylsten et al., 1990; Levashina et al., 1995; Samakovlis et al., 1990). Subsequently, AMPs were identified in vertebrates and in plants (Cammue et al., 1992; Selsted et al., 1984). Thus, AMPs are ubiquitously distributed throughout the animal and plant kingdoms, contributing a major role in the arsenal of multicellular host defense (Ganz, 2003).

Shortly after the identification of insect AMPs, the molecular characterization and cloning of AMP cDNAs was undertaken. In particular, cloning techniques pioneered by the Boman group paved the way for the sequencing of full genomic clones (Kylsten et al., 1990; Reichhart et al., 1992). This led to the characterization of promoter sequences that could induce their expression. In 1991, Ingrid Faye was the first to report the presence of a sequence motif resembling an NF-κB consensus sequence (5'-GGGGATTCCT-3') at an upstream region of *attacin* genes in *H. cecropia* (Sun et al., 1991). These sequence motifs were subsequently discovered in the promoter region of *cecropin* genes and the *diptericin* gene (Reichhart et al., 1992; Sun et al., 1992). Several groups, using *Drosophila* and other insect models, identified the

presence of nuclear proteins that bound to κB-like motifs and that these motifs were required for immune inducibility in cells and *in vivo* (Engström et al., 1993; Kappler et al., 1993; Kobayashi et al., 1993; Sun et al., 1992).

In *Drosophila*, three NF-κB family members have been identified: Dorsal, Dif, and Relish. These NF-κB proteins rapidly translocate to the nucleus upon infection and bind to κB-like motifs to drive the expression of immune response genes (Gross et al., 1996; Ip et al., 1993; Petersen et al., 1995; Reichhart et al., 1992, Reichhart et al., 1993). The *dorsal* gene was first described in a developmental context rather than in immunity as Dorsal was named for its role in dorsal-ventral patterning (Santamaria et al., 1983). Through hybridization screening of the *Drosophila* genome using the *dorsal* Rel sequence, another NF-κB protein was identified by the M. Levine group in the US (Ip et al., 1993). This NF-κB protein was named Dorsal related immunity factor (Dif) which bears ~31% identity and ~46% similarity tos Dorsal. Dif is expressed in larva, pupae, and adults, but unlike Dorsal is not expressed in the female germline and early embryo (Ip et al., 1993). Also unlike Dorsal, Dif does not appear to control developmental genes. A third member of the NF-κB family of transcription factors in *Drosophila* was discovered in D. Hultmark's group and was named Relish (Dushay et al., 1996). Relish contains both an N-terminal Rel homology domain (RHD) and C-terminal inhibitory ankyrin repeats in a similar protein architecture to mammalian p100 and p105 (Dushay et al., 1996).

In response to infection by bacteria and fungi, two classical signaling cascades, the IMD and the Toll pathways control the inducible systemic response through regulation of AMP gene expression. Both pathways are mediated by distinct NF-κB transcription factors, Dorsal and Dif in the Toll pathway, and Relish in the IMD pathway. Both pathways involve microbial sensing by genome-encoded PRRs. The PGRP and GNBP receptor families are the two principal PRRs in the *Drosophila* systemic immune response.

C. *Drosophila* IMD pathway

One of the major evolutionarily conserved signaling cascades involved in the *Drosophila* immune response is the immune deficiency (IMD) pathway. This pathway regulates the activation of the NF-κB protein Relish and controls the expression of five of seven known classes of antimicrobial peptides in *Drosophila*. Thus, the IMD pathway is indispensable for proper immune function in *Drosophila*.

Efforts to link Toll pathway mutants to the regulation of antimicrobial peptide expression had failed. Nevertheless, in 1995, Lemaitre et al., in the J. Hoffmann group discovered the *imd* gene from genetic screens utilizing the *D. melanogaster* fly line 1046Bc which was homozygous for the Bc (black cells) mutation and generated by ethyl methylsulfanate mutagenesis (EMS) in the lab of E. H. Grell (Lemaitre, 2004). These mutants were impaired in phenoloxidase activity and had a thermosensitive tumor phenotype (Lemaitre et al., 1995). Bacterial infection resulted in severely impaired antibacterial peptide gene expression (Lemaitre et al., 1995). This phenotype was not the result of the *Bc* mutation, but was found to be due to a mutation only 3.5 centimorgans away from *Bc* which was termed "*immune-deficiency*" or *imd* (Lemaitre et al., 1995). This was the first reported mutant in flies that was found to alter antibacterial peptide expression.

Homozygous *imd*-mutant flies were viable, but highly susceptible to bacterial infection as the mutation diminished the inducibility of all known antibacterial peptide genes (Diptericin, Cecropin, Defensin, Attacin, and Drosocin) in the *Drosophila* immune response (Lemaitre et al., 1995). Upon bacterial challenge, flies that had a mutation in the recessive gene *imd* were more susceptible to infection and had lower survival rate compared to wild-type flies (Lemaitre et al., 1995). This observation was the first functional evidence that antimicrobial peptides are critical for fighting bacterial infection *in vivo*. However, *drosomycin* induction was unaffected in *imd*

mutant flies, suggesting that another signaling pathway may be controlling expression of the antifungal peptide Drosomycin.

Additional genetic screens by several laboratories using EMS mutagenesis revealed other potential genes involved in the IMD pathway with phenotypes mirroring *imd* and *relish* mutants. These mutants exhibit extreme sensitivity to bacterial infection and fail to produce antimicrobial peptides (Hedengren et al., 1999; Lemaitre et al., 1995). Four additional IMD pathway genes were identified under the EMS approach: *dTAK1* (ortholog of mammalian TAK1), *DREDD* (ortholog of mammalian caspase-8) as well as orthologs of the mammalian IKK subunits IKKβ and IKKγ/NF-κB essential modulator (NEMO) encoded by genes *ird5* and *kenny* (Kim et al., 2000; Leulier et al., 2000; Lu et al., 2001; Rutschmann et al., 2000; Silverman et al., 2000; Vidai et al., 2001). Both *ird5* and *kenny* mutant flies were severely compromised in inducibility of antibacterial peptides, but not antifungal peptides (Lu et al., 2001; Rutschmann et al., 2000). *Kenny* mutants are particularly highly sensitive to bacterial infection as they die only two days after infection by *E. coli,* but had a similar response to wild-type flies upon fungal infection (Rutschmann et al., 2000). These genetic results demonstrated that the *Drosophila* IKK subunits are essential for proper immune induction.

The mammalian IKK subunits have also been shown to be absolutely essential in immune responses upon pro-inflammatory stimuli such as TNF-α, IL-1, LPS, phorbol myristate acetate, and many other stimuli that initiate the canonical NF-κB activation pathway. Elegant gene-knockout studies of IKKβ and IKKγ in mice resulted in embryonic lethality similar to NF-κB p65 knockout phenotype (Q. Li et al., 1999; Z. W. Li et al., 1999; Tanaka et al., 1999). Thus, the essentiality of IKK subunits is conserved in flies and mammals, constituting a major regulatory step in immune responses mediated by NF-κB in the *Drosophila* IMD pathway and in the mammalian canonical NF-κB activation pathway.

Soon after the discovery of key proteins in the IMD pathway, the K. Anderson group discovered that the principal PRR in this pathway is PGRP-LC, a member of the peptidoglycan recognition protein (PGRP) family (Choe et al., 2002). PGRPs are a highly conserved protein family with homologs identified in mollusks, echinoderms, arthropods and mammals (Dziarski, 2004). PGRPs share a ~160 amino acid long PGRP domain homologous to N-acetylmuramoyl-L-alanine amidases (also known as type 2 amidases) common to bacteria, bacteriophages, and T7 lysozyme (Dziarski, 2004; Kang et al., 1998). The *Drosophila* genome encodes 13 PGRP genes which are alternatively spliced into 19 isoforms (Royet et al., 2007).

PGRPs recognize peptidoglycan, a constituent of most bacterial cell walls in both gram-negative and gram-positive bacteria. Bacterial PGN is composed of a network of conserved polymers consisting of alternating sugar residues of N-acetylglucosamine and N-acetylmuramic acid linked by a β-(1,4)-glycosidic bond. N-acetylmuramic acid is cross-linked by a short stem peptide of 3-5 amino acids long (Kaneko et al., 2005). Gram-positive bacteria typically have lysine at the third position of the stem peptide, while most gram-negative bacteria have meso-diaminopimelic acid (DAP) at this position. This third amino acid is typically cross-linked to D-alanine, which is the fourth amino acid in the stem peptide (Kaneko et al., 2005). Naturally, PGN is shed from the bacterial cell wall during cell division and cell death.

PGRP-LC is the main receptor that binds directly to DAP-type PGN to trigger the activation of the IMD pathway in the systemic immune response (Figure 1.1). PGRP-LC is a transmembrane receptor that is alternatively-spliced into three known isoforms: PGRP-LCa, PGRP-LCx, and PGRP-LCy (Werner et al., 2003). These isoforms have identical transmembrane and cytoplasmic regions, but have different PGRP domains that contribute to ligand specificities (Kaneko et al., 2005). PGRP-LCx contains a deep PGN binding cleft which is typical of PGRP family of proteins and type 2 amidases accommodating both polymeric and monomeric DAP-PGN (Chang et al., 2005; Kleino et al., 2014). Structural and biochemical

studies have shown that PGRP-LCx binds to monomeric DAP-PGN known as tracheal cytotoxin (TCT) which then recruits the PGRP domain of PGRP-LCa to form a PGRP-LCx/a heterodimer (Chang et al., 2005, Chang et al., 2006). On the other hand, the function of PGRP-LCy, its mode of PGN recognition, and its specificity for a particular type of PGN ligand is not yet known, though some antagonistic effects on AMP expression upon bacterial challenge have been observed *in vivo* (Neyen et al., 2012).

Somewhat surprisingly, it was also shown that PGRP-LC mutant flies can still mount a reduced response against TCT infection (Neyen et al., 2012, Royet and Dziarski, 2007). Genetic studies revealed that PGRP-LE can contribute to the response against TCT leading to downstream signaling of the IMD pathway (Neyen et al., 2012; Royet et al., 2007). PGRP-LE can either be secreted extracellularly or reside intracellularly in the cytoplasm (Neyen et al., 2012; Royet et al., 2007). Extracellular PGRP-LE can bind to circulating TCT via its PGRP domain and can form a dimer with PGRP-LCx at the plasma membrane to act as a co-receptor and enhance PGRP-LCx mediated response to TCT (Neyen et al., 2012). PGRP-LCx:PGRP-LE mediated TCT recognition is reminiscent of mammalian MD-2 acting as a co-receptor for TLR-4 in the sensing of lipopolysaccharide. However, this PGRP-LCx-PGRP-LE mediated response is not as potent as the PGRP-LCa/x heterodimer in mediating AMP expression (Kleino et al., 2014; Royet et al., 2007).

Moreover, intracellular PGRP-LE functions independently of PGRP-LCx and binds to TCT that has crossed the cell membrane or is released from intracellular infection (Kleino et al., 2014; Royet et al., 2007). Intracellular binding of TCT to PGRP-LE results in PGRP-LE homodimerization and downstream signaling (Kleino et al., 2014). It has been proposed that PGRP-LE-mediated signaling plays a more prominent role in the midgut, while PGRP-LC mediates signaling primarily in the fat body as well as in the local responses in the respiratory and gut epithelia. This is corroborated by AMP expression levels in intestinal tissues of Gram-

infected flies with a greater reduction in PGRP-LE mutants than PGRP-LC mutants (Neyen et al., 2012). This effect is accompanied by a higher level of PGRP-LE expression than PGRP-LC in intestinal tissues (Neyen et al., 2012).

After sensing of DAP-type PGN by PGRP-LC or PGRP-LE, the signal is transduced to the adaptor protein Imd, which contains a C-terminal death domain homologous to mammalian RIP1. For many years, it was not known how PGRP-LC and PGRP-LE propagate downstream signaling through is N-terminal intracytoplasmic region as a homologous signaling domain had not yet been identified and functionally characterized. It was thought that the mechanism involved clustering of PGRP-LCx dimers and multimerization of PGRP-LE, though the precise molecular interactions and nature of assembly remained uncertain (Kleino et al., 2014). Recently, N. Silverman's group at the University of Massachussets in Worcester showed that PGRP-LC and PGRP-LE, along with Imd, activate the IMD pathway through a conserved mechanism in mammals involving formation of functional amyloids (Kleino et al., 2017).

The assembly of functional amyloid fibrils is a necessary step in the IMD pathway and is mediated by homotypic interactions of cryptic RIP homotypic interaction motifs (cRHIM) composed of a core VXXG sequence at the N-termini of the receptors PGRP-LC and PGRP-LE, as well as at the N-terminus of the adaptor protein IMD (Kleino et al., 2017). The *Drosophila* cRHIM domains bears weak homology with amyloidogenic mammalian RHIMs of RIP1/RIP3 proteins that mediate formation of functional signaling amyloid fibrils in necroptosis (Kleino et al., 2019). A putative cRHIM has been identified within the N-terminus of Relish, but has yet to be biochemically and functionally characterized (Kleino et al., 2017). Disruption of amyloid formation of the cRHIMs through mutation or small-molecule inhibition strongly interfered with IMD signaling and AMP expression in cells and in flies, but did not interfere with Toll signaling and induction of Drosomycin expression (Kleino et al., 2017). The cRHIM-containing protein Pirk is a potent negative regulator of the IMD pathway and is under transcriptional control by Relish.

It was not known for several years how Pirk can interfere with the pathway until these recent studies from the N. Silverman group showed its role in the inhibition of cRHIM-containing amyloid fibril formation. The cRHIM of Pirk interacts with the cRHIM motifs in PGRP-LC:Imd fibrils and interferes with formation of the signaling amyloids perhaps by destabilization and/or capping of nascent fibrils (Kleino et al., 2017).

Ligand binding to PGRP-LC or PGRP-LE dimers triggers receptor aggregation and amyloid formation through receptor cRHIM interactions (Kleino et al., 2017). Imd cRHIMs are recruited to the amyloid fibrils and forms a filamentous platform for the recruitment of downstream factors. It is not yet known whether nucleation of this amyloid fibril starts with PGRP cRHIM homoamyloid or a heteroamyloid with IMD cRHIMs. After formation of the amyloid fibrils, Imd then forms a signaling complex with dFADD through homotypic death domain (DD) interactions, while dFADD enlists the caspase Dredd via death effector domain (DED) interactions (Hu et al., 2000). Unlike most caspases that require proteolytic processing for activation, Dredd is activated by K-63-linked polyubiquitination by the E3-ubiquitin ligase dIAP2 (Meinander et al., 2012). Activated Dredd cleaves IMD after aspartate 30 within a caspase recognition motif $_{27}$LEKD/A$_{31}$, exposing a highly-conserved IAP-binding motif (IBM) at the neo-N-terminus of IMD (Paquette et al., 2010). A functional IBM acts as a docking site for dIAP2 which associates with the E2 ubiquitin conjugating enzymes UEV1a, Bendless (Ubc13), and Effete (Ubc5) and rapidly conjugates K-63 polyubiquitin chains onto IMD at lysine residues 137 and 153 (L. Chen et al., 2017; Paquette et al., 2010). K-63 polyubiquitination recruits and activates the Tab2-Transforming growth factor β-activated kinase-1(Tak1) complex which functions to activate the DmIKKβ:γ complex (L. Chen et al., 2017). It is also possible that the DmIKK complex is recruited to the amyloid fibrils through interactions with IMD-conjugated K-63 polyubiquitin chains and DmIKKγ, which harbors putative ubiquitin binding domains (Rutschmann et al., 2000). The activated DmIKK complex phosphorylates multiple sites within

the N-terminus of Relish (Ertürk-Hasdemir et al., 2009; Silverman et al., 2000). Signal-dependent phosphorylation of Relish at Serines 528 and 529 by the DmIKK complex is required for the efficient recruitment of RNA polymerase II at Relish target genes (Ertürk-Hasdemir et al., 2009). On the other hand, Dredd cleaves Relish after aspartate 545 within the cleavage site $_{542}$LQHD/G$_{546}$ leaving an N-terminal portion of Relish known as Rel-N or Rel-68 and the C-terminal portion called Rel-C or Rel-49 (Paquette et al., 2010). Both DmIKK-mediated phosphorylation and Dredd-mediated cleavage of Relish is required for proper transactivation of antimicrobial peptide genes. The newly liberated Rel-N can translocate into the nucleus to induce expression of most AMPs including Dipericin, Defensin, Cecropins, Drosocin, and Attacins in addition to other effector genes, while Rel-C remains in the cytoplasm (Gregorio et al., 2002; J. L. Imler et al., 2005; Stöven et al., 2000).

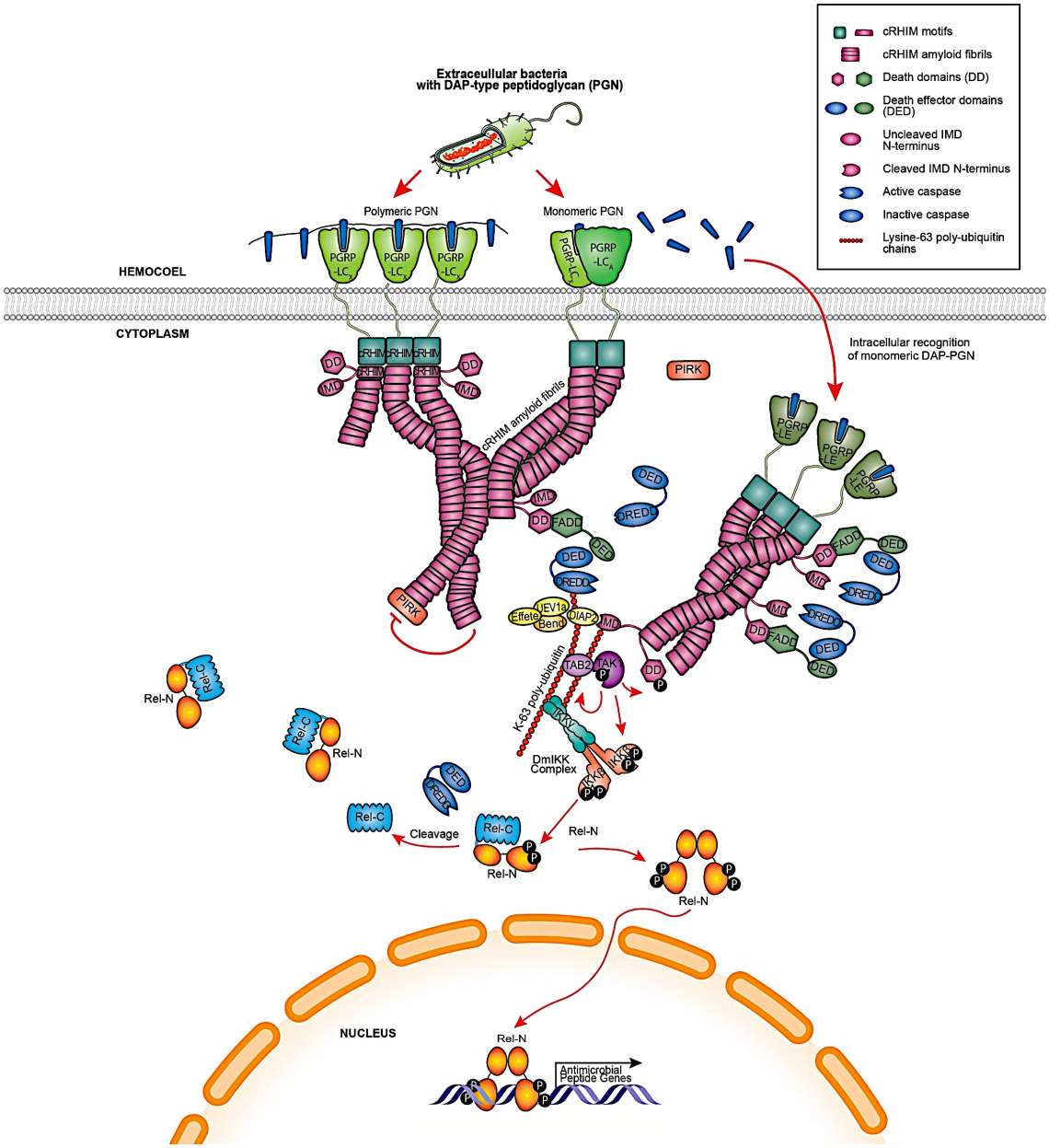

Figure 1.1: Schematic overview of *Drosophila* IMD signaling

D. *Drosophila* Toll pathway

A series of semi-saturating mutagenesis screens carried out by C. Nusslein-Volhard's group in Tubingen, Germany and by the T. Schüpbach and E. Wieschaus groups at Princeton University identified several genes that control early embryonic development in *Drosophila* (Lemaitre, 2004). Nusslein-Volhard and Wieschaus along with E. B. Lewis at Caltech were awarded the Nobel Prize in Physiology or Medicine in 1995 for discoveries in the genetic control of early embryonic development in *Drosophila*. Genetic screens carried out by K. Anderson in Nusslein-Volhard's group identified the "dorsal group" of twelve genes which include *toll*, *tube*, *pelle*, *cactus, dorsal*, and seven genes upstream of *toll* in the pathway: *nudel*, *gastrulation defective*, *windbeutel*, *pipe*, *snake*, *grass*, and *easter* (Anderson, Bokla, et al., 1985; Anderson, Jürgens, et al., 1985; Anderson et al., 1984; Belvin et al., 1996). Loss of function mutations of 11 of these genes affected dorsal-ventral polarity resulting in "dorsalized" embryos that lack ventral structures, while loss of function mutations in *cactus* resulted in "ventralized" embryos (Anderson, Bokla, et al., 1985; Anderson, Jürgens, et al., 1985; Schupbach et al., 1989).

After the initial identification of these "dorsal group" genes, K. Anderson's and other groups molecularly characterized the genes and their functions using a variety of genetic, molecular, and immunohistochemical approaches. *Dorsal* was found to encode for an NF-κB transcription factor with close homology to vertebrate *c-rel* (Steward et al., 1988). *The toll* gene was cloned in the lab of K. Anderson and found to encode a single-pass type-I transmembrane protein receptor with a large N-terminal ectodomain containing leucine-rich repeats (LRR) flanked by cysteine-rich motifs (Hashimoto et al., 1988). At the C-terminus, the Toll receptor was discovered to harbor a 105-amino acid intracytoplasmic domain which was noted to bear homology to the intracellular signaling domain of the mammalian IL-1 receptor, the sequence of which was reported at around the same time that *toll* was cloned (Gay et al., 1991; Sims et al., 1988). This domain was termed the "Toll/IL-1-R (TIR) homology domain" due to significant

similarity with the intracytoplasmic domains of mammalian interleukin-1 receptor (IL-1R) family of proteins (Bowie et al., 2000).

9 toll genes have been discovered in *Drosophila*. *Toll* encodes the prototypical Toll-1 receptor involved in regulating dorso-ventral (DV) patterning and production of AMPs through the Toll pathway. 8 other toll genes also encode for single-pass transmembrane receptor proteins (Tauszig et al., 2000). *18 wheeler* (Toll-2), *tehao* (Toll-5), and *toll-9* have been shown to play a role in supporting immune responses and AMP expression (Dushay et al., 2000; J. L. Imler et al., 2000; Luo et al., 2001; Ooi et al., 2002; Tauszig et al., 2000). On the other hand, *tollo* (Toll-8) has been shown to negatively regulate the IMD pathway in respiratory epithelium (Akhouayri et al., 2011). In addition, it was shown that the Toll-7 receptor interacts directly with vesicular stomatitis virus (VSV) and induces signaling in a similar fashion to the direct binding of ligands to mammalian TLRs (Nakamoto et al., 2012). Neveretheless, most members of the *Drosophila* Toll receptor family do not play major roles in immunity, rather they primarily control developmental processes (Tauszig et al., 2000).

The Toll pathway is initiated by gram-positive bacteria and fungi (Figure 1.2). However, unlike mammalian TLRs, the *Drosophila* Toll receptor does not directly sense microbially-derived molecular components. Instead, *Drosophila* Toll-1 is a cytokine receptor that recognizes an endogenous ligand produced in the host, a mature form of the cytokine Spaetzle, a homolog of the vertebrate β-nerve growth factor (βNGF). Under basal conditions, the Spaetzle pro-domain occludes the Toll-binding surface within the C-106 cystine knot domain, a predominantly hydrophobic region of the protein consisting of the last C-terminal 106 amino acids of the protein. Circulating extracellular recognition factors act as pattern recognition receptors to initiate proteolytic cascades activating Spaetzle in both embryonic patterning and the immune response though the extracellular factors leading to Spaetzle activation are distinct. Gram-negative binding protein-3 (GNBP-3) recognizes long β-1,3 glucans from the cell wall of fungi

and yeast while a complex of PGRP-SA and GNBP-1 sense Lysine-type peptidoglycan from gram-positive bacteria (Gobert et al., 2003; Gottar et al., 2006; Mishima et al., 2009). PGRP-SD is another circulating PRR involved in the Toll pathway, but with specificity for DAP-type peptidoglycan from Gram-negative bacteria. It also participates in the detection of Lys-type peptidoglycan via an unknown mechanism to induce the Toll pathway (Leone et al., 2008). PGRPP-SD, however, is not required in the IMD pathway (Leone et al., 2008). Activation of Spaetzle involves proteolytic cleavage causing a conformational change allowing the Toll ectodomain to associate with the now exposed Spaetzle C106 domain (Hu et al., 2004; Weber et al., 2003).

In DV patterning, a proteolytic cascade involves the serine proteases Nudel, Gastrulation Defective (GD), Snake, and Easter. The protein disulfide isomerase (PDI)-related protein chaperone Windbeutel and the sulfo-transferase Pipe are other factors that are essential in regulating the protease cascade leading to Easter activation. In particular, a Windbeutel homodimer interacts directly with Pipe to facilitate its export from the endoplasmic reticulum (Barnewitz et al., 2004). Pipe was found to be essential in the development of ventral cues and facilitating the activation of Easter by stabilizing the Snake:Easter complex (Cho et al., 2010). Once activated by proteolytic processing by Snake, Easter directly cleaves Spaetzle.

In response to microbial infection, three different proteolytic cascades trigger Spaetzle processing depending on the type of activating microbe. Fungal β-glucan binds to GNBP-3, while gram-positive lysine-type peptidoglycan binds to either a complex of PGRP-SA:GNBP-1 or to monomeric PGRP-SD (Bischoff et al., 2004). In all three of these variations of the recognition step in the Toll pathway, the serine protease Mod-SP is responsible for integrating these microbial signals to Grass which activates SPE. The serine proteases Spirit, Spheroide, and Sphinx 1/2 have been shown to be involved in this cascade by RNAi-based experiments, but the exact molecular mechanism is not currently known, though is likely to function in between Grass

and activation of SPE (Kambris et al., 2006). Activated SPE cleaves the pro-domain of Spaetzle to allow its C-106 cysteine knot domain to bind to the extracellular domain of Toll.

Damage and stress signals elicited by fungal and Gram-positive proteolytic virulence factors penetrate the insect body cavity via subtilisin-like proteolytic activity. This leads to activation of a serine protease cascade mediated by the host serine protease Persephone (Chamy et al., 2008). Interaction of microbial virulence factors and the zymogen form of Persephone leads to cleavage and maturation of Persephone by these virulence factors (Gottar et al., 2006). Matured Persephone then cleaves and activates SPE which can then process Spatzle. Thus, Persephone has dual roles as a sensor of virulence factors and as activator of the Spatzle-activating proteolytic cascade to guard against virulence factors and abnormal proteolytic activity. The detection of damage or stress signals in response to virulence factors as well as tissue injury and cell death also exists in mammals. Endogenous factors known as damage-associated molecular patterns (DAMPs) are released and are recognized by specific receptors and PRRs to initiate inflammatory responses (Boyer et al., 2011; Heil et al., 2014; Tang et al., 2012). In *Drosophila* larvae, it was shown that endogenous factors released by necrotic cells initiate a Persephone-dependent pathway resulting in active Spaetzle (Ming et al., 2014).

Once activated, Spaetzle, as a dimer, can then bind to the N-terminal extracellular ectodomain of a Toll receptor (Parthier et al., 2014). Formation of this complex initiates conformational changes in the Toll receptor resulting in an active Toll dimer for downstream signaling. The activated Toll receptor can then associate with the adaptor protein Myd88 through homotypic TIR domain interactions. Myd88 then recruits another adaptor protein Tube which then enlists the protein kinase Pelle to form a complex mediated by death-domain (DD) interactions. Formation of this signalosome leads to autophosphorylation of Pelle. The signaling cascade then proceeds to Cactus, a homolog of mammalian IκB which forms a complex with

NF-κB transcription factors Dorsal-related immunity factor (Dif) in adult flies and Dorsal in adult flies and larvae thus sequestering NF-κB in the cytoplasm. Activation of Dif and Dorsal requires phosphorylation of Cactus. However, the mechanism of signal-dependent Cactus phosphorylation in the Toll pathway is not yet clear, though an *in vitro* study points to Pelle, a homolog of mammalian IKK regulator IRAK-1, as the Cactus kinase in this pathway (Daigneault et al., 2013). However, signal-responsive phosphorylation of Cactus by Pelle has yet to be demonstrated *in vivo*. While the DmIKK complex was shown to phosphorylate Cactus *in vitro*, this does not seem to occur *in vivo* as cell-based and fly studies with mutant DmIKK did not impair *drosomycin* induction (Lu et al., 2001; Rutschmann et al., 2000; Silverman et al., 2000). Thus, the Toll pathway does not seem to involve components of the DmIKK complex, but is clearly involved in the regulation of the IMD pathway (Lu et al., 2001; Rutschmann et al., 2000; Silverman et al., 2000).

Nonetheless, signal-responsive Cactus phosphorylation triggers ubiquitination and rapid degradation by the 26S proteasome to permit the nuclear translocation of the NF-κB proteins Dif and Dorsal. This leads to the expression of immune response genes such as AMPs and genes involved in DV patterning. In adult flies, primarily in the fat body and in hemocytes, Dif is essential for the expression of immune-responsive genes, while Dif and Dorsal function redundantly in larval innate immunity (Manfruelli et al., 1999; Rutschmann et al., 2000). In both larvae and adult flies, the Toll pathway is essential for the induction of the antimicrobial peptides Drosomycin and Metchnikowin as well as the full induction of some antimicrobial peptides genes that include Cecropin, Defensin, and Attacin which are induced by the IMD pathway (Imler, 2014).

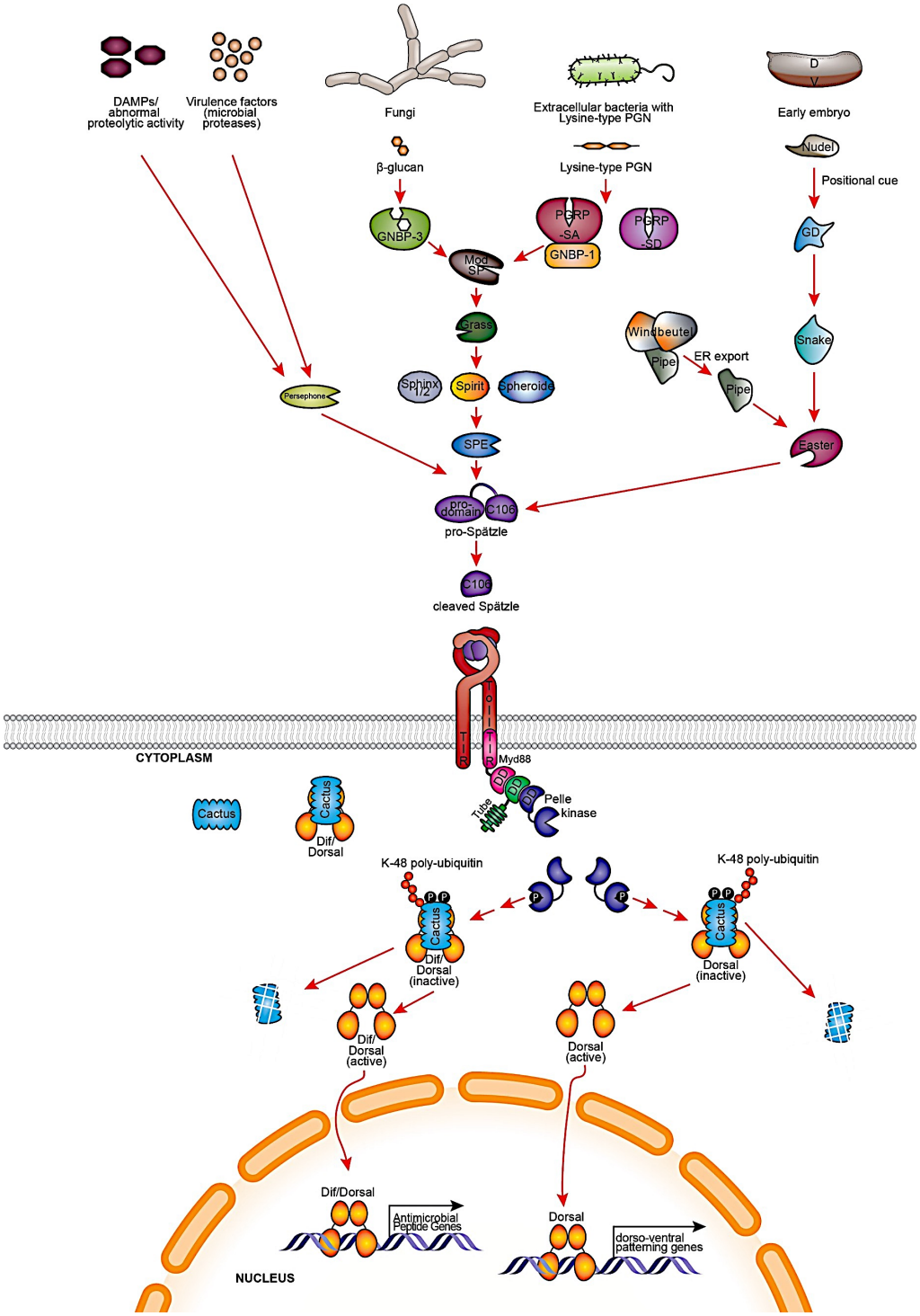

Figure 1.2: Schematic overview of *Drosophila* Toll Signaling in innate immunity and embryonic patterning

E. Antimicrobial peptides

Insect-derived AMPs are small (<100 amino acids), cationic peptides that are mainly produced in the fat body, an analogue of the mammalian liver. Microbial infection triggers the rapid secretion of an arsenal of antimicrobial peptides into the hemocoel or body cavity of the open circulatory system. Gram-positive bacteria and fungi activate the Toll pathway, while gram-negative bacteria trigger the IMD pathway. AMPs are often secreted in high concentrations into the hemolymph, the bodily fluid of the insect open circulatory system where they are maintained at such concentrations of up to 400 micromolar for several hours (Chamy et al., 2010). Moreover, insect AMPs can also be produced locally by barrier epithelial cells similar to the vertebrate AMP system (Buchon et al., 2014).

In *Drosophila*, seven distinct families of AMPs have been characterized and are active against specific types of microbes (Figure 1.3) (Imler et al., 2005). Three of these AMP families: the Diptericins, Attacins, and Drosocin, target gram-negative bacteria (Åsling et al., 1995; Bulet et al., 1993; Charlet et al., 1996; Reichhart et al., 1992; Wicker et al., 1990). On the other hand, Defensin and Metchnikowin target gram-positive bacteria (Dimarcq et al., 1994; Levashina et al., 1995). In contrast to other AMP families exerting bactericidal activity on either gram-negative or gram-positive bacteria, Cecropins target both types (Dushay et al., 1996; Dan Hultmark et al., 1982; Lemaitre et al., 1995). To combat fungi, *Drosophila* elicit the Toll pathway and induce the expression of Drosomycin (Fehlbaum et al., 1994; Michaut et al., 1996). In addition, the antibacterial peptides Cecropins, Metchnikowin, and Defensin have dual specificity and can also target fungi (Ekengren et al., 1999; Levashina et al., 1995; Samakovlis et al., 1990; Tzou et al., 2002).

Mutagenesis studies on flies lacking both IMD and Toll pathways demonstrate that AMPs are critical for proper immune responses (Lemaitre et al., 1996; Tzou et al., 2002). These mutant flies do not produce any of the known antimicrobial peptides and are extremely

susceptible to bacterial and fungal infection (Lemaitre et al., 1996). Constitutive expression of a single AMP gene such as *attacin A* or *drosomycin* in these IMD and Toll deficient flies can rescue the ability to mount a response against the target class of microorganism (gram-negative bacteria, and fungi, respectively) (Tzou et al., 2002).

In general, AMPs kill microbes by a variety of mechanisms to disrupt membrane integrity or by non-membrane targeting mechanisms to block microbial growth. Most AMPs are membrane-active by virtue of their amphipathic as well as cationic nature. It is thought that clusters of positive charges allows them to interact with the negatively charged phospholipid head groups while hydrophobic patches allow interaction with the fatty acids of the microbial membrane (Nakatsuji et al., 2012). For example, the cationic and amphipathic insect defensins are highly toxic relying on cellular destruction by disrupting membrane permeability and exerting immediate lysis (Bulet et al., 1999; Yi et al., 2014). In addition, post-translational modifications can also play a role in AMP activity as it was shown that the broad-spectrum Cecropin is amidated at its C-terminus and that this moiety stabilizes interaction with phospholipids of liposomes derived from *E. coli* (Nakajima et al., 1987; Yi et al., 2014). In contrast, the 19 amino acid peptide Drosocin exhibits a non-membrane targeting mechanism by binding to the bacterial heat shock protein DnaK. This interaction interferes with DnaK's function of folding mis-folded proteins and leads to disruption of metabolic processes and cell death (Bikker et al., 2006). Furthermore, O-glycosylation at threonine 11 is required for Drosocin activity as removal of this moiety significantly reduces bactericidal activity (Bulet et al., 1993).

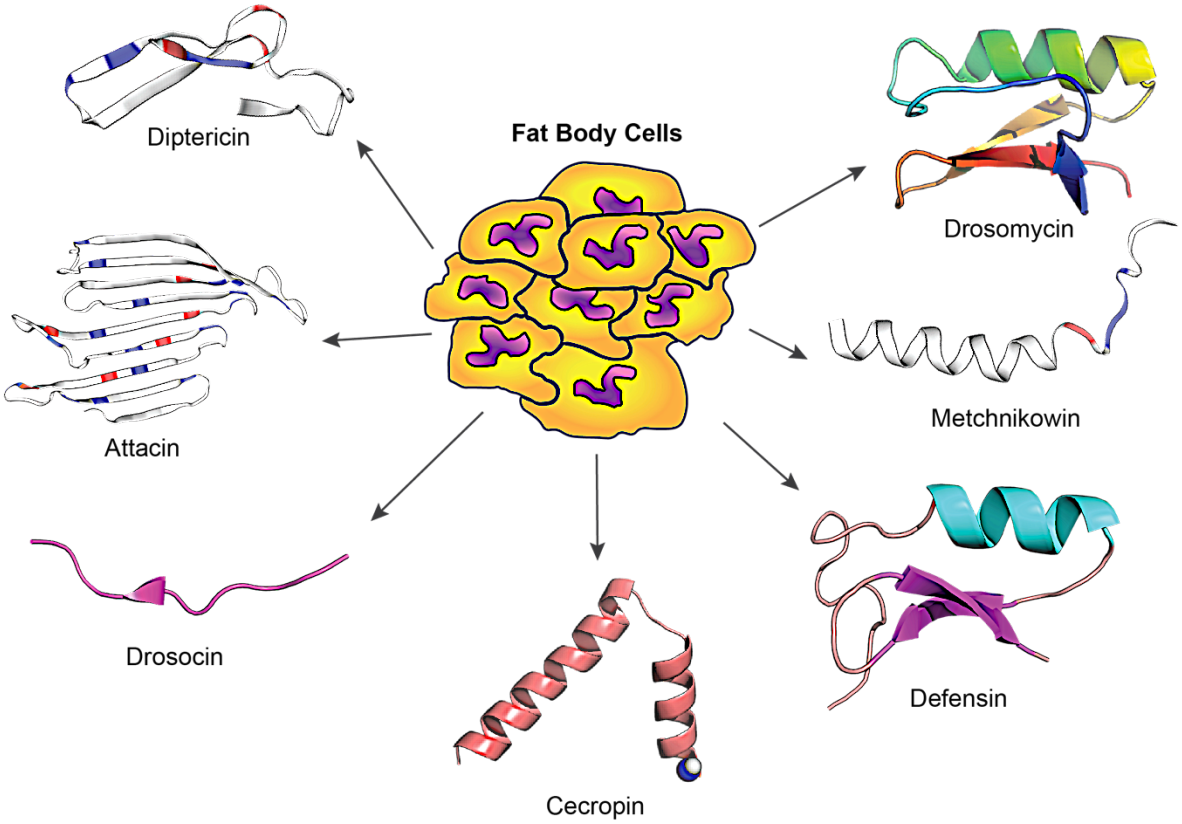

Figure 1.3: Seven classes of *Drosophila* antimicrobial peptides secreted by the fat body in the systemic immune response.
The 3D structures are from PDB files of *D. melanogaster* Drosomycin (1MYN), ortholog of Defensin (1ICA) from *P. terranova*, and ortholog of Cecropin A (2LA2) from of *P. xuthus*. The 3D structures of Diptericin, Attacin, and Metchnikowin have not been determined and were modeled using the default settings on SWISS-MODEL (https://swissmodel.expasy.org/).

F. Evolutionary conservation of NF-κB activation pathways

NF-κB activation pathways are characterized by signaling cascades in which ligand binding to receptors trigger changes in conformation or receptor stoichiometry. This facilitates binding of receptor-proximal adaptor proteins, recruitment of intermediary adaptors via protein-protein interactions and transduction to downstream factors including kinases. As such, the recruitment and activation of IKK is a key regulatory event and is thought to be dependent upon induced proximity effects or conformational changes mediated by association of adapter proteins. Intriguingly, before the mammalian IKK complex was identified and isolated, the activity was dependent on non-degradative ubiquitination by ubiquitin machinery involving the E2 ubiquitin conjugating enzymes Ubc4/Ubc5 and was hypothesized to lead to IKK activation (Z. J. Chen et al., 1996). It is now known that non-degradative poly-ubiquitin linked through K-63, linear (M-1), or even mixed linkages has been shown to be integral in the early events of NF-κB signaling, mediating protein-protein interactions with other adaptors and other upstream factors and also propagating signaling to NEMO and activation of the IKK complex (Clark et al., 2013; Ea et al., 2006; Fujita et al., 2014; Kensche et al., 2012; Skaug et al., 2009; Tokunaga et al., 2009; Xia et al., 2009). Hence, poly-ubiquitin plays a major signaling role outside of protein degradation. In contrast to other signaling cascades, these early signaling events in NF-κB activation pathways do not primarily rely on kinase cascades that are characteristic of classical signal transduction pathways such as JAK-STAT, MAPK/ERK, and JNK pathways.

Instead, the NF-κB signaling module requires, at its simplest, a dimeric NF-κB transcription factor, an upstream IκB kinase (IKK), and an inhibitor of κB (IκB) protein that sequesters NF-κB in the cytoplasm, keeping it inactive. Physiological stimuli activates IKK which then phosphorylates the IκB protein resulting in sequential ubiquitination and degradation. Liberation of NF-κB from the inhibitory protein IκB is an activating event allowing it enter the

nucleus and bind to a DNA sequence motif in promoter/enhancer regions known as “κB-sites” to control the expression of target genes.

The intracellular signaling cascades leading to NF-κB activation have been strikingly well conserved throughout evolution (Gilmore et al., 2012; Lemaitre et al., 2007). High-throughput genomic sequencing of the metazoan lineage including basal metazoan taxa such as sponges, corals, and sea anemones have revealed that NF-κB is likely to have originated one billion years ago and arose in an ancestral organism on the cusp of multicellularity (Gilmore et al., 2012). It is known that sponges (phylum: Porifera) are among the most earliest metazoan life forms appearing in the Precambrian era about 800 million years ago (Hedges et al., 2006; Kumar et al., 2017, 2011; Roy et al., 2013). Recently, NF-κB has been functionally characterized in protists which are primitive unicellular eukaryotic taxa that pre-date metazoans, originating about 1 billion years ago (Hedges et al., 2006; Kumar et al., 2017, 2011; Roy et al., 2013; Williams et al., 2021). The unicellular holozoan *Capsaspora owczarzaki* and the choanoflagellate *Acanthotheca spectabilis* have been shown to have NF-κB-like transcription factors that bind to κB sites and exhibit transactivation ability (Williams et al., 2021, 2020b). *C. owczarzaki* is thought to be the closest living unicellular relative to the metazoans and are basal to the sponges. It will not be surprising to discover more NF-κB-like homologs as well as homologs of core components in NF-κB signaling pathways in pre-metazoan taxa as more genome sequencing data is continuing to be revealed. Characteristic core components of the NF-κB signaling module exists throughout the metazoan phylogenetic spectrum and is present in the basal metazoans such as sponges, but has been lost in *C. elegans* and other taxa in Ecdysozoa such as Tardigrada (Gilmore et al., 2012; J. Hoffmann, 2011; Mapalo et al., 2020; Williams et al., 2020a). The conserved core components include the dimeric NF-κB transcription factors, the inhibitory protein IκB, and the IκB kinase (IKK) complex known as the “master” regulator of NF-κB (Gilmore et al., 2012; Hayden et al., 2012; M. Karin et al., 2000). In the

following section, I describe conserved structural and mechanistic features of the core elements in the NF-κB signaling module.

1. NF-κB proteins

Proteins of the Rel/NF-κB family are highly conserved transcription factors that control the expression of stress response genes involved in many physiological processes such as cell survival, innate immunity, induction of adaptive immunity, inflammation, cellular proliferation and many others (Hayden et al., 2012; Karin et al., 2000). Emerging from the prolific period of transcription factor discovery in the mid-1980's, NF-κB was the first transcription factor that was identified whose sequence-specific DNA binding capability could be induced by extracellular stimuli via a post-translational mechanism (Sen et al., 1986). NF-κB was discovered as a nuclear activity that was rapidly induced by LPS and with DNA-binding specificity towards the 10 base pair sequence 5'-GGGACTTTCC-3' within the enhancer of the immunoglobulin κ light chain gene in mature antibody-producing B cells (Sen et al., 1986). Since this pivotal discovery, NF-κB has been extensively studied and is a master transcription factor responding to a plethora of cellular stimuli and coordinating responses in different cell types and disease states (T. Liu et al., 2017).

There are five members in mammals: p65/Rel-A, Rel-B, c-Rel, p50 (derived from precursor p105), and p52 (derived from precursor p100), while three members exist in *Drosophila*: Dorsal, Dif, and Relish (Figure 1.4). All members of the NF-κB family of proteins share a ~300 amino acid Rel homology region (RHR) at the N-terminus which is comprised of two folded domains: an amino-terminal domain and a dimerization domain that both adopts an immunoglobulin-like fold. The RHR also harbors a nuclear localization signal (NLS). As a whole, the RHR is responsible for homo- or hetero-dimerization with other NF-κB subunits, recognition of sequence-specific DNA, nuclear localization, and binding to IκB. The mammalian NF-κB subunits p65, Rel-B, and c-Rel as well as the *Drosophila* Dorsal and Dif subunits have a

transcription activation domain (TAD) at their C-termini which is responsible for directing target gene expression. After the initial discovery of NF-κB, it was noted that the N-terminal RHR of NF-κB subunits exhibits significant homology with the viral oncogene v-Rel (Gilmore et al. 1999, Gilmore et al. 2012). On the other hand, the mammalian precursor proteins p105 and p52 in addition to the *Drosophila* precursor Relish contain C-terminal ankyrin repeats, the signature structural domain of IκB proteins. These precursors must undergo processing and proteolysis of the ankyrin repeats for full activation, otherwise the ankyrin repeats can be inhibitory as a bona fide IκB protein in contact with NF-κB dimers keeping them inactive and in the cytoplasm, thereby sequestered from transcriptional targets.

NF-κB family members are often grouped into subclasses with the precursor proteins grouped into “Class I” or also known as the “NF-κB” subclass and the TAD-containing members grouped into “Class II” also known as the “Rel” subclass (Gilmore et al., 2012; Huxford et al., 2009). NF-κB dimers that contain a “Class II” subunit have inherent potential to activate transcription, while homodimers consisting of “Class I” subunits can act as repressors or recruit additional transcriptional regulators such as co-activation machinery or general transcription machinery to activate gene expression (Ghosh et al., 2012; Smale, 2010, 2011). NF-κB dimers are directed to 10 base pair consensus DNA sequence motifs known as “κB sites” or “κB elements” present in promoter or enhancer regions composed of the sequence “5’-GGGRNNYYCC-3’” in which R is purine, Y is pyrimidine, and N is any base. Viruses such as HIV-1, herpesviruses, adenoviruses, and other viruses have evolved to abuse NF-κB transactivation by recruiting NF-κB to κB sites present in their genes (Pahl, 1999).

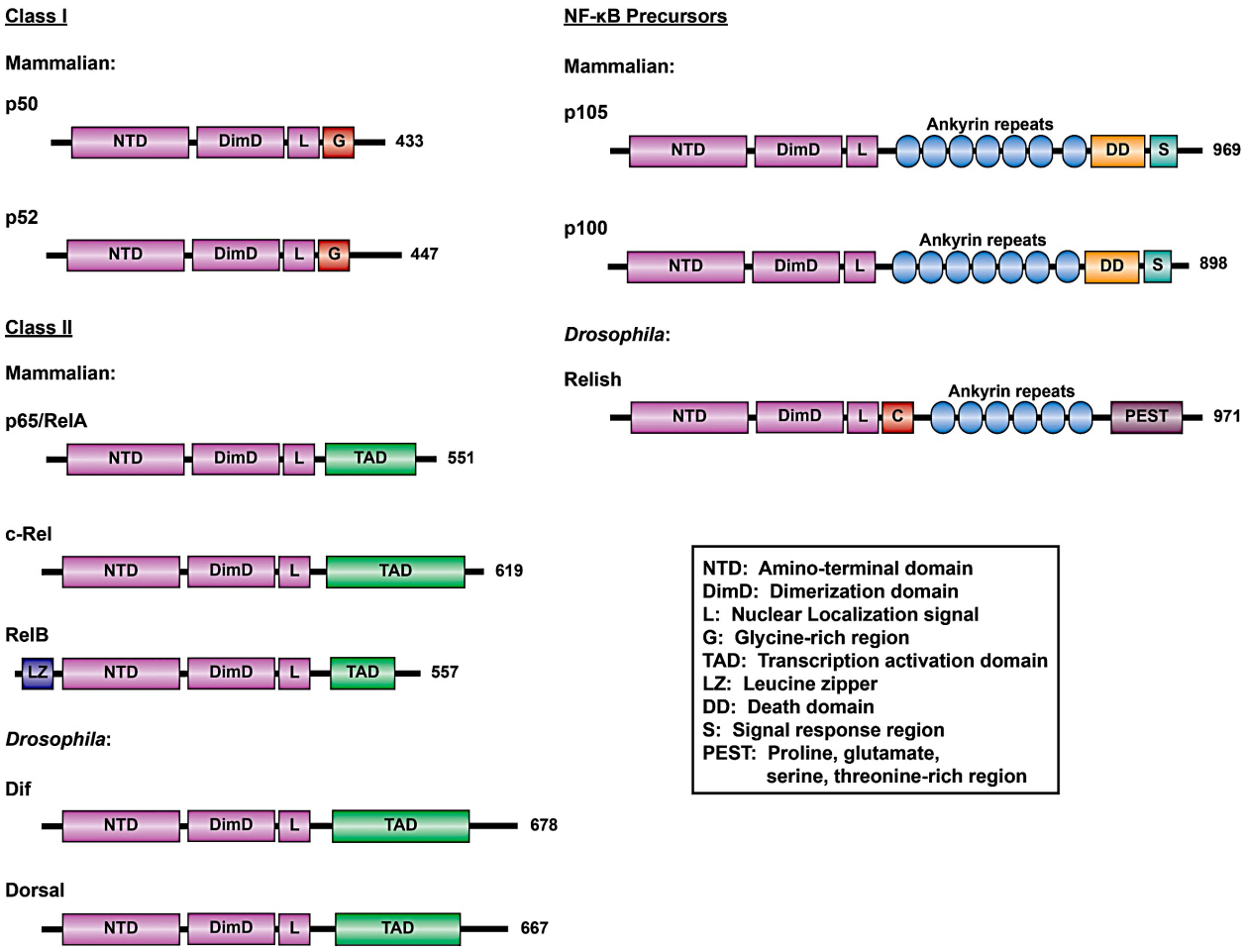

Figure 1.4: Domain structures of NF-κB proteins

2. IκB proteins

In view of the fact that NF-κB plays a vital role in the expression of a variety of genes that modulate overall cellular homeostasis, it must be tightly controlled. This control is accomplished by high-affinity non-covalent interactions with members of the IκB family of inhibitory proteins (Figure 1.5). IκB proteins can be functionally classified into three separate groups: the cytoplasmic "classical IκBs" (consisting of mammalian IkBα, IkBβ, IkBε, and *Drosophila* Cactus), the NF-κB precursors (comprising mammalian p100 also known as IκBδ, p105, as well as *Drosophila* Relish), and the nuclear or "atypical IκBs" (consisting of the seven

mammalian members IκBα, IκBβ, IκBε; Bcl-3, IκBζ, IκBη, IκBNS and a newly identified *Drosophila* IκB named Pickle/Charon) (Ji et al., 2020; Morris et al., 2016).

IκB proteins are distinguished by their signature structural motif, an ankyrin repeat domain (ARD) consisting of a stretch of 6-7 ankyrin repeats through which they exert their potent inhibition. Ankyrin repeats are sequence stretches of a ~33 amino acid consensus sequence that form repeating helix-loop-helix structures that often mediate protein-protein interactions. Specifically, the ankyrin repeats of one IκB molecule bind to the NLS of one NF-κB dimer to prevent nuclear translocation. Of these family members, IκBα is the most studied, regulating the activity of the prototypical p50:p65 heterodimer involved in the canonical NF-κB response.

Classical IκB proteins contain an ARD with 6 ankyrin repeats that are flanked by unstructured regions. N-terminal to the ARD is a flexible region containing the signal response region and C-terminal to the ARD is the PEST domain that is rich with proline, glutamic acid, serine, and threonine residues. The PEST domain is the target of several kinases and is involved in rapid proteolytic turnover with the 20S proteasome (Mathes et al., 2010). Within the signal response region are two conserved serine residues in the consensus sequence "DSGXXS" in a βTRCP degron that undergo signal-dependent phosphorylation. In mammals, upon stimulation, the catalytic IKKβ subunit in the IKK complex phosphorylates the two conserved serine residues within the consensus sequence which results in K-48 polyubiquitination on adjacent lysine residues and proteolytic degradation. In *Drosophila*, however, the kinase responsible for phosphorylation of these signal-dependent serine residues in Cactus is not known. There is, however, *in vitro* evidence that the IRAK4 homolog Pelle can phosphorylate these signal-responsive sites (Daigneault et al., 2013)

In contrast, "atypical" or "nuclear" IκB proteins typically accumulate in the nucleus and bind to NF-κB dimers that have translocated in the nucleus. Like classical κB proteins, nuclear

IκBs contain an ARD, often containing 7 ankyrin repeats. In mammals, nuclear IκB protein expression is inducible and regulated by NF-κB. These family members can coordinate expression of a "second wave" of NF-κB gene expression with a binding preference for p50 or p52 homodimers to repress or activate another subset of NF-κB target genes (Hatada et al., 1992; Trinh et al., 2008; Yamazaki et al., 2001). The mechanisms of this secondary wave of NF-κB gene regulation by nuclear IκBs is not fully understood. Nonetheless, it was shown that IκBζ, in concert with Akirin2, recruits the SWI/SNF chromatin remodeling complex to p50 homodimers that then leads to expression of proinflammatory cytokines IL-6 and IL12-b (Tartey et al., 2014, 2015). The *Drosophila* homolog of Akirin also was found to regulate the expression of a subset of Relish target genes in the IMD pathway through the recruitment of the Osa-containing-SWI/SNF-like Brahma complex (BAP) (Bonnay et al., 2014). Whether *Drosophila* Akirin exerts this regulatory function with a nuclear IκB homolog as was observed in the mammalian system with IκBζ remains to be seen. Inasmuch, one recently described *Drosophila* nuclear IκB, called Pickle or Charon preferentially binds to Relish homodimers in the nucleus and can either repress or activate specific Relish target genes (Morris et al. 2016, Ji et al. 2020). In particular, it was shown that Pickle/Charon can repress Relish homodimers by interacting with the histone deacetylase dHDAC1 and can also interact with Poly [ADP-ribose] polymerase 1 (PARP-1) to activate Relish-dependent expression of AMP genes (Morris et al. 2016, Ji et al. 2020). Thus, the interplay between *Drosophila* nuclear IκB proteins, chromatin-remodeling machinery and other transcriptional regulators such as the conserved protein Akirin in gene regulatory mechanisms remains to be seen.

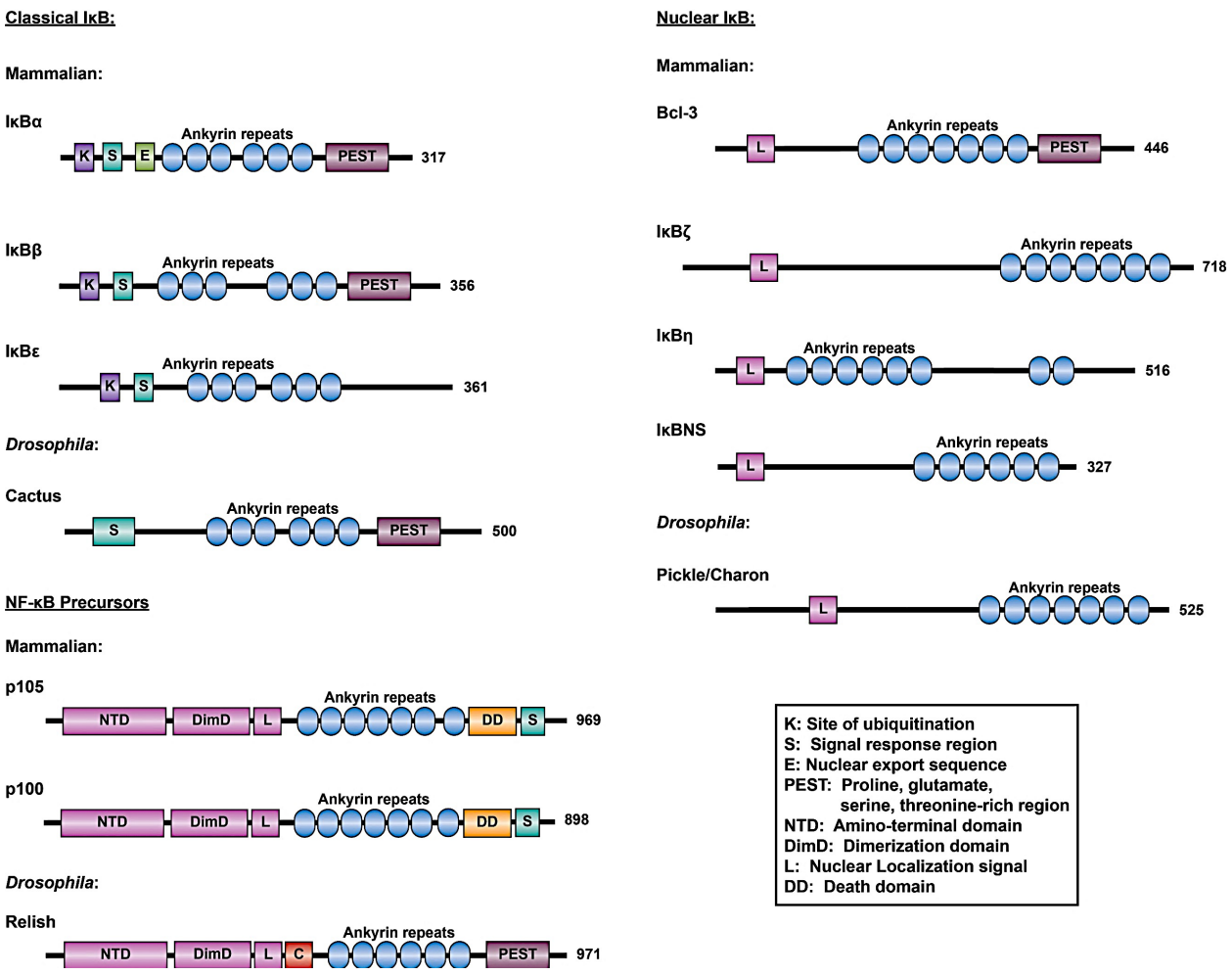

Figure 1.5: Domain structures of IκB proteins

3. IκB kinases (IKK)

Although multiple types of NF-κB dimers can be formed and regulated by different members of the IκB family under diverse stimuli, only one kinase complex composed of the same subunits is responsible for signal-dependent phosphorylation of IκB (Zandi, 1998). In 1997, multiple groups identified the kinase complex responsible for this activity and the complex was named the IκB kinase complex (IKK). The IKK complex was initially purified and characterized as a high molecular weight complex whose activity was dependent upon stimulation (Didonato et al., 1997; Mercurio et al., 1997; Régnier et al., 1997; Woronicz et al., 1997; Zandi et al., 1997). Upon stimulation of TNFα in HeLa cells, this IKK complex was purified and exhibited an apparent molecular weight of 700-900 kDa according to size-exclusion chromatography. Microsequencing and mass spectrometry revealed the presence of two highly similar serine kinases with 50% primary sequence identity and molecular weights of 85 kDa and 87 kDa corresponding to IKK1 (also named IKKα) and IKK2 (also named IKKβ), respectively (Didonato et al., 1997; Zandi et al., 1997). IKK1 was the first IKK subunit identified and was recognized to be the same protein as CHUK which was discovered two years prior as a novel and highly conserved serine-threonine kinase ubiquitously expressed in tissues (Connelly et al., 1995). Soon after the identification of the kinase-containing IKK subunits, several groups identified a third subunit of the IKK complex called NEMO (also named IKKγ, FIP3, and IKAP1) through biochemical purification, complementation of NF-κB-unresponsive cell lines, and as a factor that interacts with an adenoviral protein that inhibits NF-κB (Y. Li et al., 1999; Mercurio et al., 1999; Rothwarf et al., 1998; Yamaoka et al., 1998). In contrast, NEMO is a 48 kDa protein that does not contain a kinase domain and preferentially interacts with IKKβ over IKKα (Mercurio et al., 1999). Instead, NEMO functions as an adaptor to link the catalytic IKK subunits to receptor proximal factors, thus playing a role in the propagation of signaling towards IKK (Schröfelbauer et al., 2012). Mice knockout studies have clearly shown that NEMO is an

absolute requirement for NF-κB activation by IKK (Makris et al., 2000; Rudolph et al., 2000; Schmidt-Supprian et al., 2000).

A few years after the mammalian IKK complex was discovered, orthologs were identified in *Drosophila* and are a necessary component of NF-κB activation in the IMD pathway (Kim et al., 2000; Lu et al., 2001; Rutschmann et al., 2000; Silverman et al., 2000). IKK orthologs exist throughout metazoa, present in arthropods and other invertebrates such as hydra and sea anemone (Gilmore et al., 2012).

The IKK proteins constitute a small family of protein kinases consisting of the aforementioned catalytic subunits IKKα and IKKβ in addition to the IKK-like kinases TBK1 and IKKε (also known as IKK-i). These four IKK protein kinases are homologous, sharing a ~300 amino acid kinase domain and a unique domain architecture not observed in other protein kinases. TBK1 and IKKε exhibit 48% identity and 63% similarity globally, while the kinase domains show 69% identity and 83% similarity. In addition, the kinase domain of TBK1 and IKKε only have 30% identity with the kinase domain of IKKβ (Kishore et al., 2002). Within the kinase domain, IKKα/IKKβ and TBK1/IKKε have similar activation loops and specific serine residues must be phosphorylated to become active. Two serine residues undergo activation loop phosphorylation in IKKα/IKKβ: Serine residues 176 and 180 in IKKα and serine residues 171 and 181 in IKKβ. However, only serine residue 172 is phosphorylated in the activation loop of TBK1/IKKε.

Structural studies of *Xenopus* and human IKKα and IKKβ revealed a domain architecture with three main modules: an N-terminal kinase domain (KD) followed by a ubiquitin-like domain (ULD) and the scaffold dimerization domain (SDD) through which IKK subunits dimerize (Xu et al., 2011; Liu et al., 2013; Polley et al., 2013; Polley et al., 2016). A helical motif known as the NEMO-binding domain (NBD) present at the C-terminus of both IKKα and IKKβ mediates a high-affinity binding site for the N-terminus of NEMO (Drew et al., 2007; May et al., 2002; Rushe

et al., 2008). The X-ray crystal structure of mouse TBK1 revealed that like IKKα/IKKβ, it also has an N-terminal KD, ULD, and C-terminal SDD but does not have an NBD (Larabi et al., 2013). While serine residues 32 and 36 of IκBα is the main target of IKKβ, all IKK protein kinases can phosphorylate these sites, though TBK1/IKKε preferentially phosphorylates serine residue 36 suggesting some overlap in substrate sequence specificity (Kishore et al., 2002). TBK1 and IKKε are seen to be functionally redundant and phosphorylate the same main substrates, the transcription factors IRF3 and IRF7 which regulate the expression of Type I interferons in response to recognition of foreign nucleic acid species, viral and infection by other pathogens. TBK1/IKKε respond to stimuli recognized by TLRs, RLRs, and the cGAS-STING pathway (Honda et al., 2006; X.-D. Li et al., 2013). A TBK1 ortholog has been identified in *Drosophila* called IK2 and is involved in cytoskeleton assembly during oogenesis in a pathway independent of NF-κB (Shapiro et al., 2006). Moreover, the cGAS-STING pathway is a conserved signaling module recently described in *Drosophila* and in mammals (Goto et al., 2018; X.-D. Li et al., 2013). Both mammalian and *Drosophila* utilize cGAS to generate cyclic GMP-AMP (cGAMP) though mammalian cGAS senses cytosolic DNA, while *Drosophila* cGAS has been shown to respond to picorna-like viruses (Goto et al., 2018; X.-D. Li et al., 2013). However, in both systems, cGAMP binds to STING, though subsequent steps in the pathway differ. In mammals, upon cGAMP-STING binding, TBK1 is recruited and phosphorylates IRF3 for induction of immune response genes such as cytokines and type I interferons. The IKK complex and the catalytic activity of IKKβ is also critical in the cGAS-STING pathway and found to phosphorylate the activation loop serine 172 in TBK1/IKKε in addition to its role in the activation of NF-κB in this pathway (Fang et al., 2017). In *Drosophila* where IRFs and interferons are absent, DmIKKβ independent of DmIKKγ mediates Relish activation to induce expression of antiviral effector genes in a separate cGAS-STING pathway not involving the IMD pathway or IK2 (Goto et al., 2018). It remains to be seen whether *Drosophila* IK2 plays

additional regulatory roles, especially in the immune response. Despite this, in both *Drosophila* and mammals, there is significant cross-talk with other signaling pathways and the list of stimuli and pathways that converge upon the IKK complex continues to grow.

IKK-like kinases have been described not only in flies and mammals but also in the most basal metazoan group, the sponges (Gilmore et al., 2012). The IKK ortholog in the sponge, *Amphimedon queenslandica* is more similar in primary sequence to the IKK-like kinases TBK1 and IKKε (Gilmore et al., 2012). Consequently, the ancestral IKK may have been more similar to the sponge TBK1/IKKε and duplicated, diverging into an IKKα/IKKβ-like gene in a sponge/cnidarian ancestral lineage. It will be of interest to see if this hypothesis holds as more genomes of basal metazoans are being sequenced and characterized.

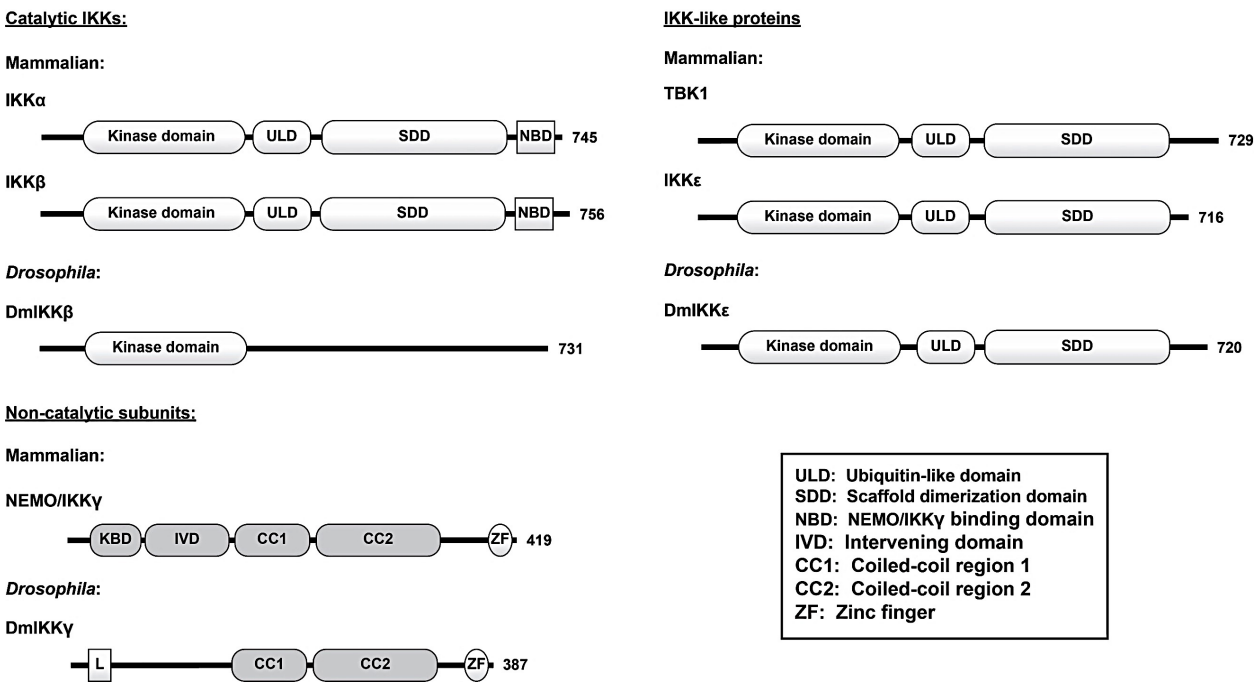

Figure 1.6: Domain structure of IKK and IKK-like proteins

G. Homology of NF-κB signaling cascades in mammals and *Drosophila*

NF-κB signaling pathways are evolutionarily ancient and play a major role in innate immune, developmental and cell survival mechanisms within the animal kingdom. From flies to mammals, the IκB kinase (IKK) complex responds to extracellular threats and transduces this signal to activate dimeric NF-κB transcription factors. The major differences in NF-κB activation pathways across the phylogenetic spectrum are in the terminal ends of pathways which are the receptors that initiate the pathway and the effector genes targeted. Unlike the mammalian system in detecting pathogens through TLRs, the *Drosophila* IMD and Toll pathways rely on PGRPs and GNBPs as pattern recognition receptors. In mammals, the activation of NF-κB induces expression of stress response genes such as cell-survival genes, cytokines and other "acute phase response" genes to clear infection as well as induction of co-stimulatory molecules. In *Drosophila*, the NF-κB homologs Dif, Dorsal, and Relish are known primarily for their role in initiating the expression of AMPs in the humoral innate immune response although

hundreds of other genes are induced and are involved in physiological processes such as aging, tumorigenesis, brain function, microbiome homeostasis, and others (Buchon et al., 2014; Gregorio et al., 2002; Hanson et al., 2020; Parvy et al., 2019). As more NF-κB target genes induced by the Toll and IMD pathways are characterized, it will not be surprising to continue to discover overlap as well as some differences in *Drosophila* and mammalian gene expression programs regulated by NF-κB signaling modules.

It is clear that there are significant differences in the microbial sensing and the effector genes expressed in NF-κB signaling in flies and mammals. This may be reflective of different evolutionary constraints and selective pressures experienced between the two groups. Given the striking conservation of NF-κB signaling components, it appears as though metazoans have started with a common background of basic macromolecular components and molecular modules of which they have utilized following the constraints and selective pressures encountered in evolution by natural selection. Understanding of molecular-level details of NF-κB activation in flies and in other basal and pre-metazoan species will undoubtedly continue to illuminate our understanding of the signaling and regulation of the vital NF-κB transcription factor underlying innate immunity and whole organism physiology. In this section, I compare the conserved features of *Drosophila* Toll and IMD pathways with that of mammalian NF-κB activation pathways.

1. Homology between the *Drosophila* IMD pathway and mammalian TNFR1 pathway

The IMD pathway exhibits similarities with the intracytoplasmic signaling factors and organization of the mammalian TNFR1/TNFR2 pathway with some molecular components also bearing similarity with mammalian TLR pathways (Figure 1.7, Figure 1.8). Although the receptors and ligand recognition are dissimilar given that PGRP-LC recognizes DAP-PGN in the IMD pathway and TNFR1 or TNFR2 senses the cytokine tumor necrosis factor α (TNFα) in the TNFR pathway, the receptor proximal adaptors bear striking homology. For instance, Imd bears

homology with both the death domains and RHIM motif of the TNFR adaptor Receptor-interacting protein kinase 1 (RIP1) forming necessary signaling complexes and assemblies in their respective pathways.

Recognition of TNFα by TNFR1/2 leads to receptor trimerization and recruitment of downstream adaptors. Unlike mammalian RIP kinases, Imd does not harbor a kinase domain. Despite this, both Imd and RIP1 facilitate the formation of functional signaling amyloids. RIP1, along with RIP3, form filamentous structures that form a scaffold for downstream signaling to trigger a form of inflammatory cell death called necroptosis. Imd and PGRP-LC form similar signaling amyloids through a cRHIM interaction for AMP gene induction. In both pathways, RHIM-mediated formation of signaling amyloids is necessary for NF-κB activation.

In mammals, The Tab1-Tab2/3-Tak1 complex functions to activate the IKK complex through phosphorylation of the IKK activation loop (human IKKβ serine 177) which may prime IKKβ activation through trans-autophosphorylation of serine residue 181. (Zhang et al., 2014). In *Drosophila*, orthologs of Tab2 and Tak1 exist and also form a complex to phosphorylate and activate the DmIKK complex (Kleino et al., 2005; Lu et al., 2001; Rutschmann et al., 2000; Silverman et al., 2000). However, Tab1 has been lost in *Drosophila*. In addition, both the TNFR and IMD pathways bifurcates to activate the c-Jun N-terminal kinase (JNK) pathway at the level of Tab-Tak1 in response to stress stimuli and contributes to inflammatory responses (Delaney et al., 2006; Silverman et al., 2003; Vlahopoulos et al., 2004).

Drosophila Dredd is a homolog of mammalian caspase-8, the latter of which functions as a molecular switch for apoptosis and nectroptosis. Caspase-8 inhibits MLKL and RIP3-mediated necroptosis, but facilitates receptor-mediated apoptosis as well as other functions in T-cell homeostasis and anti-tumor roles (Shalini et al 2015). Fadd, in both *Drosophila* and in mammals, has two domains that function to propagate signaling via homotypic interactions: the death domain (DD) and the death effector domain (DED). As such, Fadd functions as a death

adaptor that uses its DD to interact with the DD of receptor proximal adaptors (such as Imd and RIP1) and links a caspase (caspase-8 in mammals and Dredd in *Drosophila*) to its substrate (Imd or Relish in *Drosophila* and RIPK1/RIPK3 in mammals) by utilizing its DED to interact with the caspase DED (Shalini et al., 2015).

Ubiquitination is an important regulatory signaling molecule in a multitude of pathways and is critical in the regulation of NF-κB. The E3-ligase inhibitor of apoptosis 2 (IAP2) functions to ubiquitinate caspases such as Dredd in *Drosophila* and Caspase-8 in mammals. IAP2 E3 ligases also ubiquitinate other substrates such as Imd and TAB proteins (Silke et al., 2013). *Drosophila* dIAP2 and mammalian cIAP2 associates with E2 conjugating enzymes Uev1a, Ubc13 (Bendless in *Drosophila*), and Ubc5 (Effete in *Drosophila*) to transfer K-63-linked polyubiquitin to its substrates. Upon TNF signaling, mammalian NEMO/IKKγ is both poly-ubiquitinated and binds to poly-ubiquitin chains thereby propagating inducing signals to the IKK complex (Fujita et al., 2014; Xia et al., 2009). The *Drosophila* IKKγ ortholog has primary sequence similarity to mammalian NEMO, though mostly in the C-terminal half which harbors ubiquitin-binding domains (Rutschmann et al., 2000; Silverman et al., 2000). The linear ubiquitin chain assembly complex (LUBAC) is an important factor in the regulation of the IKK complex (Fujita et al. 2014). LUBAC is the only known E3 ligase that assembles linear (methionine-1) linked polyubiquitin and is composed of three subunits: the catalytic subunit HOIP, HOIL-1, and SHARPIN. (Dondelinger et al. 2016). LUBAC is known to add linear poly-ubiquitin to TNFR, RIP1, NEMO and TRADD. A *Drosophila* homolog of LUBAC was identified, called linear ubiquitin E3 ligase (LUBEL) that works in concert with DIAP2 to modify DmIKKγ with linear and K-63-linked poly-ubiquitin (Aalto et al. 2019). LUBEL, however, is not required in the systemic immune response upon septic injury, but is required in oral infection (Aalto et al. 2019). It would be of interest to see whether other ubiquitinylation machinery is involved in the systemic response and whether K-63 and linear polyubiquitin chains play significant roles in the activation

of the DmIKK complex as it does in the activation of the mammalian IKK complex. Nevertheless, the catalytic IKK subunits exhibit significant homology with the kinase domains of *Drosophila* and human IKKβ having ~50% similarity in amino acid sequences. The IKKβ orthologs both phosphorylate serines in the N-terminus of NF-κB proteins Relish in *Drosophila* and p65 in mammals for NF-κB activation (Ertürk-Hasdemir et al., 2009; Sakurai et al., 2003; F. Yang et al., 2003).

Additional factors exist in the mammalian TNFR1/2 pathway that have been lost in *Drosophila* (Figure 1.4). In the TNFR1 signaling cascade, the adaptor protein TRADD is a death-domain containing adaptor that interacts with the intracytoplasmic death domains of TNFR1 upon TNFα stimulation. A *Drosophila* ortholog of TRADD has not been identified. Three different signaling complexes are formed in the TNFR1 pathway that are either pro-survival, apoptotic, or necroptotic. TRADD recruits both RIP1 and TRAF2 through death domain interactions to form the pro-survival signaling module called “complex 1”. Two TRAF homologs have been found in the *Drosophila* genome, but none have yet to be shown to interact with members of the IMD pathway. Rather, dTRAF1 has been shown to interact with Pelle in the Toll pathway and is necessary for maximal AMP induction, while dTRAF2 regulates the JNK pathway (Cha et al., 2003; Zapata et al., 2000). In the TNFR pathway, within the TRADD-mediated signaling complex, TRADD recruits FADD through DD interactions and the complex can then bifurcate into signaling pathways leading to apoptosis or necroptosis (Peltzer et al., 2019). Recruitment of Caspase-8 to form “complex 2a” leads to apoptosis, while recruitment of RIP3 leads to the formation of RHIM-mediated RIP1-RIP3 amyloids and formation of “complex 2b”. The kinase domains of RIP1-RIP3 are activated and then phosphorylate MLKL which then forms tetramers and oligomers that function to induce necroptosis (S. Liu et al., 2017).

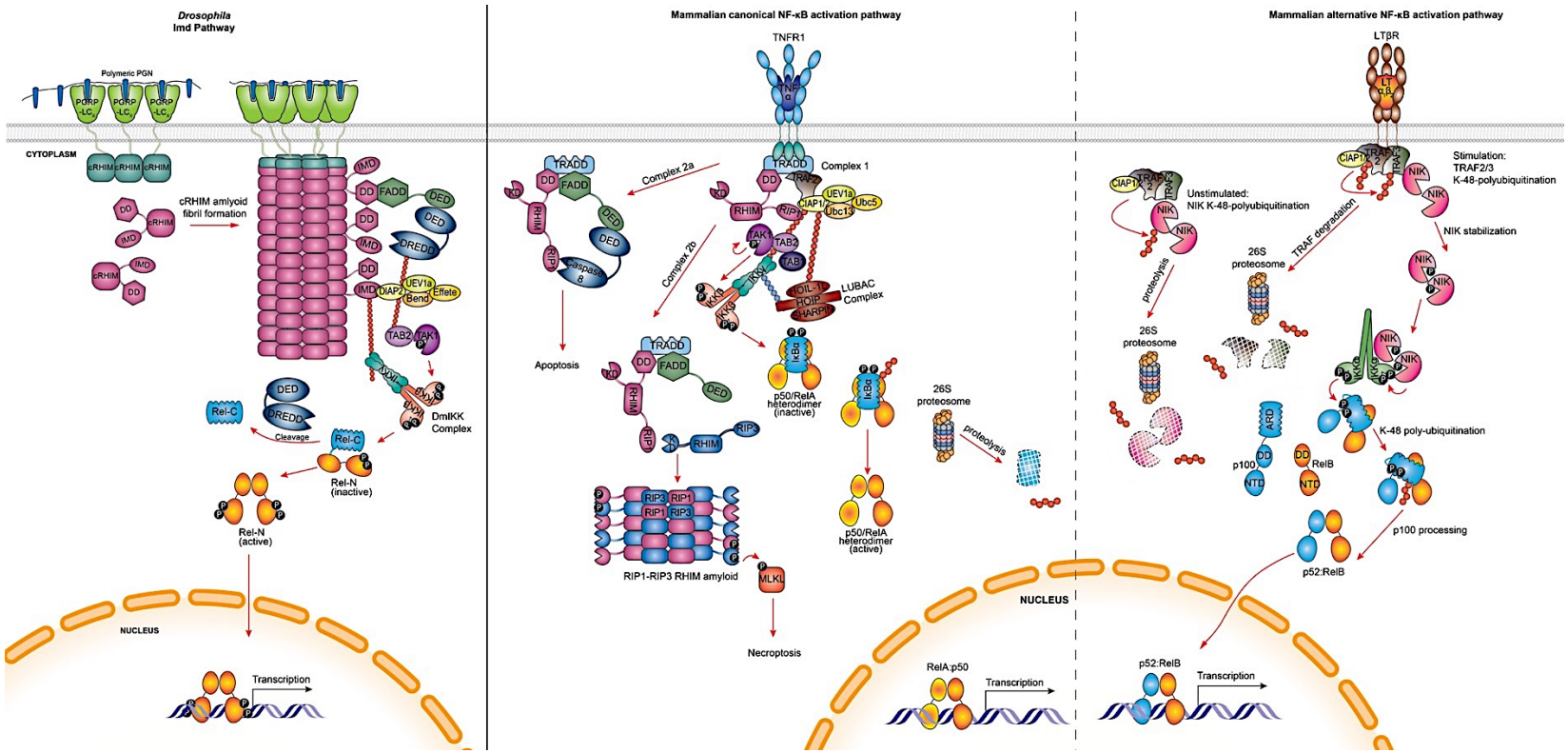

Figure 1.7: Homology of *Drosophila* Imd and mammalian canonical and alternative NF-κB signaling

It is noteworthy to mention that a homologous pathway of the mammalian alternative/non-canonical NF-κB activation pathway has been lost in *Drosophila*. The noncanonical NF-κB activation pathway involves signaling through receptors in the TNFR superfamily such as lymphotoxin β-receptor (LTβR), BAFF or RANKL receptors (Figure 1.4). Binding of cognate ligands to this subset of TNFR receptors leads to poly-ubiquitination of TRAFs such as TRAF2 and TRAF3 by CIAP1/2 which leads to its destruction via the 26S proteasome (Sun, 2011; Yang et al., 2015). This results in stabilization, accumulation, and activation of NF-κB inducing Kinase (NIK) which is necessary for the activation of IKKα, the chief catalytic IKK subunit involved in this pathway. In unstimulated conditions, NIK undergoes constitutive processing through K-48-linked ubiquitination by CIAP1/2 and subsequent proteolytic degradation. The alternative pathway is NEMO-independent and does not seem to involve the catalytic IKKβ subunit. Only one catalytic IKK subunit has been identified in *Drosophila*, and DmIKKβ has greater similarity to human IKKβ than to IKKα (Silverman et al., 2000). Activation of IKKα results in phosphorylation of p100 in a cluster of serines at both the N- and C-terminus (Xiao et al., 2004). Phosphorylation of Serines 860 and 870 facilitates binding of the β-TrCP E3-ligase for ubiquitination and proteolytic processing of the C-terminal IκB-like ankyrin repeat domains (Liang et al., 2006). This critical processing event liberates the N-terminal RHD-containing p52 subunit and permits nuclear translocation of p52:RelB dimers to drive the expression of genes involved in processes such as lymphoid organogenesis, B-cell homeostasis, activation of dendritic cells, osteoclastogenesis, and the circadian clock (Boyce et al., 2015; Lopez et al., 2016; Sun, 2011).

2. Homology between the *Drosophila* Toll and mammalian IL-1-R/TLR pathways

Starting with Toll, the intracellular signaling cascade of the Toll and TLR pathway is nearly identical with *Drosophila* orthologs present in nearly each component (Figure 1.8). However, mammalian TLRs directly interact with microbial PAMPs and Toll interacts with the

cytokine Spaetzle, a product of extracellular protease cascade initiated by recognition by PAMPs or through positional cues in embryonic development. *Drosophila* Toll and mammalian TLR and IL-1R receptors contain an intracytoplasmic TIR domain that mediate downstream signaling. IL-1R, Toll and TLRs differ in their extracellular domains as both the Toll and TLRs receptor families have an extracellular leucine-rich repeat (LRR) domain while the IL-1R family of receptors have an immunoglobulin-like (Ig) domain to bind to PAMPs. Although the extracellular domains recognize different ligands, many of the intracellular signaling proteins are the same because of the shared intracellular TIR domain. In all three of these receptors, ligand binding results in the recruitment of the receptor proximal adaptor protein called Myd88. In general, Myd88 proteins have a C-terminal TIR domain that interacts with the Toll/TLR/IL-1R TIR domain and an N-terminal death domain that interacts with the death-domain of IRAK proteins. The *Drosophila* Toll-induced signaling complex composed of Myd88, Tube, and Pelle are orthologs of mammalian Myd88, IRAK4, and IRAK1 and interact via death-domains in both systems. A major difference, however, is that the Drosophila IKK complex is not a component of the Toll pathway, while IKK is required for the activation of NF-κB in the TLR and IL-1R pathways (Lu et al., 2001; Silverman et al., 2000).

Mammalian TLR and Il-1R signaling relies on signal transduction through the ubiquitin E3 ligase TRAF6, which interacts with IRAK1 and also attaches K-63 poly-ubiquitin onto the TAB1/2-TAK1 complex via its RING domain. Recruitment of Tab1/2-TAK1 results in the phosphorylation and activation of IKK. *Drosophila* TRAF2, homologous to mammalian TRAF6, was shown to interact with Pelle and regulate AMP expression (Cha et al., 2003; Zapata et al., 2000). It is not yet known whether dTRAF2 utilizes E3-ligase activity as part of its regulatory action. The activated IKK complex then phosphorylates serines 32 and 36 of IκB which recruits the E3 ligase β-TrCP for K-48 poly-ubiquitination at lysines 21 and 22 for rapid proteasomal degradation. Slimb is the *Drosophila* ortholog of mammalian β-TrCP in the SCF E3 ubiquitin

ligase complex and is shown to play a role in Cactus degradation (Daigneault et al., 2013). The identity of the *Drosophila* Cactus kinase remains equivocal. Despite this, Cactus undergoes signal-dependent phosphorylation at N-terminal serines resulting in polyubiquitination and destruction by the 26S proteosome (Belvin et al., 1995; Bergmann et al., 1996; Cardoso et al., 2017; Daigneault et al., 2013; Spencer et al., 1999). *Drosophila* Dorsal and Dif are RHD-containing Rel proteins with ~35% and ~30% identity to RelA/p65, respectively. Release of Rel proteins from IκB allows nuclear translocation and binding to κB-motifs to induce expression of effector genes.

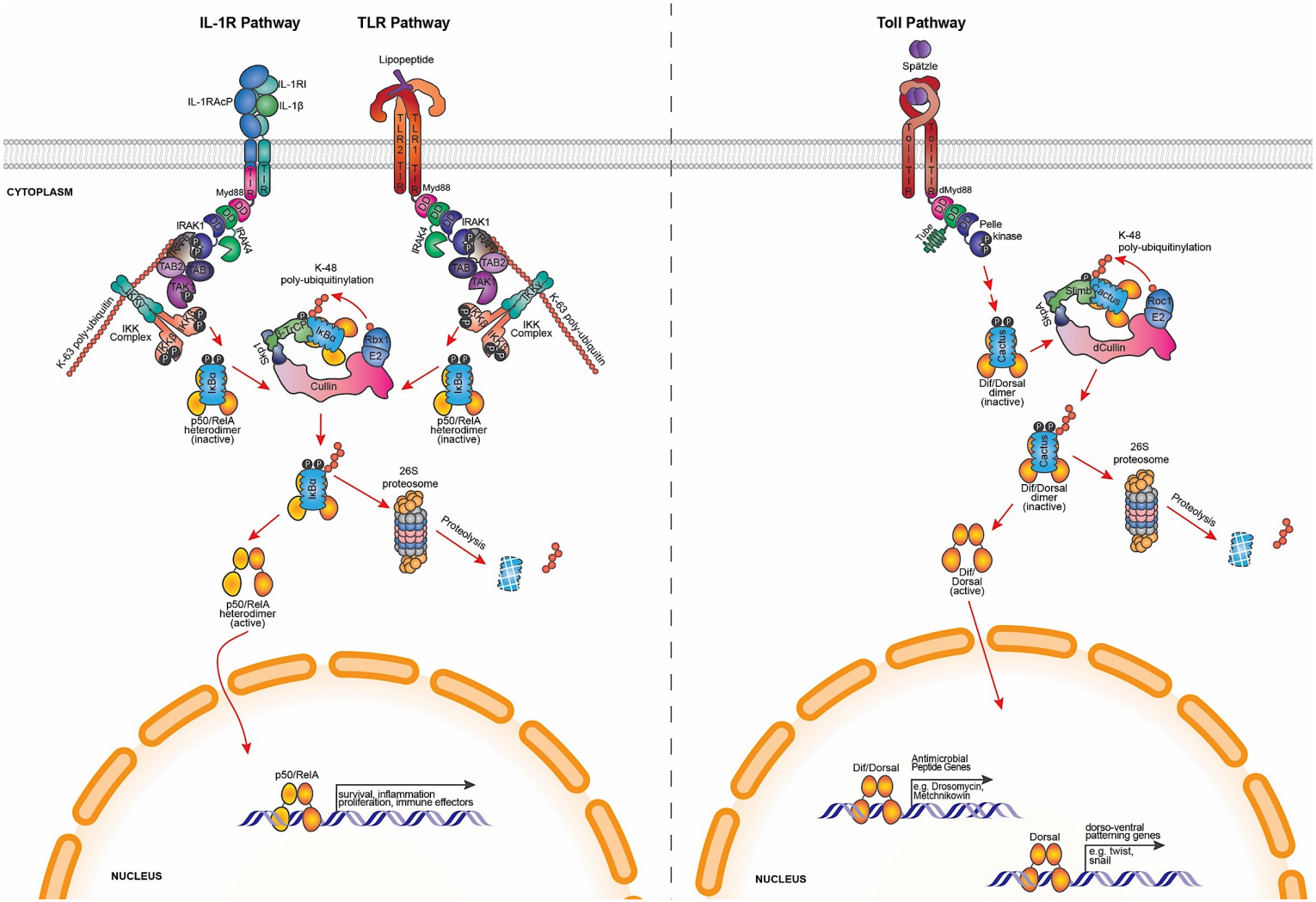

Figure 1.8: Homology of *Drosophila* Toll and mammalian TLR/IL-1R signaling

H. Focus of study

The multi-subunit IKK complex is a necessary component in all cells to be able to respond to stresses and extracellular stimuli. Since its discovery 27 years ago, there are still some fundamental questions regarding regulation of this complex as well as substrate specificity. Structural studies on mammalian IKK subunits have revealed that the catalytic subunits form dimers in solution and can form transient, higher-order oligomers that may support trans-autophosphorylation. In addition, structural studies of portions of the non-catalytic subunit NEMO show a primarily alpha-helical protein with distinct modules that function to interact with different components along the signaling pathway. These distinct modules in NEMO interact with poly-ubiquitin, IκB and with the catalytic subunits to support IKK complex regulation and activity. Nevertheless, the nature of IKK complex assembly has been uncertain since it was discovered as a very large 700-900 kDa activity, suggesting formation of multiple copies of each subunit and higher-order oligomerization. Nevertheless, there is very little structural information on a multi-subunit IKK complex as the mammalian complex is difficult to purify to homogeneity and also visualize by three-dimensional structural techniques due to instability in solution. In efforts to understand IKK biochemistry and regulation, I have undertaken structural and biophysical approaches on a multi-subunit IKK complex from the model organism *Drosophila melanogaster*. In this work, I also identify structural features that are shared with mammalian IKK and also some features that are unique to the DmIKK complex to better understand its mechanism of regulation as a key component of the *Drosophila* IMD innate immune pathway.

Chapter II

Materials and Methods

A. Preparation of expression plasmids

1. *Drosophila melanogaster* IKK expression plasmids

DmIKKβ cDNA was graciously provided by N. Silverman (University of Massachussetts Medical School). The full-length DmIKKβ cDNA was amplified by PCR and inserted into the pFastBacHtB plasmid within BamHI and NotI restriction sites to generate a construct containing an N-terminal hexa-histidine tag followed by TEV-protease recognition site. DmIKKγ was cloned by using RT-PCR of mRNA from LPS stimulated S2 cells, amplified using PCR with a reverse primer encoding a C-terminal FLAG epitope, and ligated into pFastBacHtB plasmid within BamHI and NotI restriction sites containing an N-terminal hexa-histidine tag followed by a TEV-protease recognition site. pFastBacHtB- DmIKKβ and pFastBacHtB-DmIKKγ plasmids were used to sub-clone His-DmIKKβ and FLAG-DmIKKγ constructs into pFastBacDual between BamHI and xx restriction sites for co-expression of the complex.

2. Relish expression plasmids

The Relish cDNA was kindly provided by Dr. Tony Ip (University of Massachussetts Medical School). The full-length Relish cDNA was amplified by PCR and ligated into the pFastBacHtA plasmid within EcoRI and NotI restriction sites to generate a construct containing an N-terminal hexa-histidine tag followed by TEV-protease recognition site. A His-Rel68 construct was generated by introducing a stop codon in place of glycine 546. GST-tagged Relish constructs were ligated into the pGEX-4T2 plasmid between the EcoRI and NotI restriction sites for bacterial expression. For S2* cell-based assays, a Relish construct with both N-terminal and C-terminal FLAG tags were ligated into the pMT vector (Invitrogen) with a copper-inducible promoter between the SpeI and NotI sites.

3. Human NEMO expression plasmid

Full-length human NEMO in the bacterial expression plasmid pET15b was kindly provided by Dr. Gourisankar Ghosh. The NEMO cDNA was sub-cloned between BamHI and EcoRI restriction sites. The pET15b expression vector is under the control of a T7 promoter and contains an N-terminal hexa-histidine tag.

4. GST-Tetra-ubiquitin expression plasmid

Tetra-ubiquitin was sub-cloned into pGEX-4T2 between the BamHI and NotI restriction sites from the bacterial expression plasmid pET24B-HTTEV-NFGE6-TetraUbi kindly provided by Eric Rogers. The pGEX-4T2 expression vector is under the control of a T7 promoter and contains an N-terminal GST tag.

B. Mammalian and fruit fly sequence comparison

The amino acid sequences of human (Hs) and *D. melanogaster* (Dm) IKK proteins were compared using FASTA sequences obtained from UniProt using the following UniProt IDs: Q9VEZ5 for DmIKKβ; O14920 for HsIKKβ; O15111 for HsIKKα; Q9GYV5 for DmIKKγ; and Q9Y6K9 for HsNEMO. Global alignment was performed using MUSCLE (https://www.ebi.ac.uk/Tools/msa/muscle/) for multiple sequence alignment and visualized using ESPript 3.0 (http://espript.ibcp.fr/ESPript/ESPript/). Pair-wise local alignment was performed using Lalign (https://www.ebi.ac.uk/Tools/psa/lalign/).

C. Multiple sequence alignment (MSA), evolutionary analysis, and structural conservation analysis

Multiple sequence alignments were performed using MUSCLE (https://www.ebi.ac.uk/Tools/msa/muscle/). The Jpred 4 server was used to predict human NEMO and DmIKKγ secondary structural elements (http://www.compbio.dundee.ac.uk/jpred/). Pair-wise sequence identity and similarity matrices were constructed using the default settings on the SIAS server (http://imed.med.ucm.es/Tools/sias_help.html). Pair-wise p-distances and number of amino acid differences were calculated using MEGA X. All positions containing gaps

and missing data were eliminated (complete deletion option). Using the MSA, maximum likelihood phylogenetic trees were built from the multiple sequence alignment of eight metazoan IKKβ orthologs and separate analysis using six metazoan IKKγ orthologs in MEGA X. Bootstrap analysis with 1000 replicates were performed to evaluate the support for the phylogenetic reconstruction. Neighbor-joining and BioNJ algorithims were applied in the initial heuristic search. The MSA file was input into the ConSurf server for positional amino acid conservation scoring and mapping (Ashkenazy et al., 2010, 2016; Berezin et al., 2004; Celniker et al., 2013; Glaser et al., 2003; Landau et al., 2005). Figures were made in PyMol (DeLano, 2002).

D. Recombinant virus production

Preparation of recombinant baculovirus and titering was performed using a modified version of the Bac-to-Bac system (Invitrogen) as detailed previously (Shaul et. al 2008). Sf9 cell cultures used for recombinant baculoviral production were grown in ESF 921 insect cell media (Expression systems) containing 10% fetal bovine serum (Gibco).

E. Protein expression and purification

Sf9 cell suspension cultures were grown in ESF 921 insect cell media (without fetal bovine serum) to a density of ~2 million cells/mL and infected with recombinant baculovirus for 72 hours. 500 mL of infected cells were harvested at 500*g* for 5 min and resuspended in 60 mL of lysis buffer (25mM Tris pH 8.0, 250mM NaCl, 10mM imidazole, 10% Glycerol, 0.5% Triton X-100, 5mM β-Mercaptoethanol and protease inhibitor cocktail (MedChemExpress). Lysis was performed by gentle sonication in two 10 second intervals with 1 minute rest at 20% duty cycle and power output of 3 using a Branson Sonifier 450 outfitted with a microtip. 0.17 mM PMSF was added prior to and after sonication. Lysate was clarified by centrifugation at 12,000 rpm (Sorval; SS-34 rotor) for 40 min at 4°C. Supernatant was passed through a 0.8 µm syringe-tip filter (Sartorius) and combined with Nickel Sepharose Fast Flow resin (GE Life Sciences) pre-equilibrated with lysis buffer (0.9 mL slurry per 500 mL culture). The filtered lysate and resin were batch-incubated with end-over-end mixing for 1.5-2 hours in 4°C. 0.17 mM PMSF was

again added prior to batch-incubation. Nickel resin was gently pelleted at 1000 x g for 2 min. Resin was then washed two times with 25 mL wash buffer (25mM Tris pH 8.0, 250mM NaCl, 30 mM imidazole, 10% Glycerol, 5mM β-Mercaptoethanol) at 1000*g* for 2 min. Resin was then loaded onto an empty column and washed with an additional 50-100 mL wash buffer by gravity flow. Proteins were eluted in 500 µL fractions using elution buffer (25mM Tris pH 8.0, 200mM NaCl, 250 mM imidazole, 10% Glycerol, 5mM β-Mercaptoethanol). Peak fractions were combined at a total volume of 0.5 mL for the DmIKK complex and 2 mL for His-DmIKKβ construct and were treated with 1 mM ATP, 20 mM $MgCl_2$, 10 mM NaF, and 1 mM Na_3VO_4 for 30 minutes at room temperature. The eluates were centrifuged at 15,000*g* in 4°C and loaded onto the appropriate size-exclusion column connected to an ÄKTA purifier (GE Life Sciences) pre-equilibrated with size-exclusion buffer (25 mM HEPES pH=7.2, 250 mM NaCl, 5% glycerol, and 5 mM β-Mercaptoethanol). For the DmIKK complex, a Superose 6 10/300 increase column (GE Life Sciences) was used at a flow rate of 0.5 mL/min, while a Superdex 200 16/60 size-exclusion column (GE Life Sciences) was used at a flow rate of 1.0 mL/min for the His-DmIKKβ construct. His-Relish and His-Rel-68 were expressed and purified in a similar manner as His-DmIKKβ, but was not treated with ATP and purified with a size-exclusion buffer containing 25 mM Tris pH=7.5, 150 mM NaCl, 0.5 M EDTA, 5% glycerol, and 10 mM β-Mercaptoethanol. The affinity tags were not removed in the described studies.

GST fusion proteins (Rel-49 and tetra-ubiquitin) and His-HsNEMO were expressed in *E. coli* BL21(DE3) and purified using Glutathione Sepharose 4B (GE Healthcare) and Ni Sepharose 6 Fast Flow (GE Healthcare) resins, respectively.

F. *In vitro* kinase assay and LC/MS/MS

Kinase (20-200 ng) and Relish substrate (1.5 µg) were incubated in reaction buffer (20 mM Tris-HCl, 15 mM $MgCl_2$, 10 mM KCl, 1 mM DTT, 1 mM $NaVO_4$, and 1 µM ATP) at a total reaction volume of 20 µL. For autoradiography, 0.5 µCi of γ-^{32}P ATP (Perkin Elmer) was added to each reaction and the tubes were gently mixed and incubated at room temperature for one

hour. The reactions were resolved by SDS-PAGE and dried onto #3 Whatman filter paper. The dried gels were exposed to autoradiography film for 24 hours and developed. For LC/MS/MS, the reactions were prepared by in-solution trypsin digestion and mass spectrometry was performed at the Scripps Center of Metabolomics. A total of 51 peptides were detected with 45% coverage of Rel-68 and Rel-49 constructs analyzed.

G. *Drosophila* S2* cell culture

Schneider S2* cells were kindly supplied by K. McNamara from the W. Stumph Lab (San Diego State University) and kept in an incubator at 27°C. S2* cells were cultured in S2 media (Gibco) supplemented with 10% FBS (Gibco) in 10 cm plates and were passaged upon reaching 80% confluency, about every four days.

H. S2* cell cleavage assay

Schneider S2* cells were transiently transfected with full length Relish constructs (WT, D545A, and SR1AAA) and induced with 100 mM copper sulfate. 24 hours after induction, cells were stimulated with LPS (100ng/mL) for 30 min or at the indicated time points. For immunoblot analysis, cells were lysed in lysis buffer (25 mM Tris-HCl pH 8, 50 mM Nacl, 0.1% Triton X-100) and then incubated on ice for 30 minutes. Lysates were cleared by centrifugation and total protein concentration was determined by Bradford protein assay. 10µg of total protein was resolved by SDS-PAGE and transferred onto a nitrocellulose membrane. Anti-FLAG antibody was used to probe for FLAG-Relish-FLAG cleavage.

I. Analytical size-exclusion chromatography

The apparent molecular weights of His-DmIKKβ, His-DmIKKβ:DmIKKγ-FLAG, and His-DmIKKγ-FLAG were estimated by analytical-scale size exclusion chromatography using a pre-equilibrated (25 mM Tris pH=8.0, 150 mM NaCl, and 1 mM DTT) Superose 6 10/300 GL column connected to an ÄKTA Basic chromatograph GE Healthcare). First, a calibration curve was prepared using the proteins ovalbumin (10 mg/mL), bovine serum albumin (10 mg/mL), aldolase (5 mg/mL), catalase (5 mg/mL), and ferritin (0.5 mg/mL) loaded in pairs at a volume of 0.5 mL

and flow rate of 0.5 mL/min under the same buffer conditions. Determination of the total column volume (Vc) void volume (Vo) was performed using 10μM ATP and Blue Dextran 2000 (0.5 mg/mL), respectively. Samples of freshly purified DmIKK proteins (0.5 mL) were centrifuged at 15,000*g* for 10 minutes at 4°C and loaded onto the Superose 6 column under identical conditions as the standards. Peak retention (elution) volumes (Ve) were determined by Unicorn 5 software. The logarithm of molecular weight (kDa) was plotted against K_{av} and fitted using least squares regression to the linear equation $K_{av} = -0.121\text{Log(MW)} + 2.0819$ (R^2=0.9539). K_{av} is calculated for each of the proteins using the equation $K_{av} = (V_e - V_o)/(V_c - V_o)$. The apparent molecular weights of the recombinant proteins were obtained by interpolating the K_{av} values on the standard curve.

A second calibration curve was generated to estimate the Stokes radius (R_s) of the recombinant DmIKK proteins using the Laurent and Killander method (Laurent and Killander 1964). Using the elution volumes and K_{av} values determined from the molecular weight estimation, the known R_s of the standard proteins were plotted against the square root of $-\log K_{av}$ to the linear equation $R_s = 14.31(-\log K_{av})^{1/2} - 1.316$ (R^2=0.9842). The apparent R_s of the recombinant proteins were obtained by interpolating the $(-\log K_{av})^{1/2}$ values on the standard curve.

J. SEC-MALS

One hundred microliters of freshly purified proteins was centrifuged at 15,000*g* for 10 minutes at 4°C and loaded onto a pre-equilibrated (25 mM HEPES pH=7.2, 250 mM NaCl, and 5 mM β-Mercaptoethanol) Superose 6 10/300 increase column at a flow rate of 0.5 mL/min connected to an ÄKTA Purifier coupled to a miniDAWN TREOS light scattering detector (Wyatt Technology). Protein extinction coefficients at 280 nm were calculated based on the primary sequence using ExPASy ProtParam (https://web.expasy.org/protparam/). Astra VI (Wyatt Technology) software was used to collect data and analyze light scattering from elution peak(s) for molecular weight determination.

K. Analytical Ultracentrifugation

Analytical ultracentrifugation experiments were performed at Sanford Burnham Prebys Medical Discovery Institute using a ProteomeLab XL-I (BeckmanCoulter) analytical ultracentrifuge. Absorbance at 280 nm was used for detection.

For sedimentation velocity (SV) runs protein samples from SEC peak fractions at O.D. 280nm of 0.15-0.2 for the DmIKK complex and an O.D at 280nm of 0.3 for His-DmIKKβ in buffer containing 25mM HEPES pH 7.15, 250mM NaCl and 5mm beta mercaptoethanol were loaded in 2-channel cells and span in An-50 Ti 8-place rotor at 25,000 rpm, 20 ^{o}C for 20 hours. SV data were analyzed using Sedfit software (P. Schuck, NIH/NIBIB).

For sedimentation equilibrium (SE) runs protein samples from SEC peak fractions at O.D. 280nm of 0.15-0.2 for the DmIKK complex and an O.D at 280nm of 0.3 for His-DmIKKβ in addition to two serial dilutions of them were loaded in 6-channel equilibrium cells and spun in An-50 Ti 8-places rotor at 4,000, 6,000 and 8,000 rpm, 20 ^{o}C until equilibrium was reached for each speed. AUC samples also contained 25 mM HEPES pH 7.15, 250 mM NaCl, 5mM beta mercaptoethanol and 5% glycerol. SE data were analyzed using HeteroAnalysis software (by J.L. Cole and J.W. Lary, University of Connecticut).

L. Negative stain transmission electron microscopy (TEM) sample and grid preparation

Prior to applying TEM on our recombinant DmIKKβ:γ complex, I utilized horse spleen ferritin as a control for preparation of grids and visualization of proteins using this structural method. Horse spleen ferritin (GE Healthcare, Chicago, IL) was purchased as part of a gel filtration column calibration kit and stored at a concentration of 5.0 mg/ml in storage buffer (50 mM phosphate buffer pH=7.2, 150 mL NaCl), aliquot to 100 µL in microcentrifuge tubes, flash frozen in liquid nitrogen, and stored at -80°C. For negative stain sample preparation, an aliquot of frozen ferritin was thawed and centrifuged for 10 minutes at 15,000 x g prior to dilution. Ten-fold serial dilutions were made using freshly filtered (0.2 µm) size-exclusion buffer (25 mM HEPES pH=7.2, 250 mM NaCl, and 5 mM β-Mercaptoethanol) and kept on ice.

Baculovirus-expressed His-DmIKKβ:γ-FLAG complex was purified according to methods described above. The samples were kept on ice overnight in a temperature controlled room at 4°C. The next morning, samples from peak fractions eluted from size-exclusion chromatography at a concentration of 1-2 mg/ml were used to prepare samples for negative staining. The samples were centrifuged for 10 minutes at 15,000 x g prior to dilution. Two ten-fold serial dilutions were made using freshly filtered (0.2 µm) size-exclusion buffer (25 mM HEPES pH=7.2, 250 mM NaCl, and 5 mM β-Mercaptoethanol) and kept on ice.

The samples were taken to the SDSU Electron Microscopy Facility for grid preparation and imaging. 300 mesh hexagonal carbon/formvar coated copper grids (Electron Microscopy Sciences, Hatfield, PA) were placed carbon side up on a parafilm-lined glass slide in the vacuum chamber of the glow discharge apparatus and glow discharged with 5 second pulses of electric charge repeated 2 times. 2% uranyl acetate solution was prepared each time prior to negative staining and centrifuged for 10 seconds at maximum speed to remove any precipitates. Sample adsorption onto the freshly glow discharged grids followed “side blot” method described previously (Booth et al., 2011; Scarff et al., 2018). In this sample adsorption method, 10 µL of sample was placed on the carbon support side and allowed to adsorb for 2 minutes. The excess sample was blotted on filter paper. A 20 µL drop of 2% uranyl acetate was allowed to adsorb for 10 seconds and immediately blotted on excess filter paper. Staining and blotting was repeated with another drop of 20 µL of 2% uranyl acetate. After staining, the grid was placed carbon side down on a clean piece of filter paper and allowed to dry for 5 minutes before storage. The prepared grids were examined using a FEI Tecnai T12 transmission electron microscope (FEI, Hillsboro, OR) operating at an accelerating voltage of 120 kV. Micrographs were taken using a pneumatic AMT HX41 side-mounted digital camera (Advanced Microscopy Technique, Woburn, MA).

Chapter III

Primary sequence comparison and phylogeny of DmIKK with metazoan orthologs

A. Introduction

Innate immunity is a potent, yet phylogenetically ancient defense strategy against microbial infection. It is estimated that 5-10 million metazoan species, including the most speciose metazoan group, the insects, rely only on innate immune defenses (J. A. Hoffmann et al., 2002). In particular, many insect species live in hostile environments amongst bacterial, fungal, and viral pathogens, yet rarely succumb to infection despite the lack of an adaptive/acquired immune system (Faye et al., 2016; Ferrandon et al., 2007; J. A. Hoffmann et al., 2002). A common feature of metazoan innate immunity is the pivotal role of the IKK-NF-κB signaling hub in coordinating the expression of immune response genes such as cationic antimicrobial peptides (AMPs) in insects and pro-inflammatory cytokines in mammals (J. A. Hoffmann et al., 2002; Michael Karin et al., 2000).

In *Drosophila*, there are two distinct intracellular signaling pathways that govern immune-responsive AMP expression: the immune deficiency (IMD) and the Toll pathways. Infection of gram-negative bacteria and some gram positive *Bacillus* species containing meso-diaminopimelic acid-type peptidoglycan initiates the IMD pathway eliciting the activation of a DmIKK complex containing the catalytic DmIKKβ subunit encoded by *ird5* (homologous to mammalian catalytic subunits IKKβ and IKKα, but more homologous to mammalian IKKβ) and the non-catalytic DmIKKγ subunit encoded by *kenny* (homologous to mammalian NEMO/IKKγ) (Lu et al., 2001; Rutschmann et al., 2000; Silverman et al., 2000). Activated DmIKKβ phosphorylates the NF-κB precursor protein Relish (homologous to mammalian p100 and p105) on serines 528 and 529 leading to processing and activation (Ertürk-Hasdemir et al., 2009). Unlike proteasome-mediated processing of mammalian NF-κB precursors p100 and p105, Relish is endoproteolytically cleaved by the Death related ced-3/Nedd2-like caspase (Dredd; a homolog of mammalian Caspase-8) into two fragments: a fragment called Rel-68/Rel-N containing the DNA-binding Rel-homology region and another fragment known as Rel-49/Rel-C containing IκB-like inhibitory ankyrin-repeats (Dushay et al., 1996; Ertürk-Hasdemir et al., 2009;

Stöven et al., 2000, 2003). Both phosphorylation by the DmIKK complex and proteolytic cleavage by Dredd are required for full Relish activation. Active Rel-68 regulates the expression of immune-responsive genes that include antimicrobial peptides such as *diptericin* (Ertürk-Hasdemir et al., 2009).

Upon infection of fungus and gram-positive bacteria containing lysine-type peptidoglycan, the Toll pathway is activated, resulting in phosphorylation of the IκB protein Cactus (orthologous to mammalian IκBα) and activation of NF-κB proteins Dorsal or Dorsal related immunity factor (Dif). The Toll pathway was first discovered to play a role in embryonic development involving Dorsal as a morphogen to regulate genes involved in dorsoventral patterning (Anderson, Bokla, et al., 1985; Anderson, Jürgens, et al., 1985; Hashimoto et al., 1988). Both Dorsal and Dif rapidly translocate into the nucleus following infection (Ip et. al 1993). However, it was found that Dif is the principal NF-κB subunit that acts in adult flies to regulate the expression of AMPs including the antifungal peptide *drosomycin* (Manfruelli et al., 1999; Meng et al., 1999; Rutschmann et al., 2000).

Although DmIKKβ has been shown to phosphorylate Cactus *in vitro,* cell-based and fly studies have shown that Toll pathway activation does not involve components of the DmIKK complex, but is clearly involved in the regulation of the IMD pathway (Lu et al., 2001; Rutschmann et al., 2000; Silverman et al., 2000). Nevertheless, mutation of *ird5* or *kenny* in cells and *in vivo* impairs Relish processing and blocks the induction of five of the seven classes of antimicrobial peptides in *Drosophila*, but does not block the expression of antifungal peptides that are primarily controlled by the Toll pathway (Ertürk-Hasdemir et al., 2009; Lu et al., 2001; Rutschmann et al., 2000; Silverman et al., 2000). Thus, the DmIKK complex is essential for proper immune responses in fruit flies.

In both mammals and fruit flies, a multi-subunit IKK complex is required for the regulation of NF-κB target gene expression (J. A. Hoffmann et al., 2002; Michael Karin et al., 2000). IKK1 and IKK2 double knockout mouse embryonic fibroblasts are severely impaired in

IκBalpha degradation and NF-κB activation upon stimulation of classical NF-κB activators such as LPS and TNFalpha in (Li et al 2002). In the immune response from flies to humans, the IKK complex responds to extracellular signals such as microbial infection and transduces this signal to activate NF-κB. Thus, the IKK complex has retained its role as the chief regulator of NF-κB before the evolutionary divergence of these two taxa, so we wonder whether they are structurally homologous. We would like to investigate specific structural features that are shared between the two taxa and those that are unique and whether these features are involved in the regulation mechanism specific to the two taxa.

Significant homology with mammalian IKK subunits was reported to be limited to specific regions of the subunits: the kinase domain of DmIKKβ was found to be 50% similar with the kinase domain of human (Hs)IKKβ while the DmIKKγ subunit displayed 45% similarity with human (Hs)NEMO at the C-terminal half of the protein sequence (Rutschmann et al., 2000; Silverman et al., 2000). Despite limited sequence similarity, the fruit fly and mammalian multi-subunit IKK complex are functionally homologous acting in nearly identical intracellular signaling pathways with a conserved function in phosphorylating ankyrin-repeat containing IκB protein modules. In this study, we sought out to investigate the structural features of the *Drosophila melanogaster* IKK complex by an *in silico* comparison of primary amino acid sequences with human and other metazoan taxa. With our bioinformatics approach, we aim to identify regulatory features that are conserved as well as unique to this enzyme to better understand its mechanism of regulation and biochemical functions as a key regulatory component of the IMD innate immune pathway.

B. Results

1. Identification of conserved structural features in DmIKK subunits by sequence comparison with human IKK

To investigate the structure and function of the DmIKK complex, we first examined the amino acid sequence of the individual subunits by comparison with sequences of human (Hs)

IKK orthologs. Structures of IKKα and IKKβ have been solved, while only portions of NEMO/IKKγ structures have been determined. DmIKKβ is a polypeptide of 751 amino acids in length, while DmIKKγ is a polypeptide of 387 amino acids (Figure 3.1, Figure 3.2, Figure 3.3). The mammalian catalytic subunits, IKKα and IKKβ, are organized into four ordered protein domains: an N-terminal kinase domain (KD) followed by a ubiquitin-like domain (ULD), scaffold dimerization domain (SDD), and NEMO binding domain (NBD). CD spectroscopy of mammalian NEMO/IKKγ revealed that it is primarily alpha helical in secondary structure (Catici et. al 2015). Mammalian NEMO/IKKγ is divided into seven segments: the amino-terminal segment (N), an IKK binding domain (KBD), an intervening domain (IVD), coiled-coil region 1 (CC1), coiled-coil region 2 (CC2), and a C-terminal CCHC-type zinc finger (ZF) Sequence comparison reveals that the catalytic and non-catalytic DmIKK subunits contain structural features that are similar with that of its mammalian counterparts (Figure 3.1, Figure 3.2, Figure 3.3).

Local sequence alignment of the β subunits revealed that there is a region of significant homology at the N-terminus spanning the kinase domain and part of the ULD (residues 36-392 in DmIKKβ and residues 10-350 in HsIKKβ) with 35% amino acid identity and 64% amino acid similarity (Figure 3.1A, Figure 3.2). However, throughout the length of the two polypeptides, the similarity weakens with global sequence identity at 27% and global similarity at 42% (Table 3.2). Within the individual domains of the β subunit, the similarity varies (Figure 3.1A). The kinase domains are homologous with 34% identity and 50% similarity (Figure 3.1A). It is notable to mention that in the kinase domain of mammalian catalytic subunits IKKα and IKKβ have a "DLG" motif in the magnesium binding loop instead of "DFG" that is present in most protein kinases such as PKA and CDKs (Figure 3.2). This motif is a critical regulatory sequence for protein kinases as the phenylalanine can pack into a hydrophobic pocket between a residue in the N-lobe and another in the C-lobe forming a "hydrophobic spine" that is a characteristic of active protein kinases important for a conformation conducive toward catalysis. In DmIKKβ the magnesium binding loop reverts to a typical "DFG" motif, suggesting that there might be

differences in enzyme regulation and catalysis. In addition, there is a stretch of N-terminal residues in DmIKKβ (amino acids 1-26) that does not align with the human catalytic subunits, suggesting another unique structural feature present in DmIKKβ. Moreover, there is weak-to-moderate similarity in the region spanning the scaffold-dimerization domain (SDD) with 25% identity and 41% similarity (Figure 3.1A).

Another domain present in IKKα and IKKβ is a ubiquitin-like domain (ULD) with distant homology to ubiquitin, but with strong resemblance to ubiquitin in 3D structure (Polley et. al 2013, Polley et. al 2016). The putative ULD of DmIKKβ has weak-to-moderate similarity with the ULD of HsIKKβ at 25% identity and 37% similarity (Figure 3.1A). Comparison of the ULDs with human ubiquitin primary sequences reveals that the HsIKKβ ULD exhibits 34% identity and 48% similarity, while the putative ULD in DmIKKβ has a weaker similarity to ubiquitin with 24% identity and 37% similarity. It remains to be seen whether the putative ULD in DmIKKβ adopts this fold.

At the C-terminus of mammalian IKKα and IKKβ, there is a high-affinity binding interface at the NEMO binding domain (NBD) (residues 701-745) and the N-terminus of NEMO known as the IKK binding domain (KBD) (residues 49-110) (May et. al 2002, Drew et. al 2007, Rushe et. al 2008). Sequence alignment of DmIKKβ with human IKKβ and IKKα show that the NBD is absent in DmIKKβ (Figure 3.2). Comparison of DmIKKγ and HsNEMO sequences reveal conservation of some residues throughout the length of the KBD with 24% identity and 42% similarity (Figure 3.3). The lack of an NBD in DmIKKβ and the moderate level of similarity in the region corresponding to the KBD in DmIKKγ suggests a different mode of binding between the two subunits than in mammalian NEMO.

On the other hand, like mammalian NEMO, analysis of the amino acid sequence of DmIKKγ predicted a primarily alpha-helical secondary structure comprised of coiled coil domains (Figure 3.3, Silverman et. al 2000, Rutschmann et. al 2000). Local sequence alignment of the IKKγ subunits indicated that the most similar region is within the predicted alpha-helical

region comprised of a portion of the IVD to the end of the sequence (residues 142-387 in DmIKKγ and residues 178-419 in HsNEMO) with 26% identity and 55% similarity (Figure 3.1B). Globally, the IKKγ subunits are weakly similar with 21% identity and 38% similarity demonstrating that homology is limited to the C-terminus as has been previously reported (Rutschmann et al., 2000; Silverman et al., 2000)(Table 3.2, Figure 3.3).

An LC3-interacting region (LIR) motif has been identified at the N-terminus of DmIKKγ spanning residues 5-10 (Tusco et. al 2017). The LIR motif in DmIKKγ was shown to mediate an interaction with Atg8a for the autophagic degradation of the DmIKK complex (Tusco et. al 2017). An LIR motif has not been identified in mammalian NEMO and it does not directly interact with any of the mammalian Atg8 family proteins (Tusco et. al 2017). Thus, this the LIR motif appears to be a unique regulatory region in the fruit fly IKK system which functions in the recruitment of autophagy machinery.

The remaining regions of the N-terminus are weakly similar. The N-terminal region exhibits weak similarity with 24% identity and 34% similarity (Figure 3.1B). The IVD, which is well-conserved within vertebrate IKKγ/NEMO proteins, is moderately similar at 28% identity and 39% similarity (Figure 3.1B). The two coil-coiled regions called CC1 and CC2 in mammalian NEMO exhibit some similarity in DmIKKγ: CC1 has 31% identity and 41% similarity, while the second coil-coiled region has 35% identity and 47% similarity (Figure 3.1B). Structural and biochemical studies of the mammalian CC2 show that it is a key regulatory region and that binding of poly-ubiquitin chains to the CC2 is a critical step in activation of the IKK complex (Fujita et al., 2014; Kensche et al., 2012; Rahighi et al., 2009; Tokunaga et al., 2009). Given that the C-terminus, especially the CC2, exhibits the most homology in the protein sequence, it may play similar regulatory role in DmIKKγ as a ubiquitin-binding region.

At the C-terminus, there is a proline-rich region that is weakly similar at 26% identity and 36% similarity (Figure 3.1B). This is accompanied by a lower percentage of proline residues (8%) in DmIKKγ compared to HsNEMO (21%) in this region (Figure 3.1B) A C-terminal zinc

finger was also identified in DmIKKγ by Rutschmann et al 2000 and with our sequence analysis we find that this region exhibits moderate similarity with 26% identity and 43% similarity (Figure 3.1B) (Rustchmann et. al 2000).

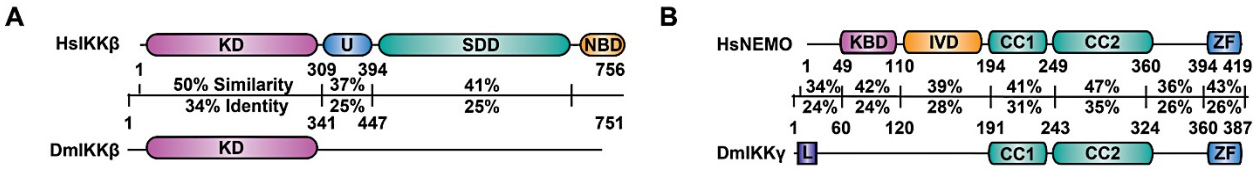

Figure 3.1: Structural features and homologous regions of human (Hs) and *D. melanogaster* IKK subunits. A) Domain architecture and regions of significant homology in IKKβ subunits. B) Domain architecture and regions of significant homology in IKKγ subunits.

Figure 3.2: MUSCLE sequence alignment of *D. melanogaster* and human IKK catalytic subunits (IKKβ and IKKα). Identical residues are boxed in black and homologous substitutions are light grey. Boxes and labels correspond to functional/structural classifications of elements within the human subunits.

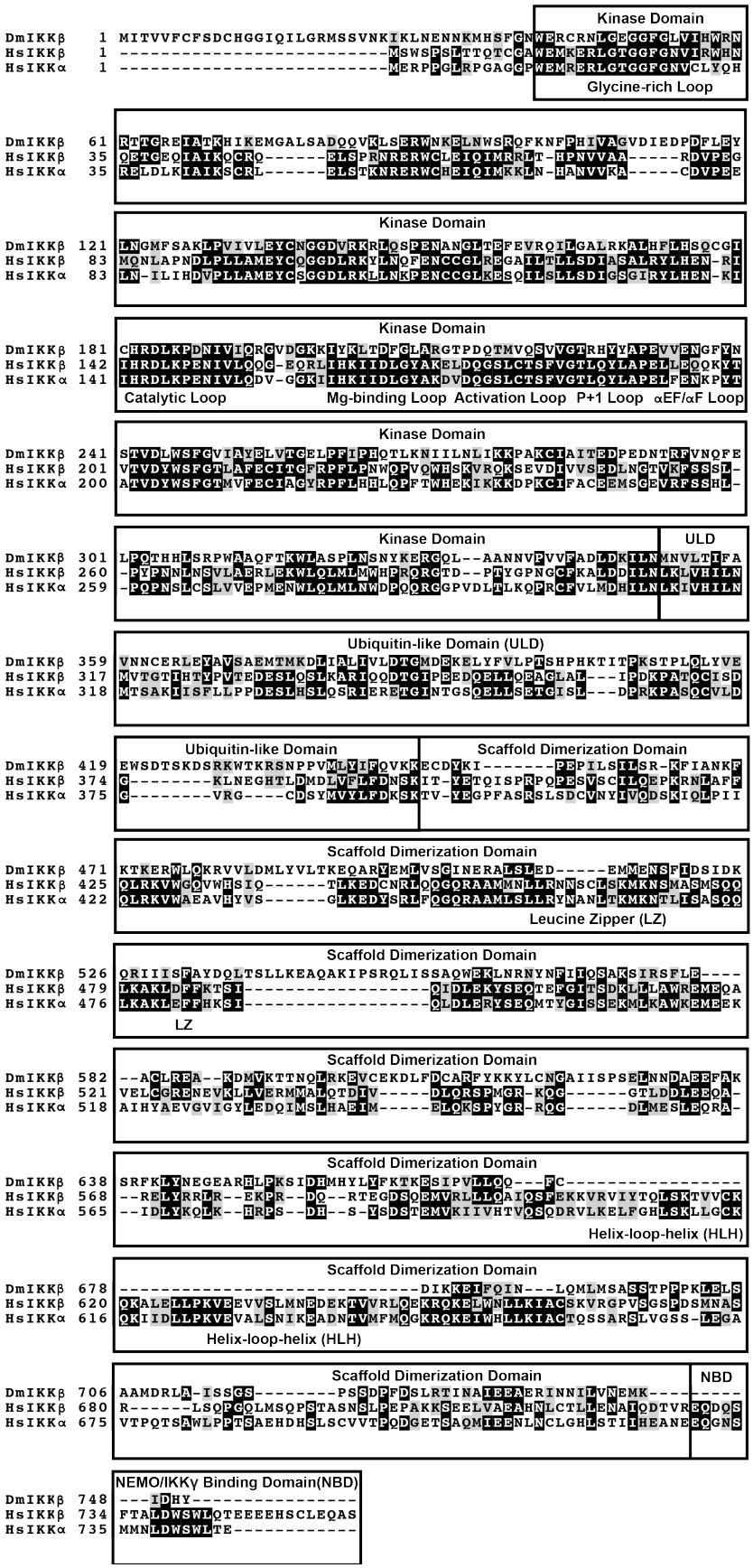
Kinase Domain
Glycine-rich Loop
Kinase Domain
Kinase Domain
Catalytic Loop
Mg-binding Loop
Activation Loop
P+1 Loop
αEF/αF Loop
Kinase Domain
Kinase Domain
ULD
Ubiquitin-like Domain (ULD)
Ubiquitin-like Domain
Scaffold Dimerization Domain
Scaffold Dimerization Domain
Leucine Zipper (LZ)
Scaffold Dimerization Domain
LZ
Scaffold Dimerization Domain
Scaffold Dimerization Domain
Helix-loop-helix (HLH)
Scaffold Dimerization Domain
Helix-loop-helix (HLH)
Scaffold Dimerization Domain
NBD
NEMO/IKKγ Binding Domain(NBD)

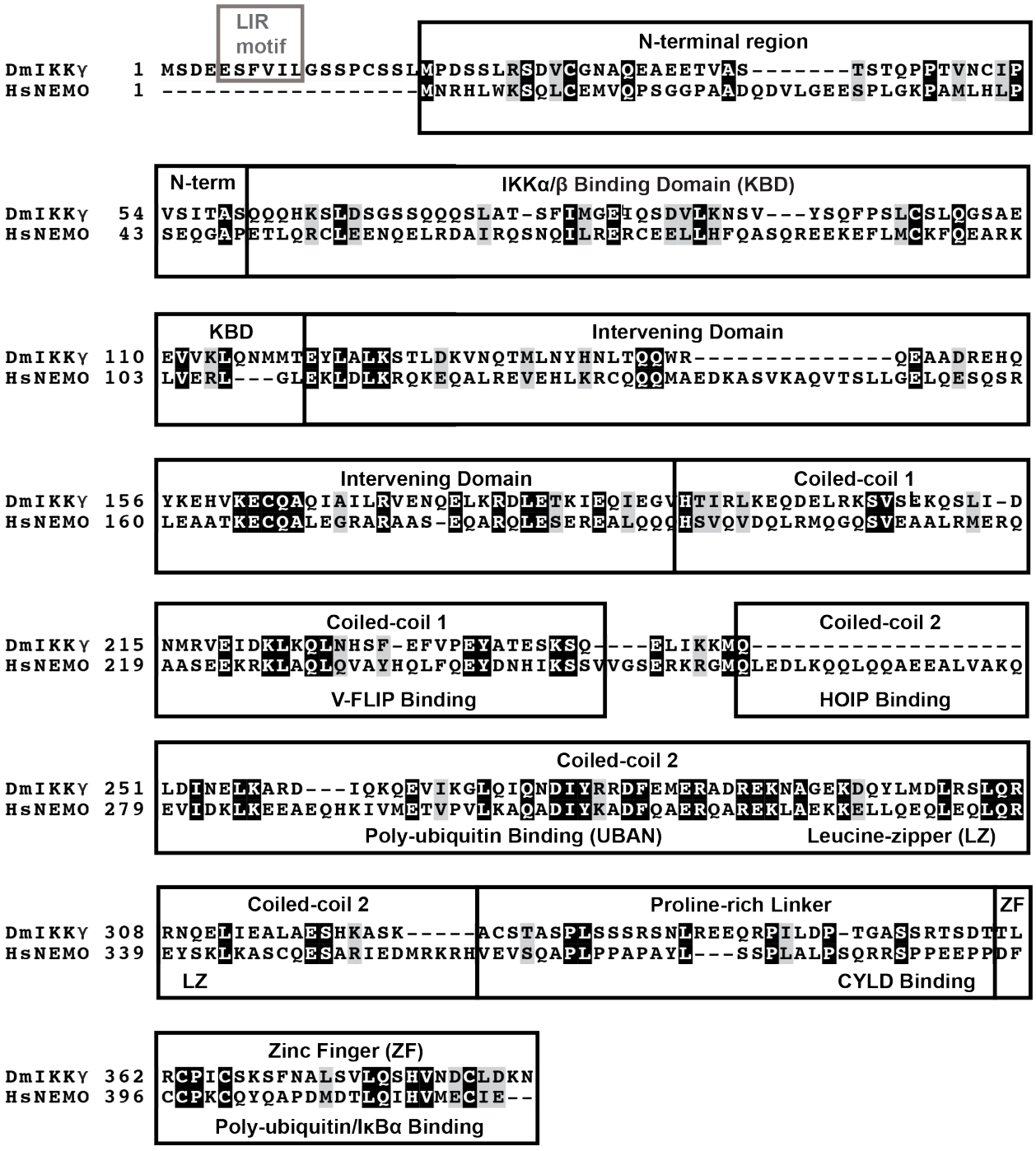

Figure 3.3: MUSCLE sequence alignment of *D. melanogaster* and human IKKγ/NEMO. Identical residues are boxed in black and homologous substitutions are light grey. Boxes and labels correspond to functional/structural classifications of elements within the human subunit.

2. Phylogenetic analysis reveals *Drosophila* IKK evolutionary divergence in the metazoan lineage

Since our comparison of fruit fly and mammalian IKK showed global primary sequence divergence in both subunits but some conserved regions such as the kinase domain in the catalytic IKKβ subunit and the CC2 domain in the IKKγ subunit, we wanted to examine these putative regulatory regions in the context of other metazoan taxa and examine the evolutionary structural divergence of DmIKK. We performed phylogenetic analyses of eight IKKβ and six IKKγ orthologs (accession numbers are listed in Table 3.1). For evolutionary and phylogenetic analyses, we first performed a multiple sequence alignment (MSA) using the MUSCLE algorithm (Figure 3.4, Figure 3.5). Using the multiple sequence alignments, we conducted pair-wise sequence identity and similarity comparisons using the Sequence Identity And Similarity (SIAS) server. Evolutionary analyses calculating interspecific pair-wise p-distances and number of amino acid differences were performed by the Molecular Evolutionary Genetics Analysis X (MEGA X) software package.

The phylogenetic reconstruction of the IKKβ orthologs revealed two distinct clades, one clade containing solely DmIKKβ and the other containing the vertebrates grouped together with two cnidarian species: *N. vectensis* and *P. damicornis* (Figure 3.6A). This result is surprising given that the cnidarian lineage diverged approximately 824 million years ago (mya) before the origin of *Drosophila* (~796 mya) (Figure 3.6C). Pair-wise sequence comparison of DmIKKβ reveals a range of only 24%-27% identity and 41%-43% similarity with other metazoan orthologs (Figure 3.6A). Following the trend observed in the phylogenetic reconstruction, IKKβ orthologs from the cnidarians (*P. damicornis* and *N. vectensis*) exhibited higher similarity and identity percentages when compared to vertebrate IKKβ orthologs with ~43-44% identity and 59-61% similarity to human IKKβ (Table 3.2). Furthermore, pair-wise analysis of DmIKKβ evolutionary distance estimations (p-distance) measuring the proportion of the number of amino acid differences (*n*) over the number of sites compared ranged from 0.75-0.77 with the number

of amino acid differences ranging from 492-501 (Table 3.3). However, the cnidarian species had lower p-distance values when compared to human IKKβ with values of 0.62 for *P. damicornis* and 0.6 for *N. vectensis* (Table 3.3). This trend is accompanied by a lower *n* value when compared to human IKKβ with *n*=406 for *P. damicornis* and *n*=398 for *N. vectensis* (Table 3.3). Thus the IKKβ orthologs from basal metazoans exhibit more structural similarity to vertebrate IKKβ than does DmIKKβ. Taken together, phylogenetic reconstruction, evolutionary analysis, and time tree analysis suggesst that the *Drosophila* catalytic IKKβ subunit has diverged from other metazoan IKKβ proteins by evolving novel structural features.

Phylogenetic analysis of IKKγ follows a similar trend as that observed in IKKβ of *Drosophila* evolutionary sequence divergence. However, IKKγ orthologs in "basal" metazoans outside of the bilaterian clade have not yet been identified. The first known appearance of a IKKγ-like protein is in *Drosophila* with homologs identified throughout the arthropod lineage (Gillmore and Wolenski 2012, Palmer and Jiggins 2015). The results show an evolutionary partitioning in which DmIKKγ is the sole member of one clade while the other clade comprises the vertebrate IKKγ orthologs (Figure 3.6B). In the MSA, we observe long stretches of insertions within the IVD in *T. guttata*, *X. laevis*, and *D. rerio* that are not similar in sequence (Figure 3.5). Nevertheless, other regions exhibited significant similarity especially within the CC1, CC2, and the zinc finger (Figure 3.5). Pair-wise comparison of the DmIKKγ amino acid sequence with metazoan orthologs shows a range of 21%-25% identity and range of 35%-38% similarity which are lower values than pair-wise % similarity and % identity comparisons amongst the vertebrate IKKγ orthologs (Table 3.4). Pair-wise DmIKKγ evolutionary distance estimations (p-distance) ranges from 0.77-0.80, which are much higher distance values than observed with pair-wise comparisons amongst the vertebrates as the next largest p-distance value is between *X. laevis* and *D. rerio* at a value of 0.49 (Table 3.5). In addition, comparison of the number of amino acid differences (*n*) with DmIKKγ and the other orthologs ranged from 236-245, which are larger values than pair-wise comparisons amongst the vertebrates as the next largest value is

between *X. laevis* and *D. rerio* at a value of *n*=151 (Table 3.5). Thus, DmIKKγ exhibits structural divergence from the metazoan taxa described in this study, suggesting that like DmIKKβ, fruit flies have adapted new functions within their IKKγ subunit.

Table 3.1: List of reference sequences and lengths of proteins used in this study	
Reference sequence ID:	**Length (residues):**
UniProtKB ID: Q9VEZ5 (IKKβ *D. melanogaster*)	751
UniProtKB ID: O14920 (IKKβ *H. sapiens*)	756
UniProtKB ID: O15111 (IKKα *H. sapiens*)	745
UniProtKB ID: O88351 (IKKβ *M. musculus*)	757
UniProtKB ID: Q6INT1 (IKKβ *X. laevis*)	742
UniProtKB ID: B0R199 (IKKβ *D. rerio*)	779
UniProtKB ID: H0Z516 (IKKβ *T. guttata*)	757
UniProtKB ID: A0A1D5PFV1 (IKKβ *G. gallus*)	753
UniProtKB ID: A0A3M6V6P6 (IKKβ *P. damicornis*)	732
NCBI Reference Sequence: XP_032238097.1 (IKKβ *N. vectensis*)	718
UniprotKB ID: Q9Y6K9 (NEMO *H. sapiens*)	419
UniprotKB ID: O88522 (NEMO *M. musculus*)	412
UniprotKB ID: Q9GYV5 (IKKγ *D. melanogaster*)	387
UniprotKB ID: Q58EN3 (NEMO *D. rerio*)	586
UniprotKB ID: Q58EW6 (NEMO *X. laevis*)	495
NCBI Reference Sequence: XP_032601643.1 (NEMO *T. guttata*)	537

Figure 3.4: IKKβ MUSCLE sequence alignment of eight orthologs. Color indicates consensus with black text having no consensus, red text as highly conserved, and white text with red background as strictly conserved. Amino acid numbering is by human IKKβ sequence. The MSA is depicted using ESPript 3.0 (https://espript.ibcp.fr/ESPript/ESPript/).

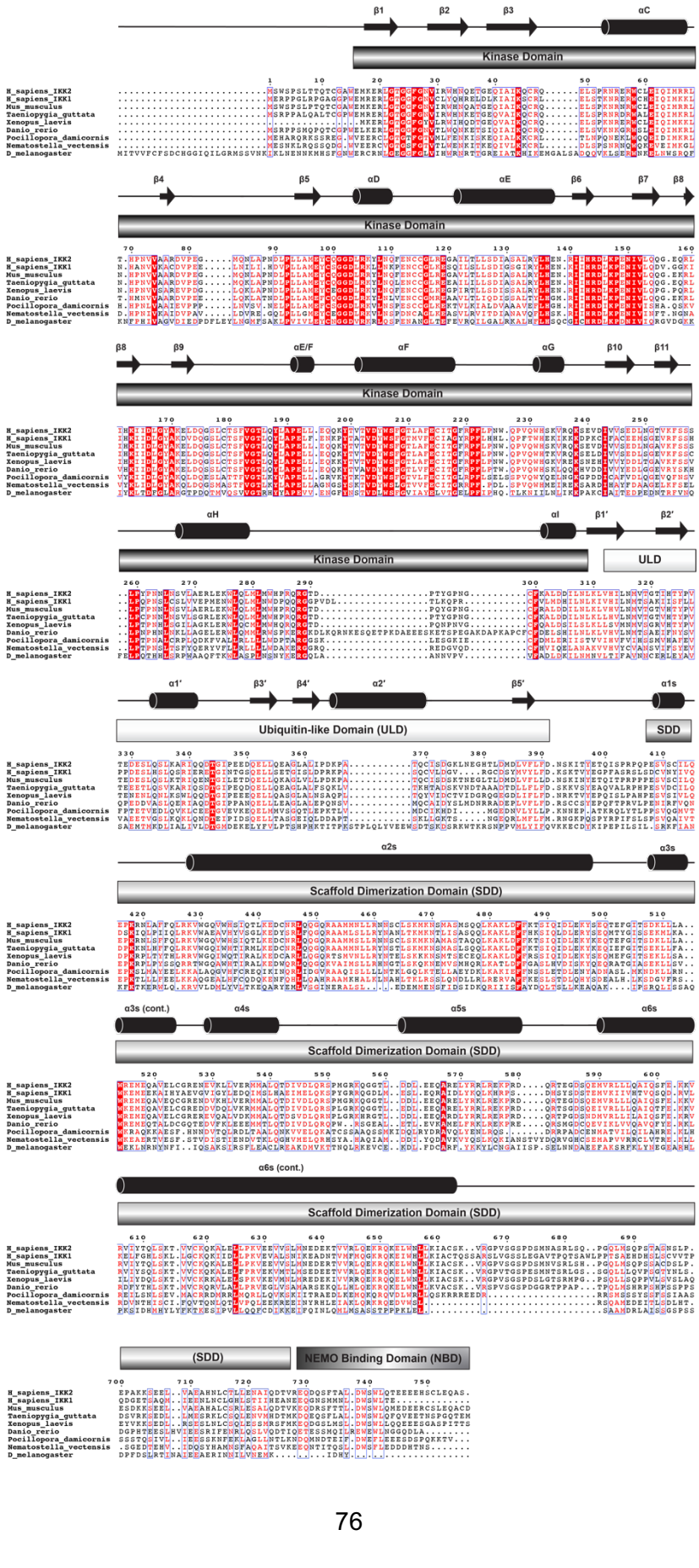
β1
β2
β3
αC
Kinase Domain
β4
β5
αD
αE
β6
β7
β8
Kinase Domain
β8
β9
αE/F
αF
αG
β10
β11
Kinase Domain
αH
αI
β1′
β2′
Kinase Domain
ULD
α1′
β3′
β4′
α2′
β5′
α1s
Ubiquitin-like Domain (ULD)
SDD
α2s
α3s
Scaffold Dimerization Domain (SDD)
α3s (cont.)
α4s
α5s
α6s
Scaffold Dimerization Domain (SDD)
α6s (cont.)
Scaffold Dimerization Domain (SDD)
(SDD)
NEMO Binding Domain (NBD)
H_sapiens_IKK2
H_sapiens_IKK1
Mus_musculus
Taeniopygia_guttata
Xenopus_laevis
Danio_rerio
Pocillopora_damicornis
Nematostella_vectensis
D_melanogaster

Figure 3.5: IKKγ MUSCLE sequence alignment of six orthologs. Color indicates consensus with black text having no consensus, red text as highly conserved, and white text with red background as strictly conserved. Amino acid numbering is by human NEMO sequence. Jpred 4 was used to depict secondary structure elements of human NEMO and DmIKKγ. The MSA is depicted using ESPript 3.0 (https://espript.ibcp.fr/ESPript/ESPript/)

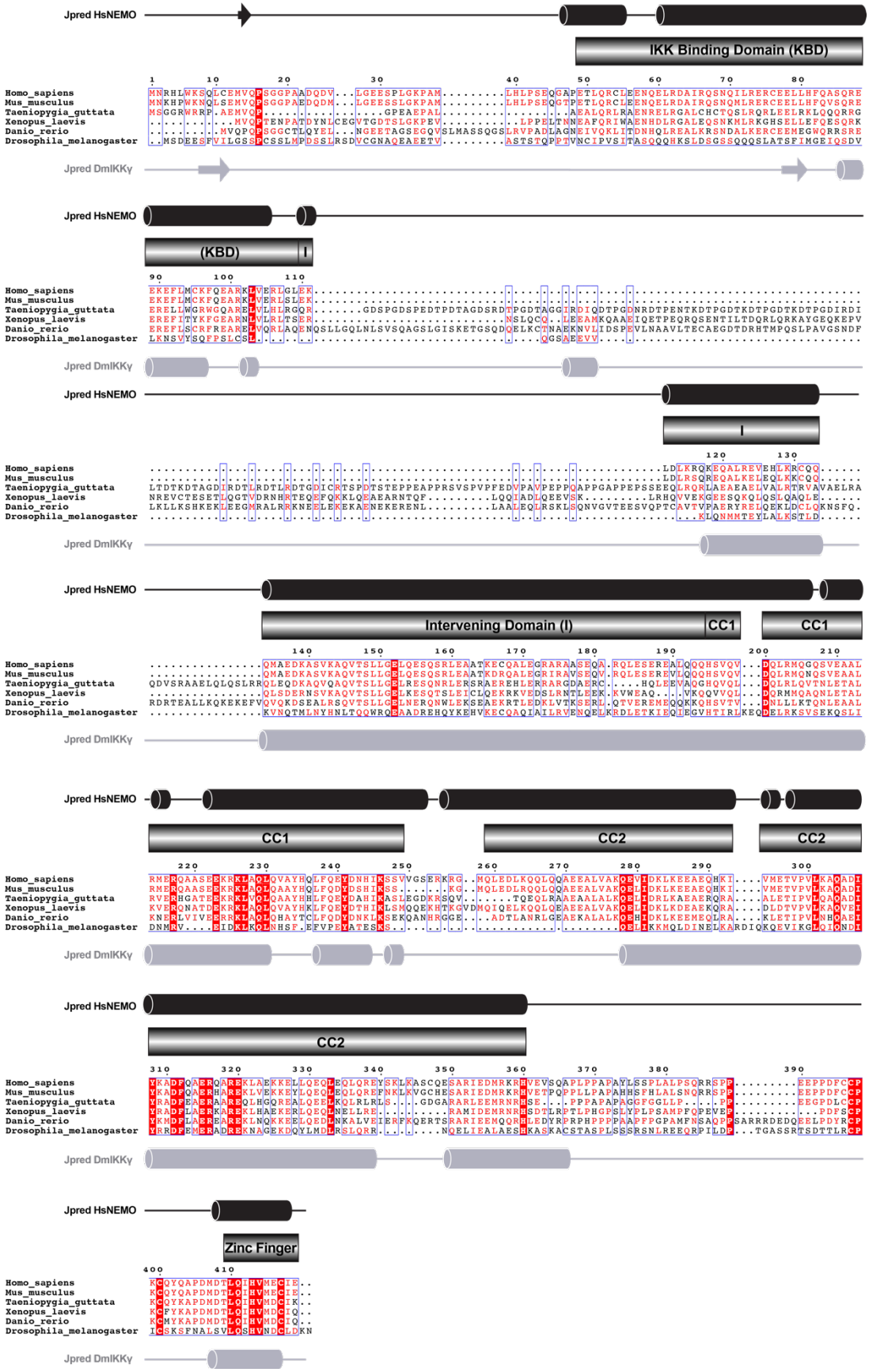
Jpred HsNEMO
IKK Binding Domain (KBD)
Homo_sapiens
Mus_musculus
Taeniopygia_guttata
Xenopus_laevis
Danio_rerio
Drosophila_melanogaster
Jpred DmIKKγ
(KBD)
I
Intervening Domain (I)
CC1
CC2
Zinc Finger

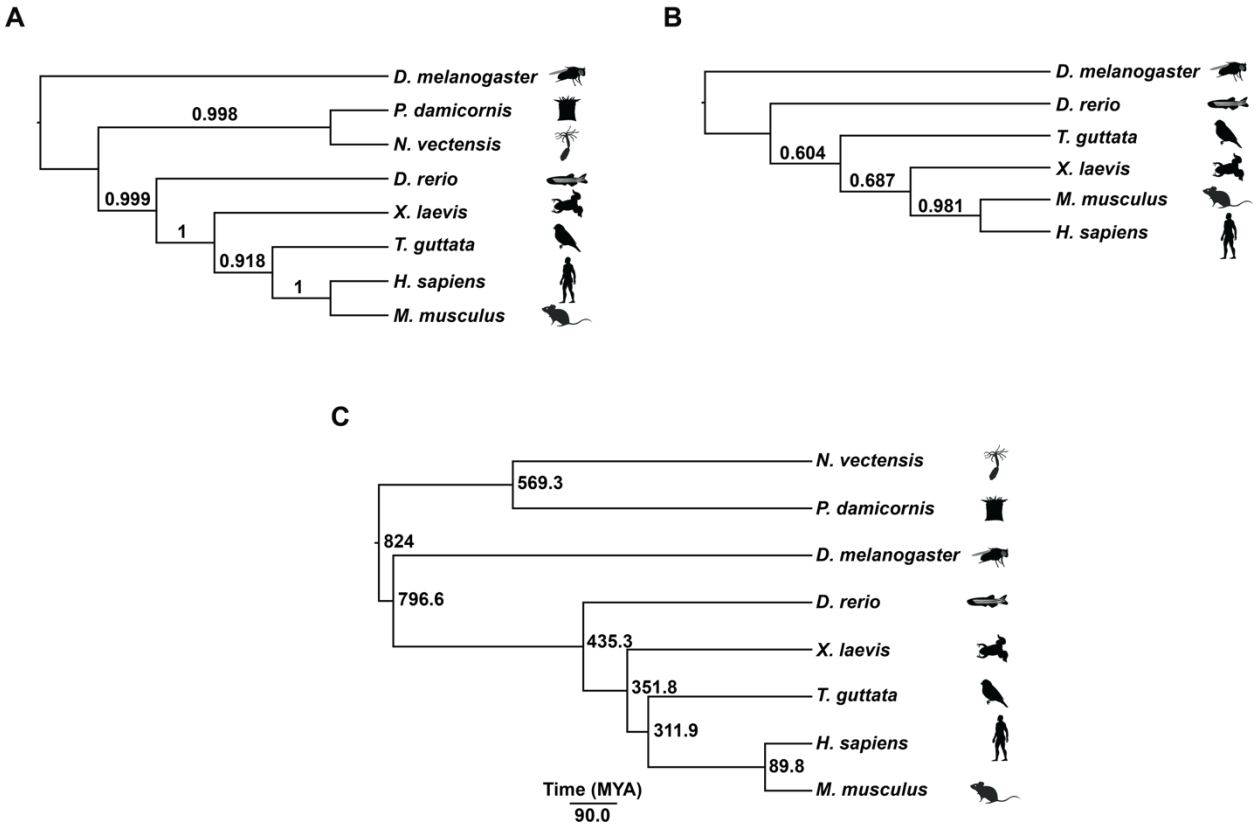

Figure 3.6: Evolutionary analysis of IKK orthologs reveals sequence divergence of *Drosophila* IKK in the metazoan lineage. A) Phylogenetic tree of IKKβ orthologs using sequences indicated and performed using maximum likelihood (ML) analysis with 1000 bootstrap replicates. Nodes indicate bootstrap support. B) Phylogenetic tree of IKKγ orthologs using sequences indicated and performed using ML analysis with 1000 bootstrap replicates. Nodes indicate bootstrap support C) Phylogenetic tree showing lineage diversification calculated using the TimeTree database (Hedges et al., 2006; Kumar et al., 2017, 2011; Roy et al., 2013). Nodes indicate divergence time in million years ago (MYA) Silhouette images were obtained from PhyloPic (http://phylopic.org).

Table 3.2: Comparison of sequence identity and similarity percentages among 8 metazoan IKKβ orthologs. A multiple-sequence alignment (MSA) was performed by MUSCLE. The MSA was input into the SIAS server (http://imed.med.ucm.es/Tools/sias.html) to calculate pairwise sequence identities (light gray box) and similarities (dark grey box). Dm and HsIKKβ identity and similarity percentage values are in bold.

Table 3.2: Interspecific pairwise identity and similarity of IKKβ primary sequences								
Species	***1.***	***2.***	***3.***	***4.***	***5.***	***6.***	***7.***	***8.***
1. *D. melanogaster*		26.25%	25.09%	26.25%	**27.22%**	26.64%	24.51%	25.86%
2. D. rerio	42.08%		61.38%	66.98%	68.72%	68.14%	43.24%	42.85%
3. X. laevis	42.27%	74.71%		77.02%	78.95%	77.02%	43.24%	41.31%
4. T. guttata	42.66%	80.11%	85.71%		89.76%	88.03%	44.78%	44.0%
5. H. sapiens	**42.08%**	80.30%	87.45%	94.78%		94.59%	43.43%	44.98%
6. M. musculus	42.08%	79.72%	85.71%	93.62%	97.49%		44.20%	44.59%
7. P. damicornis	41.11%	58.88%	58.49%	59.84%	59.84%	59.84%		50.96%
8. N. vectensis	42.85%	58.88%	59.07%	60.42%	61.38%	60.61%	67.56%	

Table 3.3: Pairwise estimates of evolutionary divergence of IKKβ orthologs.
The number of amino acid differences between the two sequences compared are shown (unshaded boxes) and the p-distance or the proportion of amino acid differences per site is shown (in shaded boxes). This analysis involved 8 amino acid sequences. All positions containing gaps and missing data were eliminated (complete deletion option). There were a total of 651 positions in the final dataset. Evolutionary analyses were conducted in MEGA X.

Table 3.3: Interspecific pairwise distances of IKKβ primary sequences								
Species	***1.***	***2.***	***3.***	***4.***	***5.***	***6.***	***7.***	***8.***
1. *D. melanogaster*	-	495	500	496	492	496	504	503
2. *D. rerio*	0.7569	-	289	253	243	246	400	408
3. *X. laevis*	0.7645	0.4419	-	176	168	180	409	419
4. *T. guttata*	0.7584	0.3869	0.2691	-	106	118	403	405
5. *H. sapiens*	0.7523	0.3716	0.2569	0.1621	-	48	406	398
6. *M. musculus*	0.7584	0.3761	0.2752	0.1804	0.0734	-	399	400
7. *P. damicornis*	0.7706	0.6116	0.6254	0.6162	0.6208	0.6101		357
8. *N. vectensis*	0.7691	0.6239	0.6407	0.6193	0.6086	0.6116	0.5459	-

Table 3.4: Comparison of sequence identity and similarity percentages among 6 metazoan IKKγ orthologs.
A multiple-sequence alignment (MSA) was performed by MUSCLE. The MSA was input into the SIAS server (http://imed.med.ucm.es/Tools/sias.html) to calculate pairwise sequence identities (light gray box) and similarities (dark grey box). DmIKKγ and HsNEMO identity and similarity percentage values are in bold.

Table 3.4: Interspecific pairwise identity and similarity of IKKγ primary sequences						
Species	***1.***	***2.***	***3.***	***4.***	***5.***	***6.***
1. *D. melanogaster*		25.21%	24.35%	21.79%	**23.93%**	22.64%
2. D. rerio	35.89%		57.26%	58.11%	59.40%	58.97%
3. X. laevis	38.46%	71.36%		62.82%	64.10%	64.10%
4. T. guttata	35.47%	71.36%	74.35%		64.52%	64.10%
5. H. sapiens	**35.47%**	73.93%	73.93%	75.64%		94.01%
6. M. musculus	35.89%	73.93%	74.78%	76.49%	95.29%	

Table 3.5: IKKγ pairwise estimates of evolutionary divergence.
The number of amino acid differences between the two sequences compared are shown (unshaded boxes) and the p-distance or the proportion of amino acid differences per site is shown (in shaded boxes). This analysis involved 6 amino acid sequences. All positions containing gaps and missing data were eliminated (complete deletion option). There were a total of 306 positions in the final dataset. Evolutionary analyses were conducted in MEGA X.

Table 3.5: Interspecific pairwise distances of IKKγ primary sequences						
Species	***1.***	***2.***	***3.***	***4.***	***5.***	***6.***
1. *D. melanogaster*		236	236	245	243	239
2. D. rerio	0.7712		151	141	136	135
3. X. laevis	0.7712	0.4935		149	148	147
4. T. guttata	0.8007	0.4608	0.4869		133	132
5. H. sapiens	0.7941	0.4444	0.4837	0.4346		27
6. M. musculus	0.7810	0.4412	0.4804	0.4314	0.0882	

3. ConSurf analysis reveals distinct regions of structural similarity and regions of divergence in DmIKK subunits

Our phylogenetic and evolutionary analyses revealed that the DmIKK subunits have diverged in the metazoan lineage, suggesting that DmIKK subunits have evolved unique structural features that may be involved in its regulation. To identify conserved regions that may be of functional relevance, we utilized the ConSurf server with our multiple sequence alignments used in the phylogenetic and evolutionary analyses to assign conservation scores at each position in the MSA (Ashkenazy et al., 2010, 2016; Berezin et al., 2004; Celniker et al., 2013; Glaser et al., 2003; Landau et al., 2005). One difference in the IKKβ ConSurf analysis was that the *Gallus gallus* (chicken) sequence (UniProtKB ID: A0A1D5PFV1) was used instead of *T. guttata* (zebra finch) to represent a bird taxa.

In general, high conservation scores were assigned to structural regions that were shown in the sequence alignments to have significant similarity percentages such as the IKKβ kinase domain and the CC2 in IKKγ (Figure 3.3, Figure 3.4, Figure 3.7, Figure 3.8, Figure 3.9). In our analysis of IKKβ, the conservation scores determined by ConSurf calculations were mapped onto the three-dimensional structure of human IKKβ (PDB 4e3c) (https://www.rcsb.org/). We observe that within the kinase domain, the activation segment (human IKKβ residues 166-194 and DmIKKβ residues 206-234) is highly conserved (Figure 3.7, Figure 3.8). There are some differences in the activation loop containing the signal-dependent phosphorylation sites (serines 177 and 181) within the signature phosphorylation motif of "SLCTS" (residues 171-181) in human IKKβ. For instance, in the cnidarians there is only one serine residue in the corresponding motif ("SLATT" in *P. damicornis* and "SMATT" in *N. vectensis*) (Figure 3.7, Figure 3.8). On the other hand, in fruit flies, the corresponding sequence is "TMVQS" (Figure 3.7, Figure 3.8). It would be of interest to see whether the threonine, serine, or both residues within the activation loop motif are phosphorylated as part of the DmIKK activation mechanism. At the extreme N-terminus, the 26 amino acid stretch in DmIKKβ is

unique among the metazoan taxa in this analysis, showing that this may be another evolved structural feature that would be of interest to functionally characterize (Figure, 3.4, Figure 3.7, Figure 3.8). Another unique feature of DmIKKβ is the lack of an NBD motif "LDWSWLQ" corresponding to human IKKβ residues 737-742 (Figure 3.4, Figure 3.7, Figure 3.8). Moreover, sequences at the extreme C-terminus flanking the NBD show lower conservation as a whole, though there are some residues that are highly conserved and are interspersed in this region. (Figure 3.7, Figure 3.8).

As observed in the IKKγ MSA, regions of significant structural similarity are CC1, CC2, and the zinc finger (Figure 3.5). The rest of the sequence alignment is variable and there are long stretches of non-conserved regions in the IVD of non-mammalian vertebrates (Figure 3.5). Since the human NEMO CC2 and the zinc finger domains have been shown to be critical in mammalian IKK activation by binding to ubiquitin, we sought to investigate the possible functional conservation of these domains through ConSurf analysis. High conservation scores are mapped to a region within the CC2 called the "CoZi" domain (human NEMO residues 257-346) using the x-ray crystal structure (PDB 3f89) (https://www.rcsb.org/) (Figure 3.9). Within the CoZi domain, polar residues D311, R316, R319, and E324 (human NEMO numbering) that mediate binding to linear di-ubiquitin are conserved in the orthologs, including DmIKKγ (Figure 3.9). High conservation scores are also observed in the zinc finger (human NEMO residues 394-419) mapped to a solution NMR structure (PDB 2jvx), especially with residues shown to be functionally important in ubiquitin binding and NF-κB signaling (M407, Q411, V415, and M415 human NEMO numbering), although the M415 position is N381 in DmIKKγ (Figure 3.9). Nonetheless, these results suggest a conserved binding interface for ubiquitin at both the zinc finger and the CoZi regions (Figure 3.9).

Figure 3.7: Color-coded MSA of IKKβ with ConSurf conservation scores on each amino acid site from turquoise indicating a variable site (1) to dark pink representing a conserved site (9). Domains are indicated according to the human sequence.

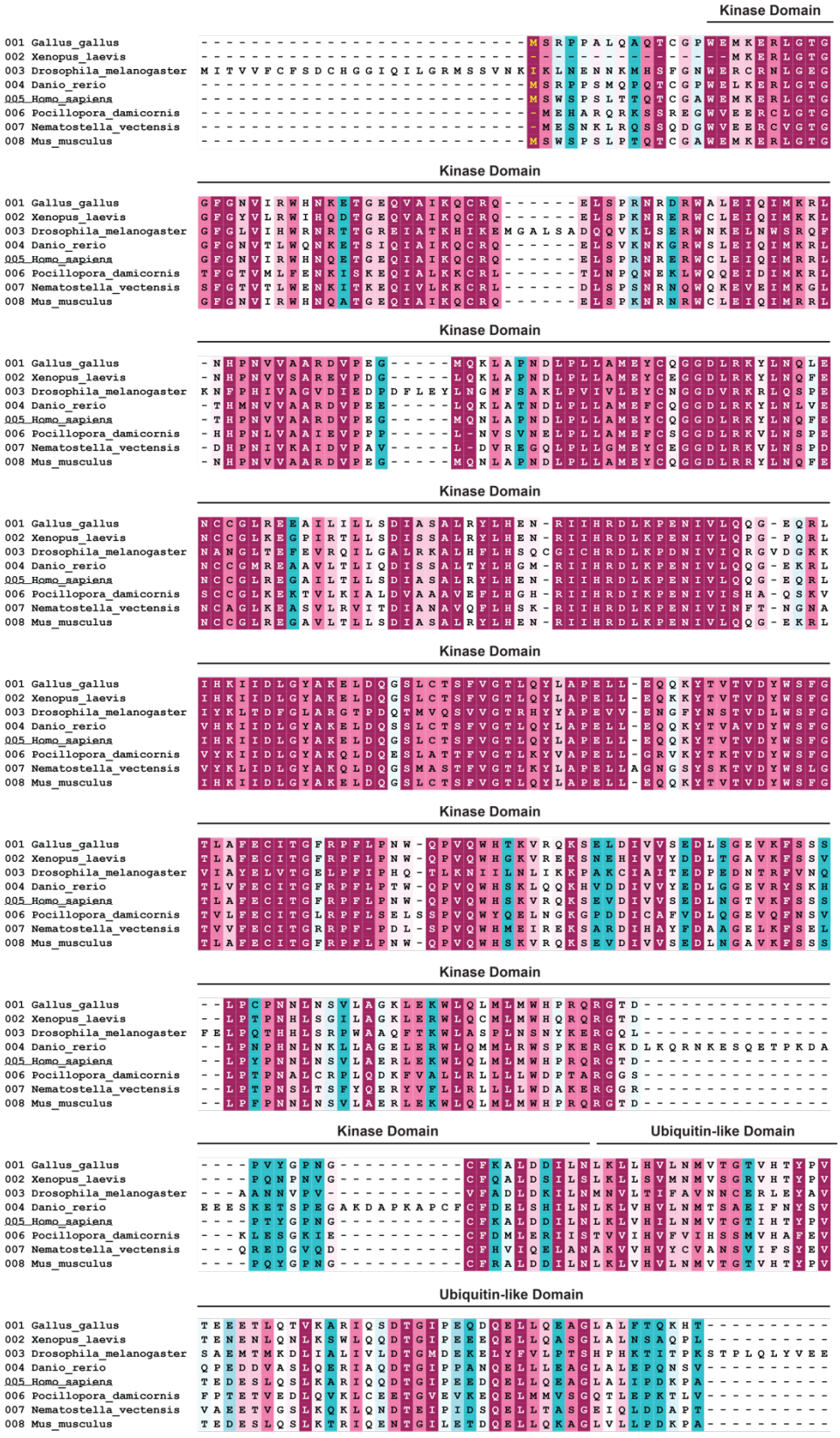
Kinase Domain
001 Gallus_gallus
002 Xenopus_laevis
003 Drosophila_melanogaster
004 Danio_rerio
005_Homo_sapiens
006 Pocillopora_damicornis
007 Nematostella_vectensis
008 Mus_musculus
Kinase Domain
Kinase Domain
Kinase Domain
Kinase Domain
Kinase Domain
Kinase Domain
Ubiquitin-like Domain
Ubiquitin-like Domain
1 2 3 4 5 6 7 8 9
Variable Average Conserved
X - Insufficient data - the calculation for this site was performed on less than 10% of the sequences.

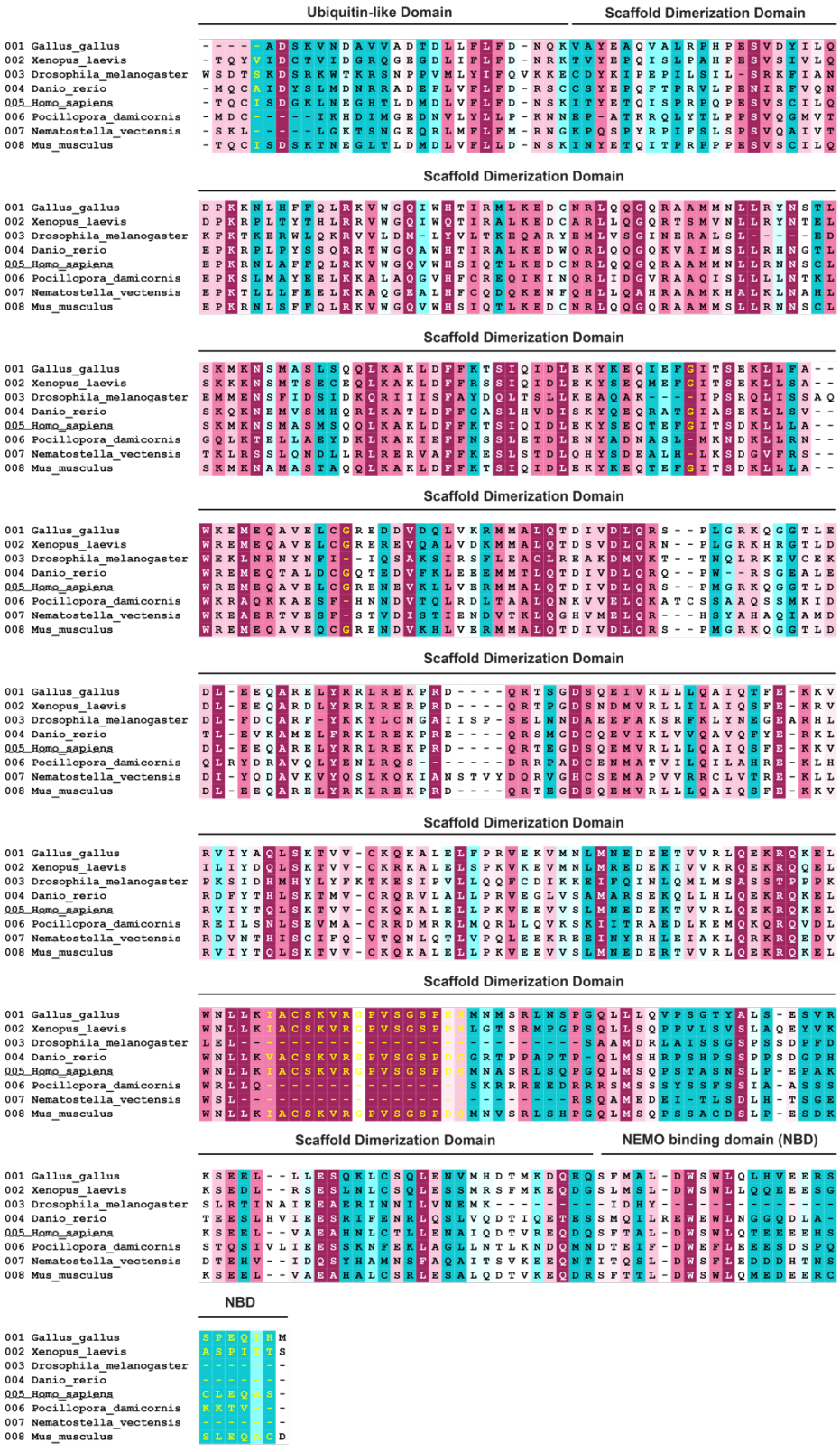

Figure 3.7: continued

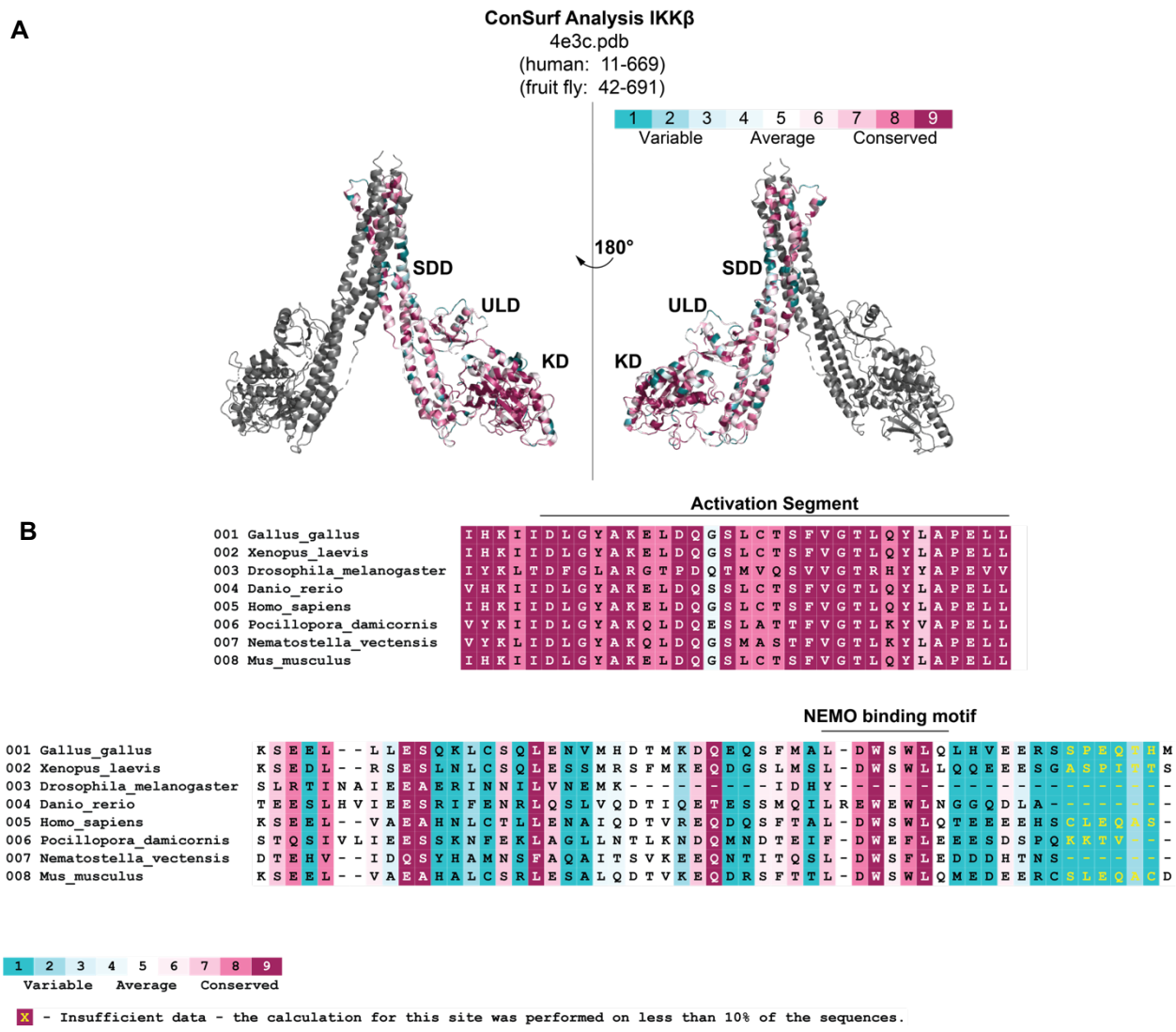

Figure 3.8: ConSurf analysis for IKKβ using same color and conservation scheme as in Figure 3.7. Amino acid sites in which there was insufficient data (calculation using less than 10% of sequences) are denoted in yellow lettering. A) The PDB 4e3c file from the Protein Databank (https://www.rcsb.org/) was used to structurally map conservation scores and is shown using the PyMol output file generated by the ConSurf server. Only one β subunit within the dimer is colored in the conservation scheme, and the partner β subunit is colored in grey. On the left is the amino acid conservation displayed on the surface of human IKKβ after rotation of 180 degrees about the y axis. B) The color-coded MSA with ConSurf conservation scores on each amino acid site for the activation segment and the C-terminal NEMO binding motif (NBD) reveals high conservation in the activation segment and absence of an NBD in *Drosophila.*

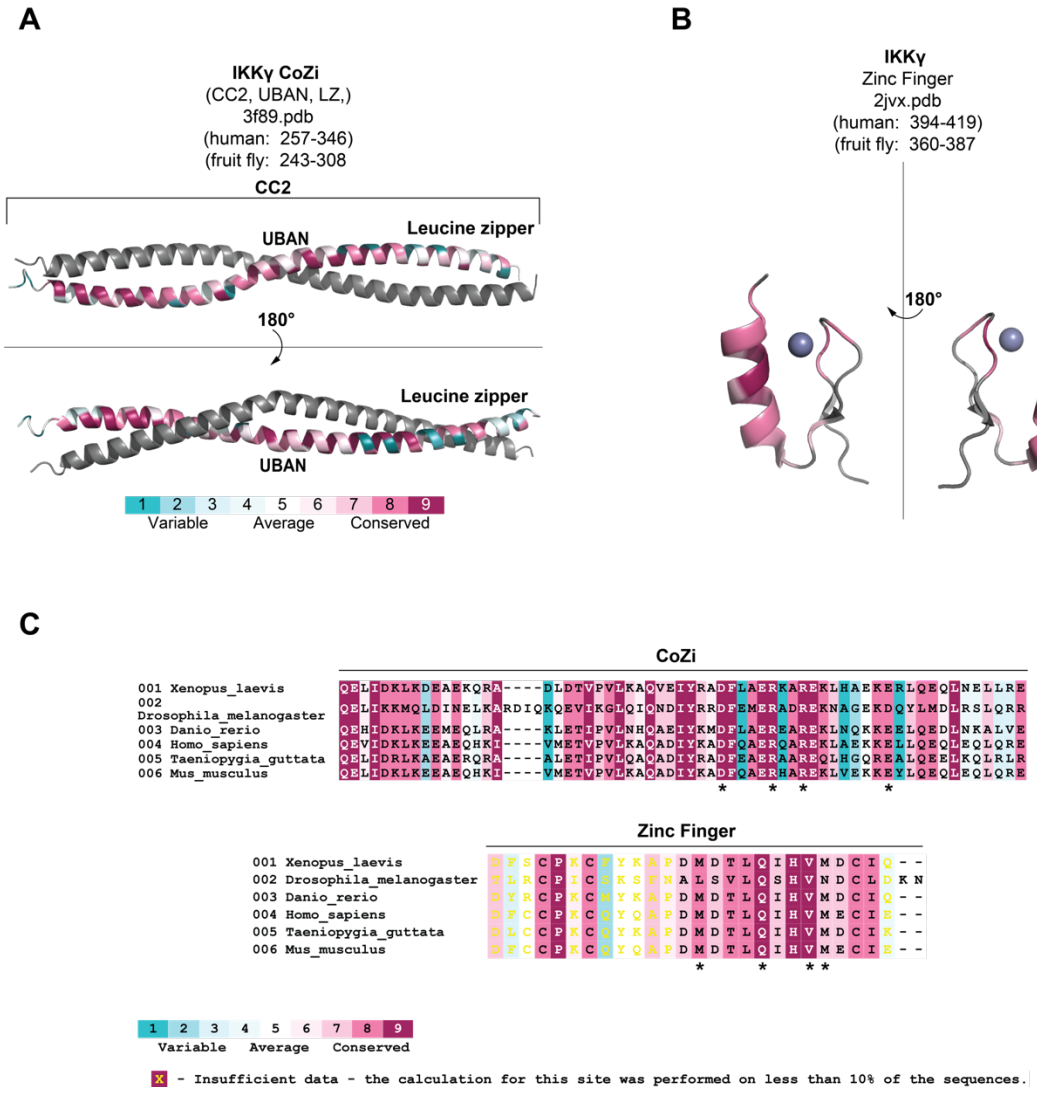

Figure 3.9: ConSurf analysis for IKKγ using the same color and conservation scheme as in Figure 3.7 and Figure 3.8. Amino acid sites in which there was insufficient data (calculation using less than 10% of sequences) are denoted in yellow lettering. A) The CoZi structural model (PDB 3f89) from the Protein Databank (https://www.rcsb.org/) was used to structurally map conservation scores and is shown using the PyMol output file generated by the ConSurf server. Only one γ subunit within the CoZi dimer is colored in the conservation scheme, and the partner γ subunit is colored in grey. On the bottom is the amino acid conservation displayed on the surface of the CoZi domain after rotation of 180 degrees about the x axis B) The zinc finger (PDB 2jvx) from the Protein Databank was used to structurally map conservation scores and is shown using the PyMol output file generated by the ConSurf server. On the left is the amino acid conservation displayed on the surface of zinc finger after rotation of 180 degrees about the y axis. C) Color-coded MSA with ConSurf conservation scores on each amino acid site for the CoZi region (top) and the zinc finger (bottom) showing high degree of conservation in these regions overall. Asterisks (*) denote residues shown to be important in mediating ubiquitin binding in mammalian NEMO.

C. Discussion

IKK is evolutionarily ancient, with orthologs of IKKβ catalytic subunits present in basal metazoans such as the cnidarians, which originated over 800 million years ago (Hedges et al., 2006; Kumar et al., 2017, 2011; Roy et al., 2013). However, the non-catalytic IKKγ subunit has not yet been found in the genomes of basal metazoans such as the cnidarians, but appears in the panarthropod lineage. This suggests that IKK regulation mechanisms involving the non-catalytic subunit first appear in the common ancestor to panarthropods which originated ~700 million years ago (Hedges et al., 2006; Kumar et al., 2017, 2011; Roy et al., 2013). Unless IKKγ orthologs from more basal metazoans are discovered, this remains a plausible hypothesis. Nonetheless, it is clear that the IKK-NF-κB signaling hub is a key component in innate immune responses throughout the metazoan phylogenetic spectrum. Each taxa has utilized this signaling hub under their own selective pressures to derive a functional IKK activity in the rapid response to microbial infection.

In this study, I show that both catalytic DmIKKβ and non-catalytic DmIKKγ subunits are divergent in the metazoan lineage in terms of primary amino acid sequences. I identified specific structural features that are shared and features that are unique to the multi-subunit, *Drosophila* IKK complex. When compared to the mammalian IKK orthologs, the regions that correspond to known structural domains are largely conserved in both subunits (Figure 3.8, Figure 3.9). An exception to this is the NEMO binding domain (NBD) at the C-terminus of mammalian catalytic IKK subunits as this sequence is completely absent in DmIKKβ. In mammals, the NBD mediates a high-affinity interaction surface (K_D of 3-25 nM) with the N-terminus of NEMO (May et al., 2002). The specific interaction surfaces that mediate DmIKK complex formation between the two subunits remains to be seen. Given the lack of homology in the C-terminus of the DmIKKβ, the mode of interaction is likely to be significantly different than that of the mammalian system. Moreover, it was shown that full-length human IKKβ elutes as a tetramer in SEC analysis, but a construct with the last 92 amino acids removed (1-664) ran as a dimer (Shaul et al., 2008). This

suggests that the sequence containing the human IKKβ NBD may be a structural feature that mediates oligomerization. This observation guided the structural determination of the human IKKβ and the construct that was crystallized (11-669) lacked the NBD and surrounding serine-rich cluster (Polley et al., 2013). Additionally, the serine-rich cluster was found to be hyperphosphorylated upon TNF stimulation, playing a role in negative regulation of IKK catalytic activity to prevent prolonged activation (Delhase et al., 1999). In contrast, full length DmIKKβ was used in this study and we observe a single species in our biophysical measurements suggesting that in DmIKKβ the lack of the IKKβ NBD and the serine rich environment surrounding this motif supports dimerization. There are some serine residues interspersed throughout the extreme C-terminus of DmIKKβ so we cannot rule out the possibility that these residues might be phosphorylated as part of a regulatory mechanism. In addition, the 26 amino acid region in DmIKKβ that is not present in the metazoan taxa analyzed in this study further suggests a novel structural feature that may somehow be involved in DmIKK regulation. Structural and biochemical characterization of this region may reveal its functional significance and add to our understanding of IKK regulation.

Sequence comparison of the non-catalytic IKKγ subunit reveals that the C-terminal half of the protein containing CC2 and the zinc finger is the most conserved region in all of the metazoan IKKγ orthologs in this study. MSA and ConSurf analysis demonstrated that within the N-terminal half of the protein, large stretches of insertions are present in the IVD of *T. guttata*, *D. rerio*, and *X. laevis* suggesting that there are particular sequences that have evolved in these taxa under specific selection pressures that may be useful for activity and/or regulation of these multi-subunit IKK complexes. Another point of divergence is in the presence of an LIR motif involved in autophagic degradation at the N-terminus of DmIKKγ (residues 5-10) which regulatory feature that is truly novel in this taxon. Moreover, I observed high conservation in two ubiquitin binding domains that are functionally significant in mammalian NEMO: the CoZi domain and the zinc finger domain. Given the conservation of many components in mammalian

and fruit fly IKK signaling, it would be of interest to characterize ubiquitin binding in DmIKKγ and whether it plays a role in regulation. As a whole, a biochemical and structural assessment of these unique and shared structural features may reveal functional significance and illuminate our understanding of DmIKK complex regulation within the immune response.

Chapter IV

In vitro characterization of a multi-subunit *Drosophila melanogaster* IκB Kinase complex

A. Introduction

Innate immunity evolved early in evolution as the “first line of defense” against microbial aggressors. This defense relies on genome-encoded pattern recognition receptors (PRRs) to recognize molecular components of pathogens (Janeway, 1989). In the signaling pathways that regulate innate immune defenses, there is remarkable similarity in the receptors and molecular signaling components from flies to humans (J. A. Hoffmann et al., 1999). The IKK-NF-κB signaling hub is a major component of the innate immune response throughout the animal kingdom acting in the control of immune response genes and its rapid induction upon infection (Chamy et al., 2010; Gilmore et al., 2012; Hayden et al., 2012; Michael Karin, 1999). Thus, basic mechanisms of pattern recognition and quick activation of the response is highly conserved in metazoans.

Insect innate immunity is a potent and multifaceted response against a broad spectrum of pathogens. For instance, *Drosophila* can withstand and clear large bacterial burdens that, relative to size, would otherwise be lethal to humans (Cantacuzène,1923; Hoffmann, Jules A et al., 1997). Within 3 hours of bacterial infection, protection is observed and a strong, heat-stable, and massive bacteriolytic activity is apparent in the hemolymph (Metalnikow 1927; Porchet 1928). This rapid bacteriolytic activity is from the action of secreted antimicrobial peptides (AMPs) in the systemic response with circulating concentrations as high as 300 μM in the fly hemolymph (J. L. Imler et al., 2000).

In *Drosophila*, the expression of antimicrobial peptide genes is controlled by members of the NF-κB transcription factor family via the Toll and Immune Deficiency (IMD) pathways. Flies that are deficient in Toll or IMD signaling are highly susceptible to infection and cannot produce any of the known AMPs (Lemaitre et al., 1996). The Toll pathway is initiated upon fungal infection and by bacteria with lysine-type peptidoglycan (PGN) controlling the expression of antifungal peptides *drosomcyin* and *metchnikowin*. On the other hand, the IMD pathway is known as the “antibacterial arm” of the *Drosophila* systemic innate immune response and is

activated by infection of bacteria with meso-diaminopimelic-type PGN controlling the expression of five classes of AMP genes including *diptericin*, *cecropin*, *defensin*, *drosocin*, and *attacin*. Thus, the IMD pathway is critical for the *Drosophila* immune response. A multi-subunit IKK complex is the principal regulator of NF-κB and is an integral component of AMP induction in the IMD pathway.

There has been extensive research into the identification of key signaling components within the Toll and IMD pathways, but the molecular details of regulation are still poorly understood. In the previous chapter, I showed that the DmIKK complex shares many structural features with mammalian IKK and other metazoan orthologs, but exhibits some unique structural elements that might play a role in its regulation and activation. In this chapter, as part of our effort to understand the biochemistry, substrate specificity, and activation mechanism of this unique small family of regulated signaling kinases, I report the *in vitro* characterization of a multi-subunit *Drosophila melanogaster* (Dm) IKK complex. I have undertaken recombinant expression, purification, and biophysical characterization of this enzyme complex.

B. Results

1. DmIKKβ:γ can be expressed and purified as a stable recombinant protein complex

In order to perform *in vitro* studies on the DmIKK complex, I have optimized large-scale recombinant expression and purification of His-DmIKKβ:γ-FLAG complex from Baculovirus-infected Sf9 insect cell suspension cultures (Figure 4.1, Figure 4.2). For co-expression, the DmIKKβ and DmIKKγ cDNA were sub-cloned into the pFastBac Dual plasmid. Specifically, DmIKKβ with an N-terminal hexa-histidine tag, is under the control of one of the two promoters, the polyhedrin promoter. In addition, we designed the construct to have DmIKKγ with a C-terminal FLAG tag under the control of the p10 promoter, the second promoter in the pFastBac Dual plasmid. The DmIKKγ cDNA was isolated from LPS-stimulated *Drosophila* S2 cells through RT-PCR. The individual subunits were also subcloned into pFastBacHT B expression plasmids with an N-terminal hexa-histidine tag (Figure. 4.5). Two pFastBacHT B constructs with DmIKKγ-

FLAG were created: one with an N-terminal hexa-histidine tag (His-DmIKKγ-FLAG) and another without (DmIKKγ-FLAG). These pFastBacHT B and pFastBac DUAL constructs were used to generate Baculovirus for the infection of 0.4-0.5L Sf9 insect cell suspension cultures. With these constructs in hand, we tested two different expression and purification methods to produce recombinant DmIKK complex: 1) co-expression with subsequent purification and 2) expression of individual subunits in separate suspension cultures followed by mixing of lysates which was then subjected to purification. In both methods, we use a two-step purification scheme starting with nickel affinity chromatography in batch binding mode and polishing of the sample by size-exclusion chromatography. Purification under our two-step scheme shows a pure, homogenous protein complex (Figure 4.1) Both subunits elute together as visualized by Coomassie-stained SDS-PAGE (Figure 4.1). Purification of the individual subunits via nickel affinity chromatography and SEC shows pure, homogenous proteins (Figure 4.2). Either co-expression or expression of subunits separately in insect cells followed by mixing of lysates individually expressing DmIKKβ and DmIKKγ yielded a stable complex of both subunits as shown by FLAG immunoprecipitation and nickel-NTA affinity pull-down (Figure 4.3, lanes 4 and 5). We also purified His-DmIKKβ and His-DmIKKγ-FLAG constructs separately using our two-step purification method for *in vitro* analysis. Typically, we obtained ~5 mg of DmIKK complex per 0.5 L of infected Sf9 cell suspension cultures. Lower yields (<5 mg) of highly pure, homogenous protein were obtained with individually expressed DmIKKγ-FLAG, while 10-15 mg of His-DmIKKβ were obtained per 0.5 L of infected Sf9 cell suspension cultures. We utilized our co-expressed DmIKKβ:γ complex for subsequent biophysical and biochemical characterization.

2. Purified recombinant DmIKKβ:γ is catalytically active

To assess the stability of our purified kinase complex and whether our recombinant DmIKKβ:γ complex is folded properly, we tested its catalytic activity using *in vitro* kinase assays. In these assays, we utilized recombinant Relish proteins His-Rel-68 (expressed in Baculovirus-infected Sf9 insect cells) and GST-Rel-49 constructs (expressed in *E. coli*) (Figure 4.4A). As

shown in the autoradiographs of the kinase assays, DmIKKβ:γ phosphorylates Relish in both His-Rel-68 and GST-Rel-49 constructs (Figure 4.4B-D). To identify the sites of phosphorylation, we performed LC/MS/MS of samples from the *in vitro* kinase assays (Figure 4.4E). Mass spectrometric analysis shows that recombinant DmIKKβ:γ phosphorylated some of the same sites (Serine 32 and 528) as identified previously (Ertürk-Hasdemir et. al 2009). It has been shown that DmIKKβ phosphorylates serines 528 and 529 *in vitro* and upon immune challenge in cells (Ertürk-Hasdemir et al., 2009). In addition to the immune-responsive phosphorylation site at the N-terminus of Relish, our LC/MS/MS analysis revealed that recombinant DmIKKβ:γ phosphorylated serine 517 in Rel-68 and serine 828 in Rel-49 within a serine-rich region (Figure 4.7E). Kinase assays show that mutation of serine 826, 827, and 828 to alanine (SSS826/827/828AAA) in this serine-rich region inhibited phosphorylation of a GST-Rel-49 constructs *in vitro* (Figure 4.4C, D). Mutation of serine 831 and 832 to alanine (SS831/832AA) within the serine-rich region, however, did not inhibit phosphorylation of GST-Rel-49 suggesting that S828 is the only site that can be phosphorylated within Rel-49 *in vitro*. Upon LPS stimulation, the same serine to alanine mutations (SSS826/827/828AAA and SS831/832AA), however, did not inhibit Relish processing in cells (Figure 4.5). The result of these *in vitro* assays are consistent with results showing that C-terminal serine and threonine residues in the last 107 amino acids are not the major target of DmIKKβ upon immune stimulation and that processing and phosphorylation are independent events in the activation of Relish (Ertürk-Hasdemir et al., 2009). It has been proposed that these non-signal-dependent sites of Relish phosphorylation may play a role in mediating interactions with DmIKKβ (Ertürk-Hasdemir et al., 2009)

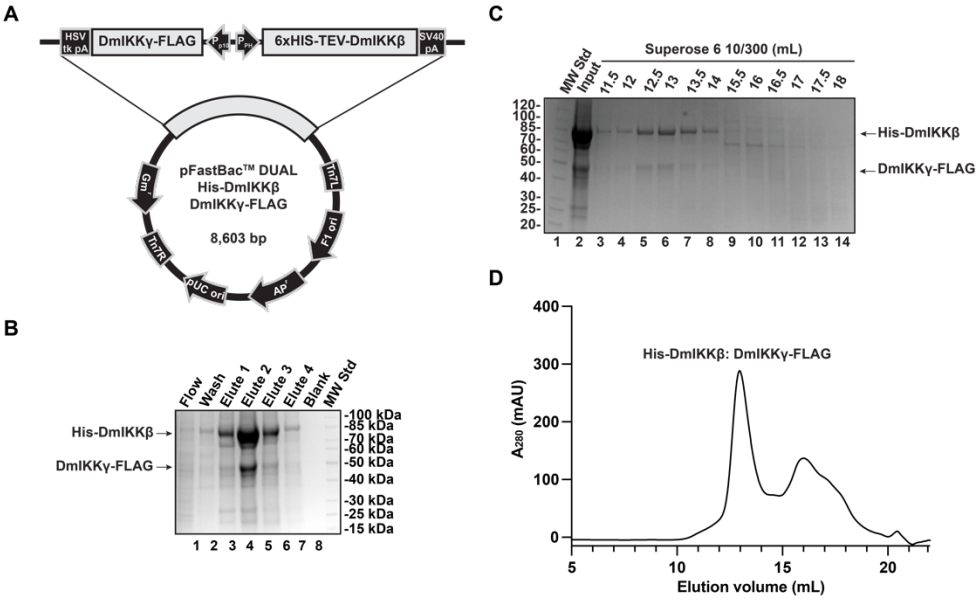

Figure 4.1: Co-expression and purification of recombinant DmlKKβ:γ complex. A) Plasmid map showing construction of recombinant Baculovirus vector for co-expression of His-DmlKKβ:γ-FLAG in Sf9 insect cells. B) A coomassie-stained SDS-PAGE gel monitoring the Ni-NTA affinity purification of co-expressed His-DmlKKβ:γ-FLAG. Lanes 1-6 represent the purification (lanes 1 and 2 are column flow and combined washes lanes 3-6 are 0.5 mL eluted fractions). C) A coomassie-stained SDS-PAGE gel monitoring the size exclusion chromatography of Ni-NTA-purified His-DmlKKβ:γ-FLAG. Lanes 2-14 represent the purification (lane 2 is the input using Ni-NTA eluted fraction #2 and lanes 3-14 are 0.5 mL eluted fractions from size-exclusion chromatography. D) Chromatogram for His-DmlKKβ:γ-FLAG purification on a Superose 6 10/300 column (GE Healthcare).

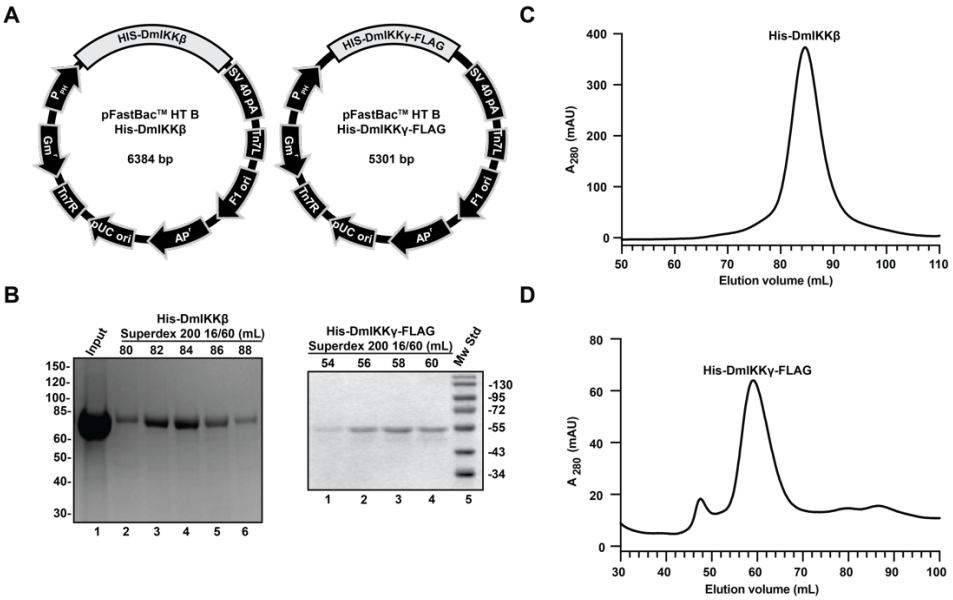

Figure 4.2: Expression and purification of individual DmIKK subunits. A) Plasmid maps showing construction of recombinant Baculovirus vectors for expression of His-DmIKKβ and His-DmIKKγ-FLAG in Sf9 insect cells. B) Coomassie-stained SDS-PAGE gels monitoring the size exclusion chromatography of Ni-NTA-purified His-DmIKKβ (left) and His-DmIKKγ-FLAG (right). For His-DmIKKβ (left), lanes 1-6 represent the purification from size exclusion chromatography (lane 1 is the input from pooled Ni-NTA elution fractions and lanes 2-6 are from 2 mL eluted peak fractions from size exclusion chromatography. For His-DmIKKγ-FLAG (right), lanes 1-4 represent the purification from 2 mL eluted peak fractions from size exclusion chromatography. C) Chromatogram for His-DmIKKβ purification on a Superdex 200 16/60 column (GE Healthcare). D) Chromatogram for His-DmIKKγ-FLAG purification on a Superdex 200 16/60 (GE Healthcare).

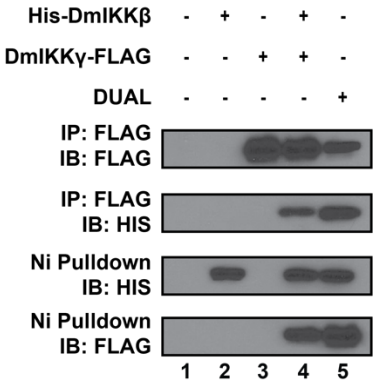

Figure 4.3: FLAG and Ni-NTA affinity pull-down assays show that both individually expressed His-DmIKKβ and DmIKKγ-FLAG (construct lacks a His-tag) or co-expressed DmIKK subunits associate to form the DmIKKβ:γ complex.

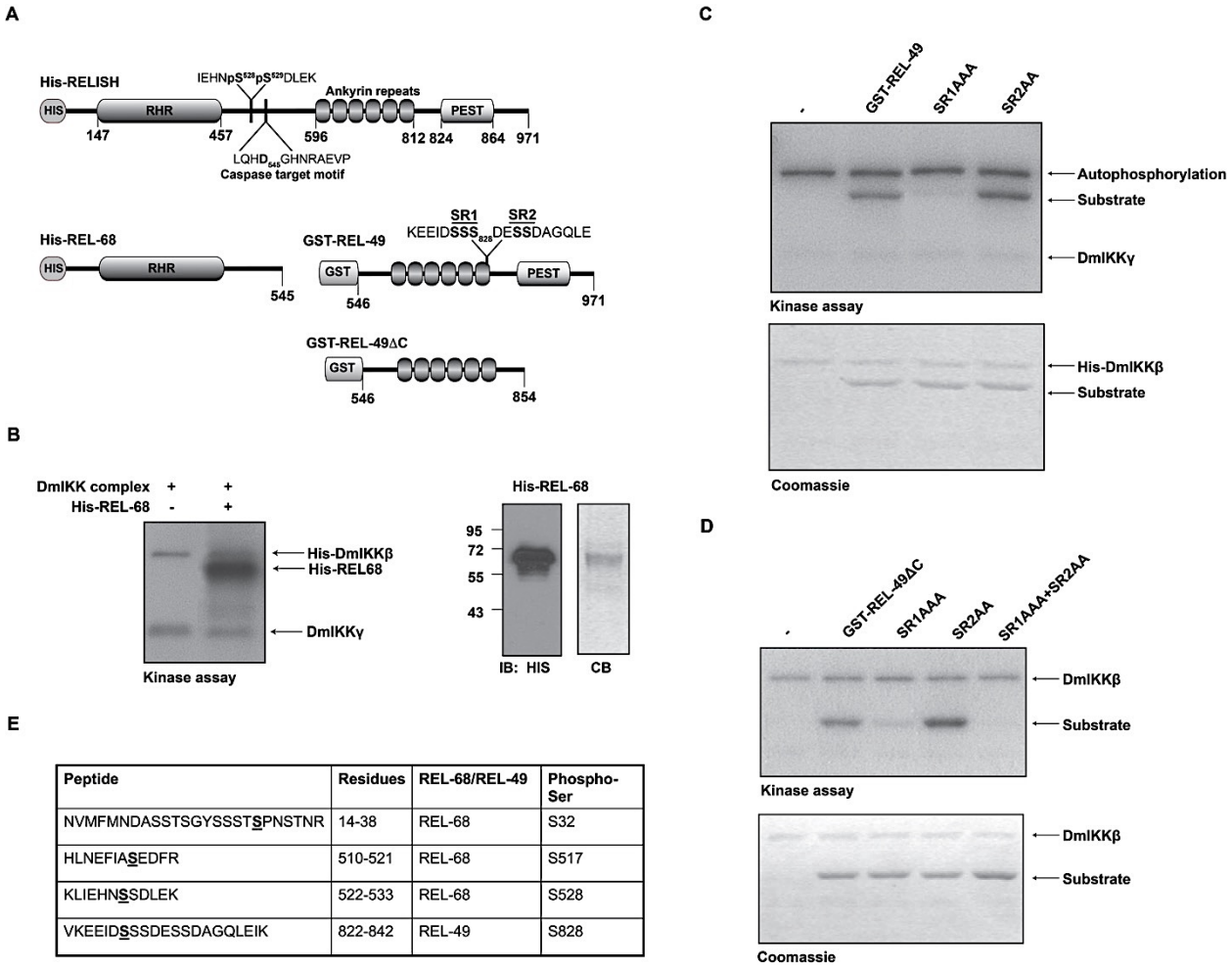

E

Peptide	Residues	REL-68/REL-49	Phospho-Ser
NVMFMNDASSTSGYSSST**S**PNSTNR	14-38	REL-68	S32
HLNEFIA**S**EDFR	510-521	REL-68	S517
KLIEHN**S**SDLEK	522-533	REL-68	S528
VKEEID**S**SSDESSDAGQLEIK	822-842	REL-49	S828

Figure 4.4: Catalytic activity of recombinant DmIKKβ:γ. A) Schematic diagrams of substrate constructs used in *in vitro* kinase assays. His-tagged or GST-tagged Relish substrates contain three possible segments depending on the construct: an N-terminal Rel homology region (RHR), a central ankyrin repeat-containing domain (ARD), and a C-terminal PEST domain that is rich with proline, glutamic acid, serine, and threonine residues. Adjacent to the RHR is a region that is phosphorylated by DmIKK, followed by a motif targeted by the caspase Dredd for Relish proteolytic processing. B) Autoradiography of *in vitro* kinase assay shows Rel-68 as a substrate for DmIKK (left). Western blot with anti-His antibody and Coomassie blue (CB) stained SDS-PAGE gel of Rel-68 substrate (right). C) Autoradiography (top) and Coomassie-stained SDS-PAGE gel (bottom) of *in vitro* kinase assays with purified DmIKK complex and GST-Rel-49 as substrate. SR1 and SR2 refer to serine-rich regions at the carboxy-terminal ankyrin repeats of Rel-49. Serines within these regions were mutated to alanine for SR1AA and SR1AAA constructs. B) The same experiment as in C) but performed on GST-Rel49ΔC construct lacking the PEST domain showing that serine residues in SR1 are the main target of GST-Rel-49. E) LC/MS/MS on purified and Rel-68 and Rel-49 proteins after they had been separately phosphorylated *in vitro* by recombinant DmIKKβ:γ complex revealed phosphorylation sites within the SR1 loop of Rel-49 and at three additional sites in Rel-68 including the known signal-dependent phosphorylation site of serine 32.

3. DmIKKβ:γ complex size characterization by analytical-scale SEC

Having established that our recombinant DmIKKβ:γ complex can be purified to homogeneity and is a stable enzyme with the ability to phosphorylate Relish on multiple sites, we examined its structural characteristics through biophysical methods. We first used analytical scale size-exclusion chromatography (SEC) to determine the solution molecular weight (M_w) and to characterize the size of the DmIKKβ:γ complex. Analytical SEC was performed utilizing the calibration of globular protein standards (Figure 4.5, Table 4.1). Recombinant DmIKKβ:γ eluted at a peak with volume corresponding to a globular protein of Mw of ~1.2 MDa and a calculated Stokes radius (R_s) of 8.47 nm (Figure 4.5, Table 4.1). This suggests that DmIKKβ:γ forms a large complex composed of multiple copies of each subunit since DmIKKβ has a predicted monomeric molecular weight of 86.373 kDa and DmIKKγ has a predicted monomeric molecular weight of 43.879 kDa. Analytical SEC analysis of the DmIKKβ subunit alone resulted in as a single peak at a volume corresponding to a Mw of 175.7 kDa with an R_s of 5.43 nm, suggesting that it exists as a β_2 dimer (Figure 4.5). His-DmIKKγ-FLAG runs as a very large species with a molecular weight of 1.0 MDa and R_s of 8.15 nm (Figure 4.5). Because size characterization by analytical SEC is based on hydrodynamic elution volume of globular protein standards, M_W determination from SEC analysis of non-globular, elongated proteins or proteins with non-ideal column interactions is often overestimated (Erickson, 2009; Kunji et al., 2008; Štulík et al., 2003). In a recent report, human NEMO has been shown to have a short retention time in SEC, eluting as a particle >700 kDa, while their SEC-MALS analysis demonstrates that human NEMO (monomer weight of 48 kDa) is primarily a dimer with a molecular weight of ~100 kDa, suggesting that the elongated coiled coil structure is responsible for the discrepancies in SEC analysis (Ko et al., 2020). Because DmIKKγ is predicted to be largely alpha-helical with coiled coil domains like its mammalian ortholog, we then pursued shape-independent biophysical techniques for DmIKK complex molecular weight characterization.

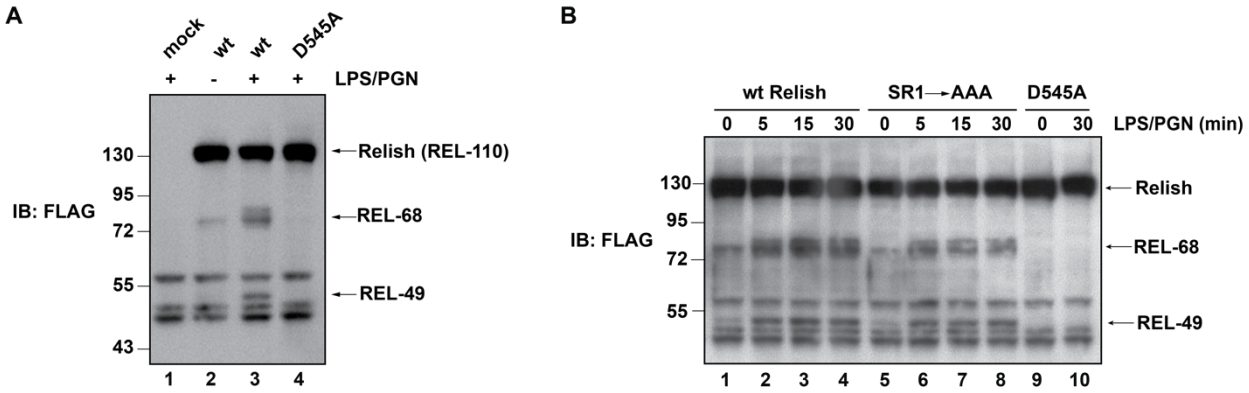

Figure 4.5: Cleavage assays reveal that mutation of phosphorylation sites is not sufficient to inhibit processing of Relish. A) Immunoblot with anti-FLAG antibody shows the proteolytic processing of a FLAG-Relish-FLAG construct transiently transfected into *Drosophila* S2 cells. Induction by LPS/peptidoglycan leads to Relish processing and production of Rel-68 and Rel-49 fragments (Left panel, Lane 3). Processing is dependent upon Dredd proteolytic activity at Asp545 of Relish as confirmed by lane 4. B) Immunoblot reveals that Relish proteolysis proceeds even when serines within the SR1 of Rel-49 are mutated to Ala. These mutations inhibit Rel-49 from being phosphorylated *in vitro* by the DmIKK complex.

4. Shape-independent size analysis by SEC-MALS

For shape-independent size characterization, we employed size-exclusion chromatography coupled to multi-angle light scattering (SEC-MALS). The SEC-MALS chromatogram for the complex at 16 μM protein concentration shows a single species with a solution molecular weight (M_w) of 271.57±4.5 kDa (Figure 4.7A). This is in agreement with the theoretical molecular weight of a β_2:γ_2 heterotetramer which is calculated to be 260.5 kDa. SEC-MALS of DmIKKβ subunit alone at 23 μM protein concentration resulted in a Mw of 161.1±6.5 kDa suggesting that it assembles primarily as a dimer in solution (Figure 4.7A). We did not observe the presence of minor peaks in the SEC-MALS chromatograms for the complex and the DmIKKβ subunit alone at the protein concentrations used.

5. AUC-SV analysis of DmIKK solution properties

Analytical ultracentrifugation sedimentation velocity (AUC-SV) further confirm DmIKK complex subunit stoichiometry of two β and two γ subunits (Figure 4.7C) The C(s) distribution of the DmIKK complex was dominated by a single peak (~80% total protein) with an apparent Mw of 248.26±9.14 kDa (Figure 4.7C). We observed a minor peak (~2% of total protein) with an apparent Mw of 586.6 kDa that may be due to the detection of a trace contaminant or nonspecific aggregation. The presence of a large, dominant peak in the AUC-SV data demonstrate that our DmIKK complex preparation is highly pure and monodisperse as this technique is sensitive to impurities. AUC-SV also reveals an extremely elongated shape for the complex with a prolate axial (a/b) radius ratio (ratio of semimajor axis a to semi-minor axis b) of 18.7. The a/b radius ratio is derived from frictional coefficients calculated from AUC-SV data using Perrin's analysis of molecules modeled as an ellipsoid of revolution. Perrin's analysis of AUC-SV data has been suggested to overestimate the asymmetry of molecules when compared to the protein dimensions obtained by other biophysical and structural techniques such as electron microscopy, atomic force microscopy, and small angle x-ray scattering (Erickson 2009, Hesterberg et. al 1981, Martin et. al 2003, Li et. al 2006). It has, however, been used to observe general trends about protein shape such as asymmetry (Godamudunage et. al 2017).

AUC-SV analysis of the DmIKKβ subunit alone show a major peak (85.3% of total protein) with an apparent Mw of 261.25±5.30 kDa and an a/b radius ratio of 15.3 suggesting an elongated trimer (Figure 4.7B). We also detected a few minor peaks (~2% each of total protein) with apparent Mw of 22.0 kDa and 114.6 kDa that may be due to detection of contaminants. The apparent Mw of the major peak are in contrast to the Mw values obtained from analytical SEC (175.7 kDa, Figure 4.6, Table 4.1) and SEC-MALS (161.1±6.5 kDa, Figure 4.7A).

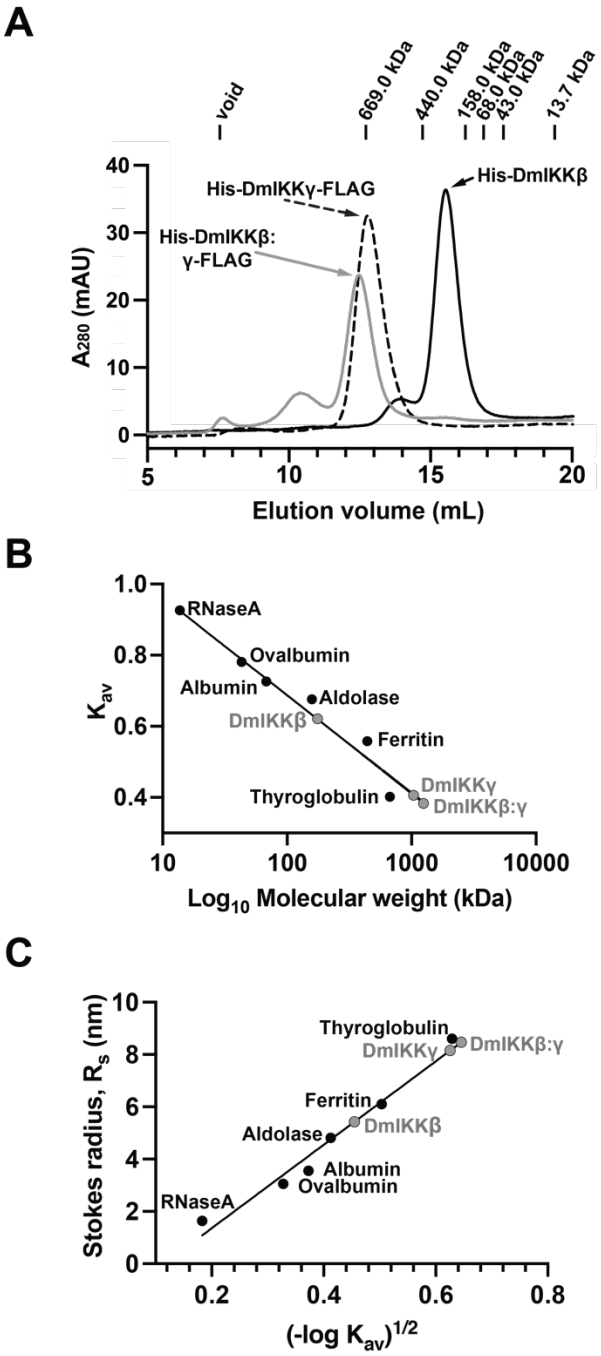

Figure 4.6: Analytical size-exclusion chromatography (SEC) of recombinant DmIKK constructs. A) Analytical SEC chromatograms of His-DmIKKβ:γ-FLAG (gray line), His-DmIKKγ-FLAG (black dashed line), and His-DmIKKβ (solid black line). B) Molecular weight analysis of DmIKK constructs based on elution volume of calibration standards. C) Determination of hydrodynamic radius (Stokes radius) by comparison with calibration standards.

Table 4.1: Data for size determination of DmIKK protein constructs in solution by analytical size-exclusion chromatography

Species	Molecular weight (MW)	Elution vol. V_e (mL)	K_{av} *	Calculated MW †	Stokes Radius (R_s) (nm)	Calculated R_s (nm)
Standards used to determine total column volume (V_c) and void volume (V_o)						
Column vol.		20.37 (V_c)				
Void volume	>5,000,000	7.56 (V_o)				
Standards used to determine column calibration curve						
RNase A	13,700	19.42	0.926		1.64	
Ovalbumin	43,000	17.56	0.781		3.05	
Albumin	68,000	16.86	0.726		3.55	
Aldolase	158,000	16.22	0.676		4.81	
Ferritin	440,000	14.71	0.558		6.10	
Thyroglobulin	669,000	12.71	0.402		8.60	
Experimental samples						
DmIKKβ		15.51	0.621	175,756		5.43
DmIKKγ		12.76	0.406	1,036,092		8.15
DmIKK complex		12.47	0.383	1,249,265		8.47

$K_{av} = (V_e - V_o)/(V_c - V_o)$
† Determined from the equation: $K_{av} = -0.121\text{Log}(MW) + 2.0819$

In AUC-SV, it is known that molecular shape influences sedimentation in that two proteins with the same mass but different shape (i.e. globular vs. elongated) can sediment at different rates leading to distorted Mw estimations. In asymmetric proteins, there is increased drag and larger frictional coefficients that are attributed to this distortion in Mw observed in AUC-SV (Herr and Conrady 2011). It may be that the discrepancies observed in the Mw measurements from AUC-SV for our recombinant His-DmIKKβ is due to the influence of increased drag and friction as a result of asymmetry in DmIKKβ. For asymmetric molecules,

analytical ultracentrifugation sedimentation equilibrium (AUC-SE), is often performed as a complementary experiment to AUC-SV (Cole et. al 2008, Lebowitz et. al 2009, Zhao et. al 2013). In AUC-SE, the molecular weight is determined independent of the hydrodynamic shape by analysis of the protein concentration distribution at equilibrium when the rate of diffusion is balanced by the rate of sedimentation (Herr and Conrady 2011).

6. DmIKK subunit stoichiometry analysis by AUC-SE

Since AUC-SV revealed that both the DmIKK complex and the DmIKKβ subunit alone exhibit extreme asymmetry, we performed AUC-SE on these proteins. The apparent molecular weight of the DmIKKβ:γ complex from AUC-SE was measured to be 265.77±0.74 kDa (Figure 4.7D). This agrees with AUC-SV and SEC-MALS analysis (Figure 4.7). For DmIKKβ stoichiometry, the apparent molecular weight from AUC-SE ($M_{w,\,app}$=153.37±11.4 kDa) confirms that it assembles as a dimer in solution in absence of the non-catalytic subunit DmIKKγ (Figure 4.7D). This is in agreement with analytical-scale SEC and shape-independent SEC-MALS analysis (Figure 4.7D).

7. The DmIKKβ:γ complex interacts with linear poly-ubiquitin

Our primary sequence comparison and ConSurf analysis described in Chapter III reveals that DmIKKγ harbors two putative ubiquitin binding domains: one in the CC2 region and the other at the zinc finger (Figure 3.9). The CoZi domain of mammalian NEMO preferentially binds to linear-polyubiquitin over K-63-linked polyubiquitin (Hadian et al., 2011; Komander et al., 2009; Lo et al., 2009; Rahighi et al., 2009). A ubiquitin-binding zinc finger (UBZ) domain is present in HsNEMO (residues 407-417) which was shown to bind to linear and K-63 linked poly-ubiquitin, with a preference for the latter type (Cordier et al., 2009, Laplantine et al., 2009). Furthermore, core residues in the CoZi domain that mediate non-covalent association with linear and K-63 linked di-ubiquitin are conserved in DmIKKγ (Figure 3.9). Both ubiquitin binding domains have been shown to regulate mammalian IKK and ablation of either domains results in diminished

IKK activation (Cordier et al., 2009; Rahighi et al., 2009). In this study, we chose to focus on whether linear poly-ubiquitin interacts with DmIKKβ:IKKγ complex in a non-covalent manner. To test this, we performed an *in vitro* GST pulldown binding assay using our purified, recombinant DmIKK proteins and a recombinant GST-tetra-ubiquitin construct that acts as a mimic for linear (M1-linked) tetra-ubiquitin. Full-length, recombinant His-tagged human NEMO was used as a positive control for GST-tetra-ubiquitin binding (Figure 4.8, lanes 4 and 8). GST was used as a control of nonspecific binding (Figure 4.8, lanes 5-8). We note, however that there is some background binding with His-DmIKKγ-FLAG as seen in the anti-His and anti-FLAG immunoblots, but this background is much lower in intensity than the experimental lane (Figure 4.8, lanes 3 and 7). GST-tetra-ubiquitin pulled down the DmIKKβ:IKKγ complex, but not the DmIKKβ subunit alone (Figure 4.8, lanes 1 and 2). We also show that the DmIKKγ subunit alone can interact with GST-tetra-ubiquitin (Figure 4.8, lane 3). We conclude that the DmIKKβ:IKKγ complex can non-covalently interact with linear poly-ubiquitin *in vitro* via the DmIKKγ subunit.

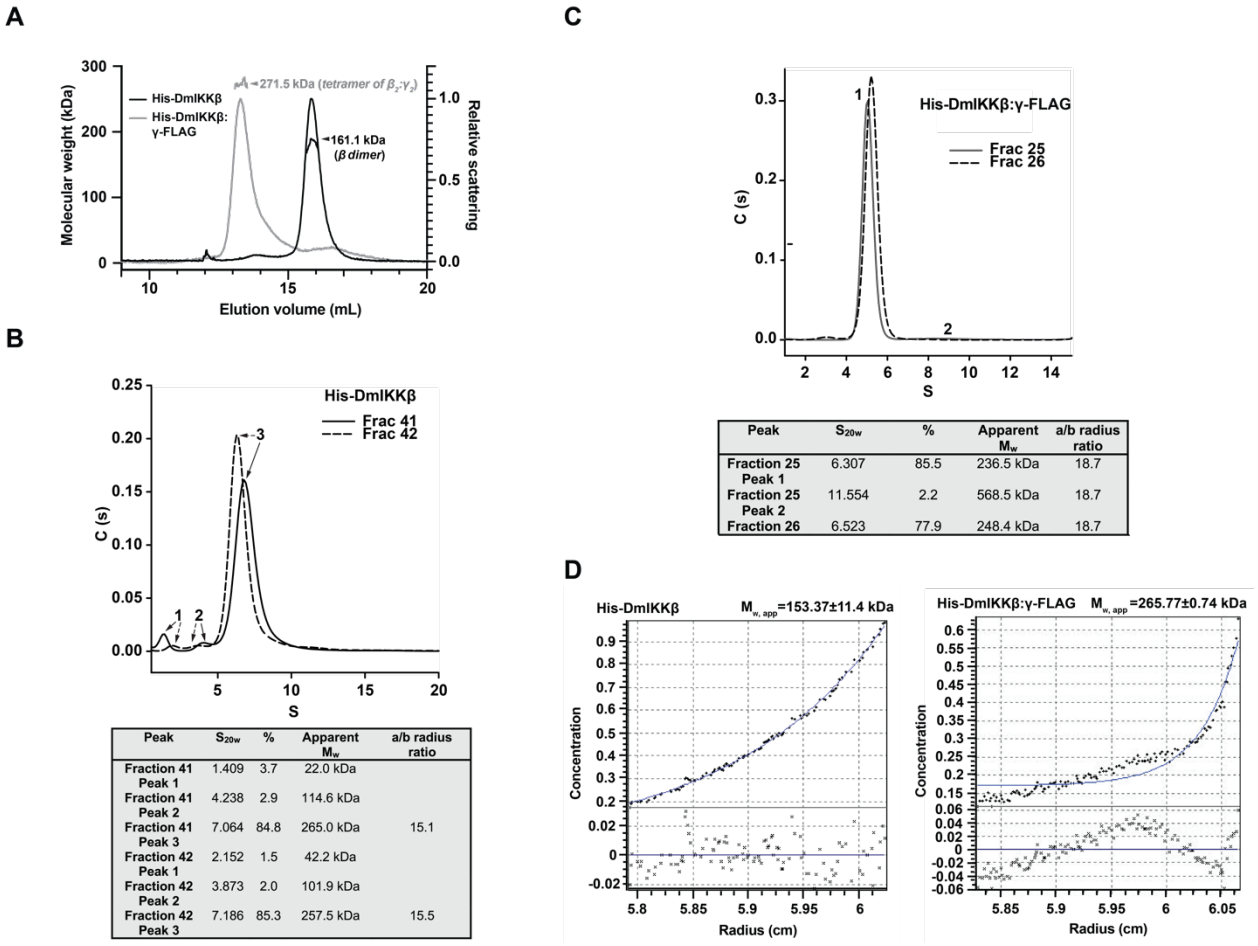

Peak	S_{20w}	%	Apparent M_w	a/b radius ratio
Fraction 41 Peak 1	1.409	3.7	22.0 kDa	
Fraction 41 Peak 2	4.238	2.9	114.6 kDa	
Fraction 41 Peak 3	7.064	84.8	265.0 kDa	15.1
Fraction 42 Peak 1	2.152	1.5	42.2 kDa	
Fraction 42 Peak 2	3.873	2.0	101.9 kDa	
Fraction 42 Peak 3	7.186	85.3	257.5 kDa	15.5

Peak	S_{20w}	%	Apparent M_w	a/b radius ratio
Fraction 25 Peak 1	6.307	85.5	236.5 kDa	18.7
Fraction 25 Peak 2	11.554	2.2	568.5 kDa	18.7
Fraction 26	6.523	77.9	248.4 kDa	18.7

Figure 4.7: Biophysical characterization of DmIKK constructs. A) Shape-independent molecular weight analysis by SEC-MALS reveals DmIKKβ dimerization and hetero-tetramerization of the complex (DmIKKβ_2:γ_2) in solution. Chromatograms show His-DmIKKβ:γ-FLAG (gray line) and His-DmIKKβ (black line). B) AUC-SV of His-DmIKKβ from peak fractions in SEC purification. C) AUC-SV of His-DmIKKβ:γ-FLAG from peak fractions in SEC purification. Data for AUC-SV is represented by peaks assigned to a percentage value of total protein detected, approximate molecular weight, and a/b major axis ratio. AUC-SV a/b radius ratio data from B) and C) reveal elongated shape of DmIKKβ and DmIKKβ:γ which may affect molecular weight estimation by this method. D) Shape-independent molecular weight analysis by AUC sedimentation equilibrium (AUC-SE) experiments confirms model of DmIKKβ dimerization and a hetero-tetramer assembly of DmIKKβ_2:γ_2. AUC-SE profiles and residuals of His-DmIKKβ (left) and His-DmIKKβ:γ-FLAG (right).

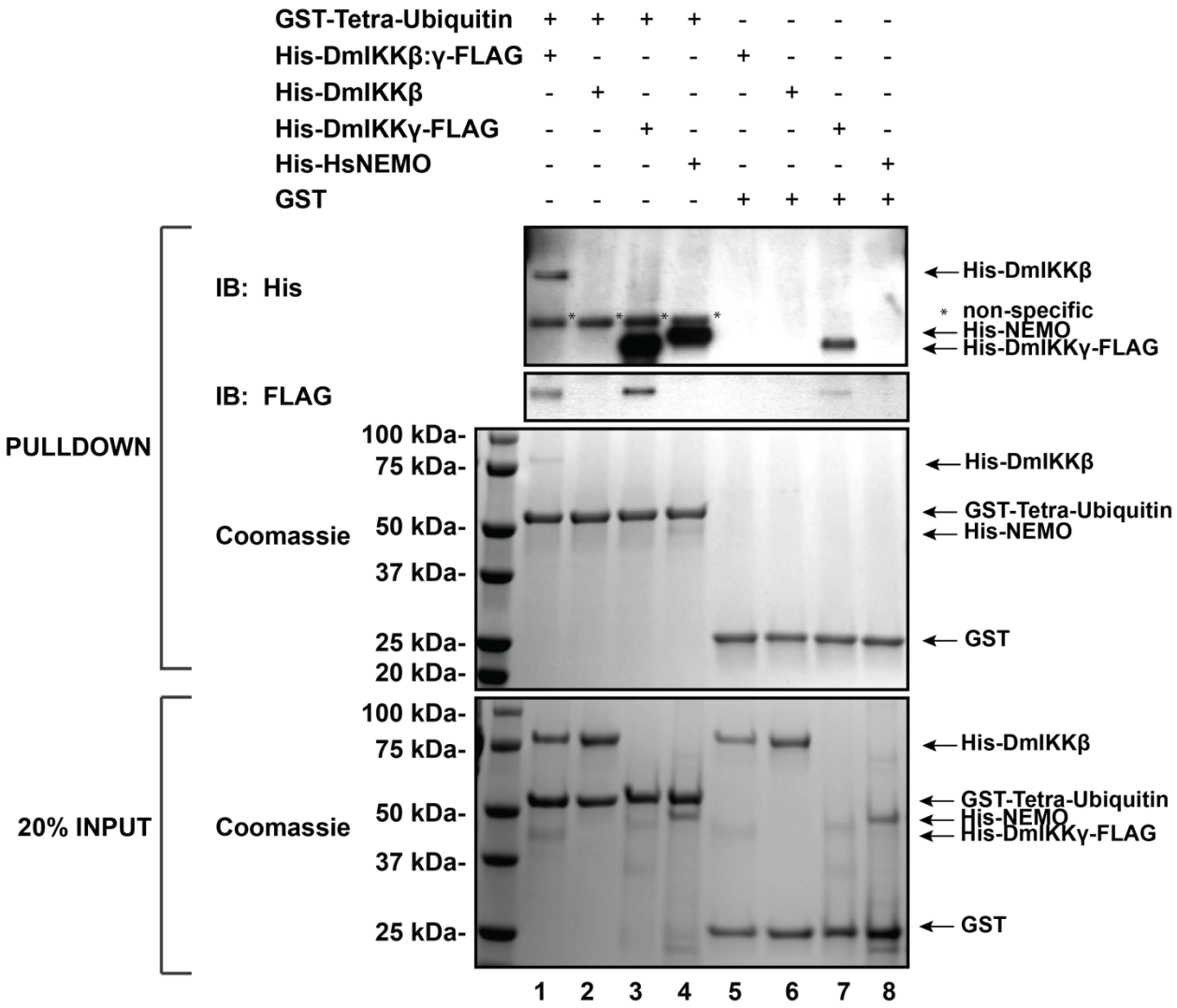

Figure 4.8: *In vitro* GST pull-down assay of recombinant DmIKK purified protein constructs shows that DmIKKβ:γ and DmIKKγ, but not DmIKKβ can associate with linear-tetraubiquitin. DmIKK constructs were pulled down by GST-M1 linked tetraubiquitin. Immunoblot (IB) panels indicate primary antibodies used to probe possible interactions.

C. Discussion

The IKK complex was first isolated in stimulated HeLa cells and characterized to be a 700-900 kDa activity by SEC analysis suggesting an arrangement of multiple copies of the catalytic and non-catalytic subunits (Zandi et al., 1997). Since this initial characterization of the mammalian IKK complex, the assembly and subunit stoichiometry of a multi-subunit IKK

complex has been controversial. Soon after the discovery of the mammalian IKK complex, the *Drosophila* IKK complex was discovered as an essential regulatory component in the IMD innate immune pathway (Lu et al., 2001; Rutschmann et al., 2000; Silverman et al., 2000). Our analytical SEC analysis of purified recombinant DmIKKβ:γ showed that it eluted as a ~1 MDa complex exhibiting short retention times in SEC as observed with the mammalian IKK complex.

Three-dimensional structures and biochemical studies of human catalytic IKKα and IKKβ has revealed much about the structural organization, homodimerization, as well as its propensity of catalytic IKK subunits to form higher-order oligomers in solution (Polley et al., 2013; Polley et al., 2016). Structures of domains and specific fragments of the mammalian non-catalytic subunit NEMO have been solved, revealing extensive homodimerization through coil-coiled domains (Rushe et al., 2008; Bagnéris et al., 2008; Lo et al., 2009; Rahighi et al., 2009; Yoshikawa et. al 2009). Structures of free NEMO dimer segments and bound to other factors have been solved including structures of the IKKβ binding Domain (KBD) of NEMO bound to the NEMO binding domain (NBD) of IKKβ/α in addition to structures of dimeric coiled-coil regions of NEMO bound to linear di-ubiquitin, lysine-63-linked di-ubiquitin, and the viral activator vFLIP (Rahighi et. al 2009, Yoshikawa et. al 2009, Bagnéris et al 2008). These studies have revealed that NEMO can act as a scaffolding protein to interact with different macromolecular components and to transduce signaling towards activation of IKK. The three-dimensional structures and biochemical studies of the individual subunits have given some insight into the architecture and regulatory interactions within each subunit, but without a high-resolution three-dimensional structure of a multi-subunit IKK complex, the regulation mechanism remains equivocal.

In this study, we focused on the solution characteristics of the multi-subunit DmIKK complex to gain insight into subunit assembly and features of its regulation mechanism. Recombinant expression and purification of the DmIKKβ:γ complex from Baculovirus-infected Sf9 cells yielded a homogenous complex that phosphorylates the NF-κB substrate Relish on

multiple sites. Size characterization via analytical size-exclusion chromatography (SEC) indicates that the DmIKKβ:γ complex migrates as a high molecular weight particle with a large hydrodynamic radius. SEC analysis of the DmIKKβ subunit alone revealed that, like mammalian IKKβ, it primarily assembles as a dimer.

Shape-independent molecular weight analysis by size-exclusion chromatography coupled to multi-angle light scattering (SEC-MALS) and analytical ultracentrifugation (AUC-SV and AUC-SE) reveals that the complex assembles as a hetero-tetramer containing two copies of each subunit, while the DmIKKβ subunit assembles as a dimer thereby corroborating analytical SEC results. A recent report shows that the human IKK complex also primarily assembles as a hetero-tetramer of $IKK\beta_2$:$NEMO_2$, but higher-order oligomers of $(IKK\beta_2:NEMO_2)_n$ are also observed (Ko et al., 2020). However, unlike mammalian IKK solution behavior, we did not observe any evidence of oligomerization with our recombinant DmIKKβ either alone or in complex with DmIKKγ. This reveals a unique feature of DmIKK complex regulation mechanism in that activation does not seem to involve higher-order oligomerization. Instead, the DmIKK complex exerts is function as a distinct heterotetrameric module of $IKK\beta_2$:$IKK\gamma_2$.

In chapter III, I showed that DmIKKγ contained putative ubiquitin-binding domains in the CC2 and zinc finger by primary sequence comparison and ConSurf analysis. The ubiquitin-binding properties of mammalian NEMO have been structurally and biochemically characterized. Linear-ubiquitin chains have been shown to be essential for IKK activation in cells (Lo et al., 2009; Rahighi et al., 2009; Fujita et al., 2014). NEMO mutations as well as disease-linked mutations in the linear-ubiquitin-binding interface in the CC2 fail to induce NF-κB activation (Rahighi et al., 2009; Fujita et al., 2014). Because of the functional importance of linear-ubiquitin non-covalent association with NEMO at the CC2, we sought to test whether this association also occurs in DmIKKγ. Our *in vitro* GST pull-down reveals that the DmIKKβ:γ complex can non-covalently interact with linear poly-ubiquitin suggesting, a conserved role of linear-ubiquitin:DmIKKγ association in the IMD pathway. Future work delineating the molecular

determinants of poly-ubiquitin binding to the DmIKK complex and the structural consequences upon its binding will undoubtedly provide insights into its activation mechanism.

Chapter V

Electron microscopy of the multi-subunit DmIKK complex

Introduction

Structural elucidation and molecular size characterization are necessary to understand mechanisms involving macromolecular assemblies. Transmission electron microscopy (TEM) is a common technique used to image macromolecules and gain essential structural information to uncover molecular features important for protein function and regulation. Although it is limited in resolution to ~18-20 Å, TEM is often used as a relatively simple and quick method to assess the homogeneity, quality of protein preparation and assembly of complexes for high resolution structural techniques such as cryo-electron microscopy (Cryo-EM). A major goal of the Huxford Laboratory is to attain a high-resolution structure of a multi-subunit IKK complex. The *Drosophila melanogaster* IKK complex is an attractive choice for high-resolution structural studies because the fruit fly system is simpler for two reasons: 1) it has only one catalytic subunit, unlike the vertebrate IKK complex which contains two catalytic subunits (IKKα and IKKβ) and 2) we do not see evidence of higher-order oligomerization in this complex so it allows for investigation of the intra-complex interactions between the β and γ subunits within the tetrameric complex separate from any signal-induced oligomerization of the complex (as is evident in the mammalian complex). This is also important as it is difficult to perform high-resolution structural studies on heterogenous mixtures of complexes of different sizes. After optimization of purification and storage conditions, the DmIKK complex is also a relatively stable particle in solution and we observe no evidence of aggregation in our biophysical measurements as has been observed when working with mammalian IKK complexes in our laboratory.

As such, a prerequisite for any three-dimensional structural study is the purification of homogenous protein in milligram amounts. In the previous chapter, we have shown that our recombinant *D. melanogaster* IKK proteins expresses well in the baculoviral system and can be purified to homogeneity. With our optimized purification scheme, we can attain ~5 milligrams of highly pure His-DmIKKβ:γ-FLAG complex from 0.5 L of baculovirus infected cultured Sf9 insect

cells. Our biophysical characterization has also shown that the DmIKK proteins are stable in solution and that the His-DmIKKβ:γ-FLAG primarily assembles as a single hetero-tetrameric species composed of β_2:γ_2. We have also shown that DmIKKγ is a highly-elongated macromolecule that migrates with a large hydrodynamic radius in SEC and AUC, contributing to the initial biophysical observations that the DmIKK complex elutes as a very large complex >1 MDa in size. In contrast, we have shown that DmIKKβ primarily exists as a dimer with no indication of any higher order oligomeric assemblies using the same biophysical methods. This is in contrast to human IKKβ, which is also primarily dimeric but was also shown to have some populations of oligomeric species in solution (Polley et. al 2013). A recent biophysical study from our laboratory revealed that the human IKKβ:γ complex also primarily assembles as a heterotetramer composed of a β_2:γ_2 assembly, but that there are also oligomeric species present in solution suggesting that human IKKβ is oligomerization prone in solution with our without NEMO (Ko et. al 2020). Our biophysical analysis of the DmIKKβ:γ complex suggests that there are some structural differences to the mammalian complex in that the propensity towards catalytic IKK subunit oligomerization is absent. Instead, a single hetereotetramer species predominates in solution.

Although three-dimensional structures of individual IKK subunits in mammals has given some mechanistic insights into the function of IKK proteins, the mechanism of regulation and biochemistry of a multi-subunit IKK complex remains equivocal. In efforts to investigate the three-dimensional macromolecular structure of the *D. melanogaster* IKKβ:γ complex we have applied negative stain TEM on our purified complex to assess the sample preparation conditions for future studies using high-resolution Cryo-EM.

Results

Before pursuing three-dimensional negative-stain-TEM structural studies on our recombinant DmIKKβ:γ complex, I sought to gain experience in this technique by using a well-behaved protein control. Given the symmetrical assembly of the 24-mer spherical cage of the

iron-storage protein ferritin and its availability as a highly pure sample used in size-exclusion chromatography calibration in our laboratory, I pursued initial grid preparation and imaging on a sample of horse spleen ferritin (GE Healthcare).

With this control protein in hand, I first applied glow discharge on carbon-formvar coated copper grids (Electron Microscopy Sciences, Hatfield, PA) using the glow discharge apparatus in the SDSU Electron Microscopy Facility. This apparatus is custom built and composed of a vacuum controlled chamber to which grids are placed and short bursts of electric charge is administered. After glow discharge, I placed ferritin samples onto the treated grids and stained the sample with drops of 2% uranyl acetate stain. The grids were allowed to dry on filter paper and kept in a storage box until visualization with the TEM. Figure 5.1 shows TEM micrographs of negatively-stained horse spleen ferritin at ~0.5 mg/mL concentration at different magnifications. Regions of stained protein are visible against a dark “halo” of stain showing image contrast of the protein structures. We observe inner and outer diameters of the ferritin cage structure at 7.269 nm and 12.66 nm, respectively. These values are in accordance with electron microscopy studies on ferritin that demonstrated the inner core to be ~8 nm and the outer diameter of ~12.5 nm (Iancu et al. 2017, Iancu, 2011). The defocus settings, however, could be optimized as the micrographs obtained are blurred (Figure 5.1).

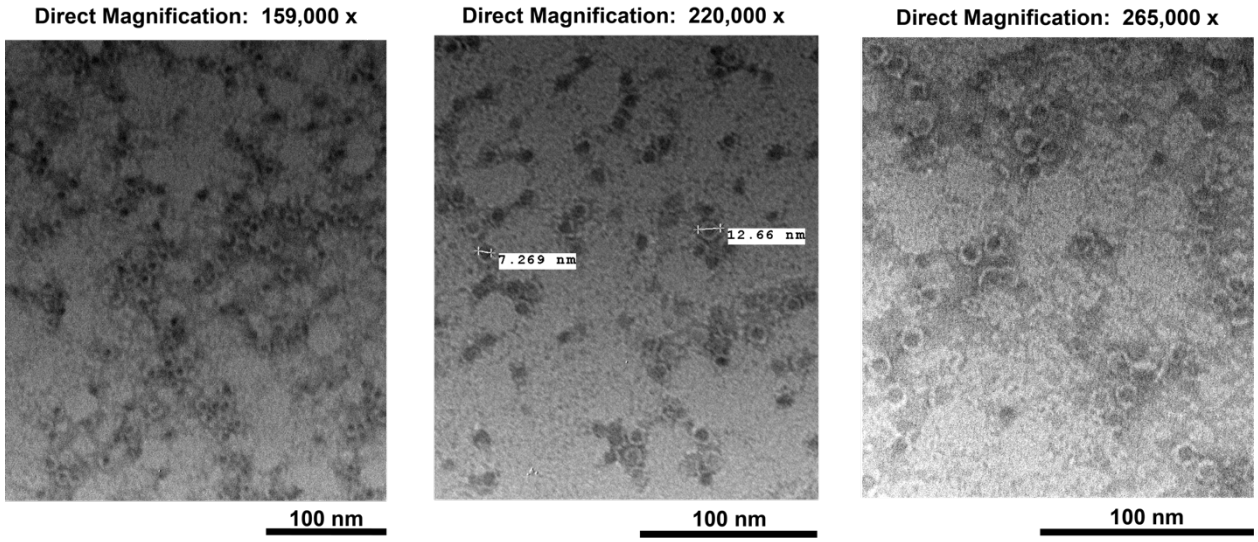

Figure 5.1: TEM micrographs of control protein horse spleen ferritin at the indicated magnifications. In the middle panel, measurements indicate approximate inner and outer diameters in nanometers (nm).

Having shown protein imaging capabilities through negative stain TEM of horse spleen ferritin, we then applied this technique to our recombinant, Baculovirus-expressed DmIKKβ:γ complex. Initially, we did not observe particles of our complex on the prepared grids (Figure 5.2A). In addition, for negatively-stained DmIKKβ, we observe some particles, but inadequate particle distribution on the prepared grids (Figure 5.2B, C). The lack of particles on the prepared grids suggested that grid preparation must be optimized. Therefore, I chose to investigate glow discharge conditions. I was able to use carbon-formvar coated copper grids that were glow-discharged using a commercially available machine prepared by SDSU EM Facility director Ingrid Niesman at the UCSD EM Facility.

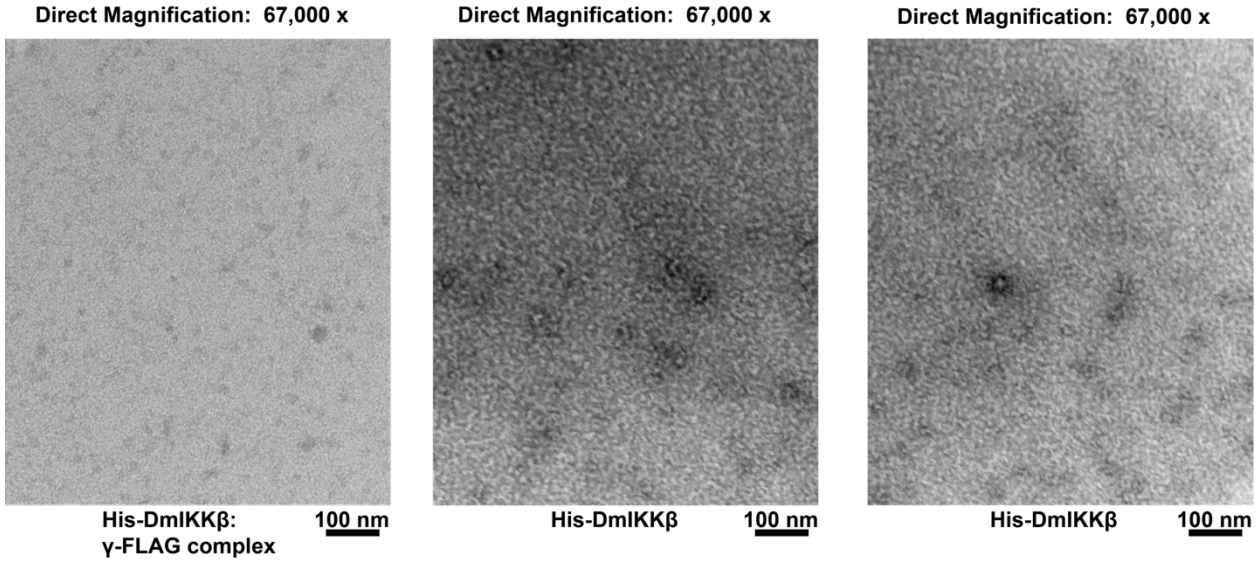

Figure 5.2: Representative TEM micrographs of recombinant DmIKK proteins complex at the indicated magnifications. The grids were prepared using the glow discharge apparatus at the SDSU Electron Microscopy.

Observation of these previously glow-discharged grids shows sample heterogeneity and large globular types of particles (Figure 5.3). Representative EM micrographs show that most particles were ~150-200 nm in size (Figure 5.3). Despite our biophysical measurements showing a monodisperse sample as shown in Chapter IV, we observe particles of different sizes in our negative-stain TEM images. It is important to note that the age of the glow-discharge grids is not known and there may be some influence of possible contaminants that might be present on the surface of the grids. Because this may be an issue, I prepared new samples and prepared grids soon after glow discharge (within a week).

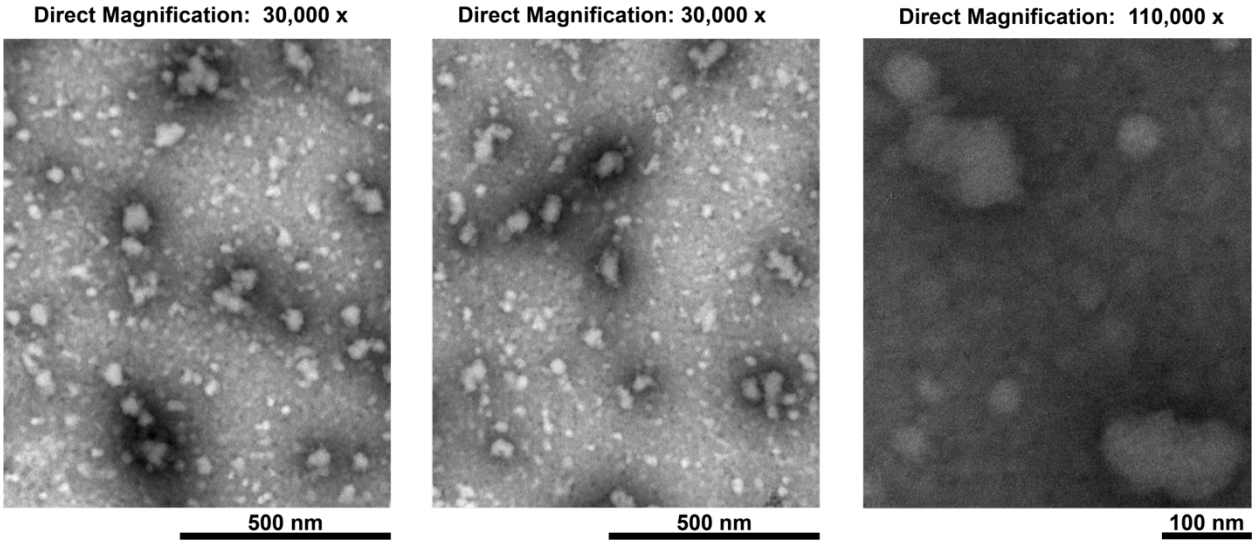

Figure 5.3: Representative TEM micrographs of recombinant DmIKKβ:γ showing large globular assemblies (~150-250 nm in diameter) at the indicated magnifications. Each panel is an image of particles located at different positions of the grid. The grids were prepared by commercial glow discharge apparatus, but have been stored for an unknown period of time prior to sample adsorption and staining.

However, the micrographs of freshly glow-discharged grids also show heterogeneity in the particle size and shape. Larger particles are ~250 nm in size, while smaller particles are about half the size. The smaller particles do not exhibit much contrast however so it is difficult to visualize structural content. Other types of particles are also present in the micrographs obtained. In Figure 5.4, some slightly elongated assemblies exhibiting more surface rugosity are observed in contrast to particles seen in the older glow-discharged grids (Figure 5.3). These particles range in size of ~75-124 nm (Figure 5.4). In Figure 5.5, globular type of particles that are ~115-170 nm in length are observed. Nevertheless, we cannot draw conclusions as to the structure of the complex and further study on its behavior and sample stability using the negative stain technique is warranted for TEM studies on the DmIKK complex.

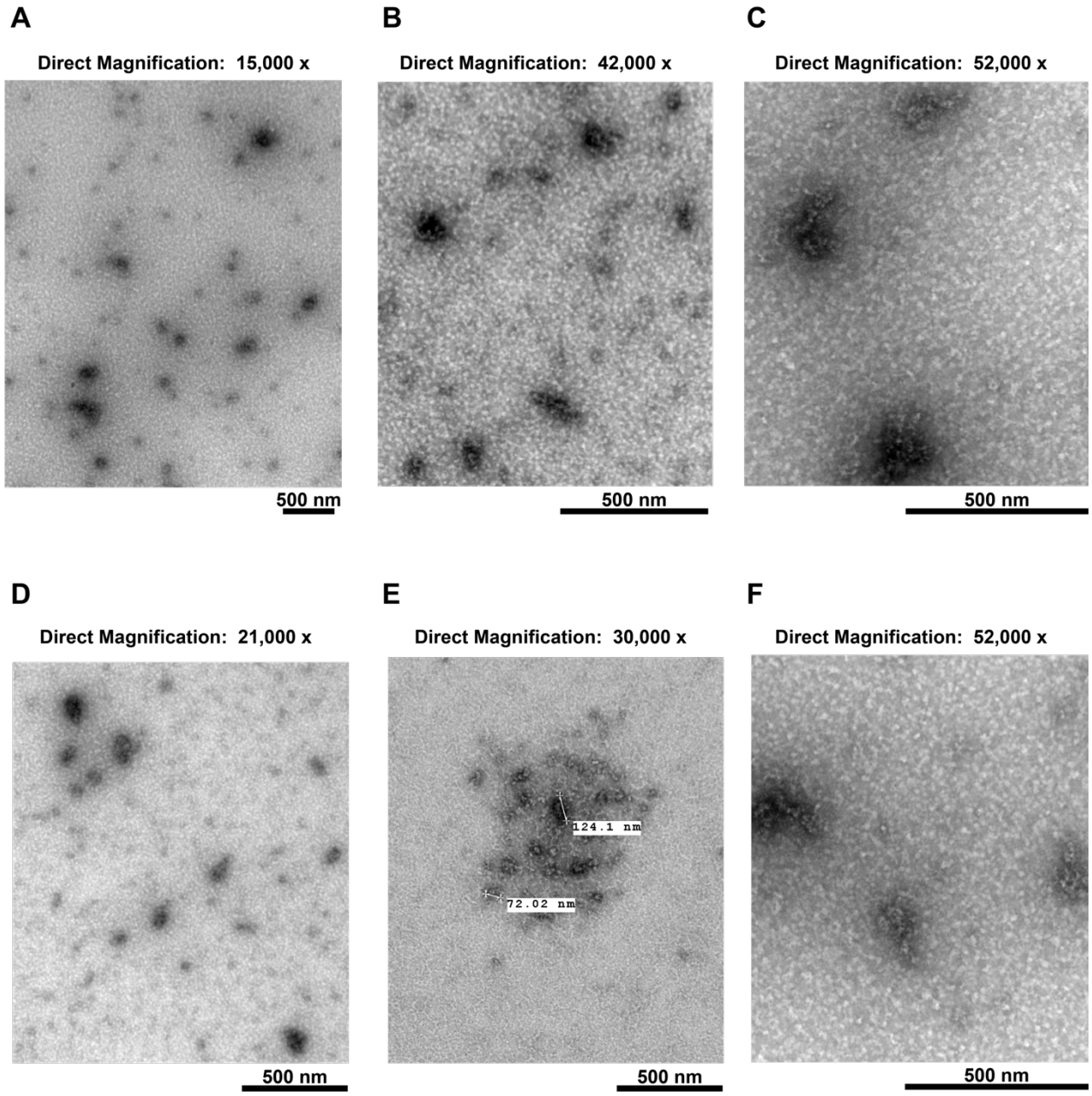

Figure 5.4: TEM micrographs of recombinant DmIKKβ:γ complex showing particles ~75-124 nm in diameter at the indicated magnifications. Each panel is an image of particles located at different positions of the grid. In panel E, measurements indicate approximate size of the particle measured in nanometers (nm).

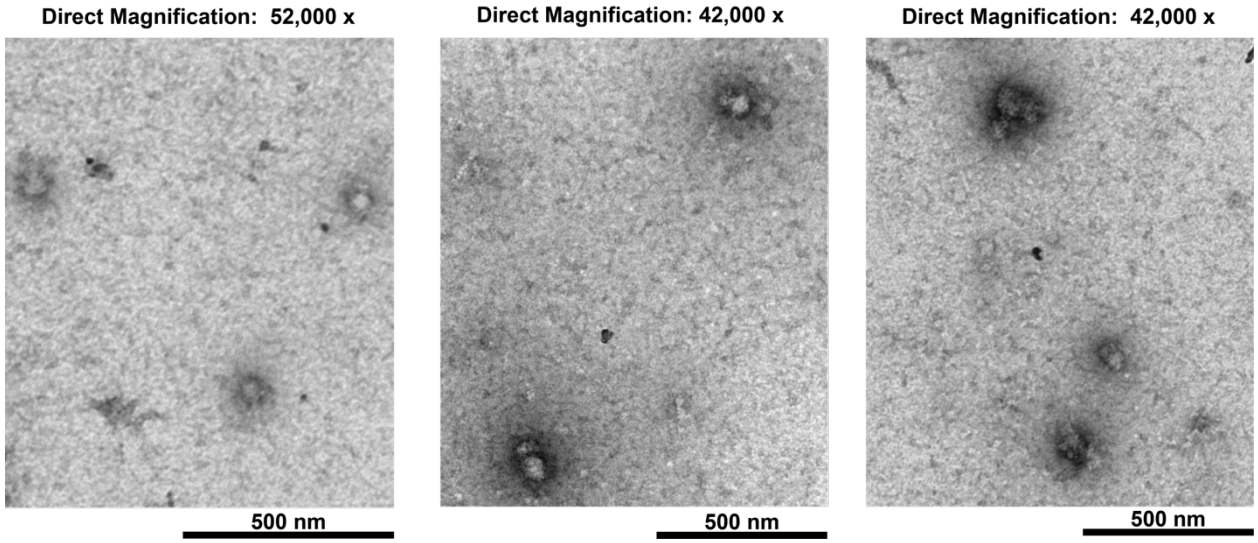

Figure 5.5: TEM micrographs of recombinant DmIKKβ:γ complex showing globular-type particles of ~115-170 nm in length. at the indicated magnifications. Each panel is an image of particles located at different positions of the grid.

Discussion

In negative-stain TEM, we observe particles of different sizes and shape with globular type particles and slightly elongated rugose particles ranging from 75-250 nm in size. Further sample optimization must be done to assess whether this heterogeneity may be due to the complex dissociating upon grid adsorption or whether the chemical composition of the uranyl acetate negative staining agent may be causing deleterious structural effects. For issues on particle dissociation, a chemical crosslinking method called GraFix may improve sample quality (Stark, 2010)

Another reason for the observed heterogeneity despite the sample being “biochemically pure” may be due to intrinsic flexibility in the complex from the primarily alpha-helical and coiled-coil structure of the noncatalytic subunit DmIKKγ. This intrinsic flexibility may be contributing to a broad ensemble of structural conformations that may be obscuring the imaging of precise structural features in the sample. Addition of ligands, substrates, Fab fragments, and small molecule inhibitors as stabilizing agents have been commonly used successfully in high-resolution structural techniques such as x-ray crystallography and also in EM (Maeda et al.,

2018; Vedadi et al., 2006; Wu et al., 2012). It is possible that addition of an IKK complex binding partner may stabilize the complex for structural studies. Our *in silico* and *in vitro* analysis of the DmIKKβ:γ complex revealed the possibility of poly-ubiquitin binding. Addition of poly-ubiquitin may act as a stabilizing agent for the DmIKKβ:γ complex and decrease its conformational heterogeneity that was observed in these EM studies. Future structural work on the DmIKKβ:γ complex utilizing poly-ubiquitin as binding partner may reveal additional details on the regulation mechanism and essential molecular interactions for its biochemistry and catalysis.

REFERENCES

Adams, M. D., Celniker, S. E., Holt, R. A., Evans, C. A., Gocayne, J. D., Amanatides, P. G., Scherer, S. E., Li, P. W., Hoskins, R. A., Galle, R. F., George, R. A., Lewis, S. E., Richards, S., Ashburner, M., Henderson, S. N., Sutton, G. G., Wortman, J. R., Yandell, M. D., Zhang, Q., … Craig Venter, J. (2000). The genome sequence of Drosophila melanogaster. *Science*, *287*(5461), 2185–2195. doi: 10.1126/science.287.5461.2185

Akhouayri, I., Turc, C., Royet, J., & Charroux, B. (2011). Toll-8/tollo negatively regulates antimicrobial response in the drosophila respiratory epithelium. *PLoS Pathogens*, *7*(10). doi: 10.1371/journal.ppat.1002319

Anderson, K. V., Bokla, L., & Nüsslein-Volhard, C. (1985). Establishment of dorsal-ventral polarity in the drosophila embryo: The induction of polarity by the Toll gene product. *Cell*, *42*(3), 791–798. doi: 10.1016/0092-8674(85)90275-2

Anderson, K. V., Jürgens, G., & Nüsslein-Volhard, C. (1985). Establishment of dorsal-ventral polarity in the Drosophila embryo: Genetic studies on the role of the Toll gene product. *Cell*, *42*(3), 779–789. doi: 10.1016/0092-8674(85)90274-0

Anderson, K. V., & Nüsslein-Volhard, C. (1984). Information for the dorsal-ventral pattern of the Drosophila embryo is stored as maternal mRNA. *Nature*, *311*(5983), 223–227. doi: 10.1038/311223a0

Ashkenazy, H., Abadi, S., Martz, E., Chay, O., Mayrose, I., Pupko, T., & Ben-Tal, N. (2016). ConSurf 2016: an improved methodology to estimate and visualize evolutionary conservation in macromolecules. *Nucleic Acids Research*, *44*(W1), W344–W350. doi: 10.1093/nar/gkw408

Ashkenazy, H., Erez, E., Martz, E., Pupko, T., & Ben-Tal, N. (2010). ConSurf 2010: Calculating evolutionary conservation in sequence and structure of proteins and nucleic acids. *Nucleic Acids Research*, *38*(SUPPL. 2), 529–533. doi: 10.1093/nar/gkq399

Åsling, B., Dushay, M. S., & Hultmark, D. (1995). Identification of early genes in the Drosophila immune response by PCR-based differential display: the Attacin A gene and the evolution of attacin-like proteins. *Insect Biochemistry and Molecular Biology*, *25*(4), 511–518. doi: 10.1016/0965-1748(94)00091-C

Bagnéris, C., Ageichik, A.V., Cronin, N., Wallace, B., Collins, M., Boshoff, C., Waksman, G. and Barrett, T. (2008). Crystal structure of a vFlip-IKKγ complex: insights into viral activation of the IKK signalosome. *Molecular cell*, *30*(5), 620-631. doi: 10.1016/j.molcel.2008.04.029

Barnewitz, K., Guo, C., Sevvana, M., Ma, Q., Sheldrick, G. M., Söling, H. D., & Ferrari, D. M. (2004). Mapping of a substrate binding site in the protein bisulfide isomerase-related chaperone wind based on protein function and crystal structure. *Journal of Biological Chemistry*, *279*(38), 39829–39837. doi: 10.1074/jbc.M406839200

Belvin, M. P., & Anderson, K. V. (1996). A conserved signaling pathway: The Drosophila toll-dorsal pathway. *Annual Review of Cell and Developmental Biology*, *12*, 393–416. doi: 10.1146/annurev.cellbio.12.1.393

Belvin, M. P., Jin, Y., & Anderson, K. V. (1995). Cactus protein degradation mediates Drosophila dorsal-ventral signaling. *Genes and Development*, *9*(7), 783–793. doi: 10.1101/gad.9.7.783

Berezin, C., Glaser, F., Rosenberg, J., Paz, I., Pupko, T., Fariselli, P., Casadio, R., & Ben-Tal, N. (2004). ConSeq: The identification of functionally and structurally important residues in protein sequences. *Bioinformatics*, *20*(8), 1322–1324. doi: 10.1093/bioinformatics/bth070

Bergmann, A., Stein, D., Geisler, R., Hagenmaier, S., Schmid, B., Fernandez, N., Schnell, B., & Nüsslein-Volhard, C. (1996). A gradient of cytoplasmic Cactus degradation establishes the nuclear localization gradient of the dorsal morphogen in Drosophila. *Mechanisms of Development*, *60*(1), 109–123. doi: 10.1016/S0925-4773(96)00607-7

Bikker, F. J., Kaman-van Zanten, W. E., De Vries-van De Ruit, A. M. B. C., Voskamp-Visser, I., Van Hooft, P. A. V., Mars-Groenendijk, R. H., De Visser, P. C., & Noort, D. (2006). Evaluation of the antibacterial spectrum of drosocin analogues. *Chemical Biology and Drug Design*, *68*(3), 148–153. doi: 10.1111/j.1747-0285.2006.00424.x

Binggeli, O., Neyen, C., Poidevin, M., & Lemaitre, B. (2014). Prophenoloxidase Activation Is Required for Survival to Microbial Infections in Drosophila. *PLoS Pathogens*, *10*(5). doi: 10.1371/journal.ppat.1004067

Bischoff, V., Vignal, C., Boneca, I. G., Michel, T., Hoffmann, J. A., & Royet, J. (2004). Function of the drosophila pattern-recognition receptor PGRP-SD in the detection of Gram-positive bacteria. *Nature Immunology*, *5*(11), 1175–1180. doi: 10.1038/ni1123

Boman, H. G., Nilsson, I., & Rasmuson, B. (1972). Inducible antibacterial defence system in Drosophila. *Nature*, *237*(5352), 232–235. doi: 10.1038/237232a0

Bonnay, F., Nguyen, X., Cohen-Berros, E., Troxler, L., Batsche, E., Camonis, J., Takeuchi, O., Reichhart, J., & Matt, N. (2014). Akirin specifies NF -κB selectivity of Drosophila innate immune response via chromatin remodeling . *The EMBO Journal*, *33*(20), 2349–2362. doi: 10.15252/embj.201488456

Booth, D. S., Avila-Sakar, A., & Cheng, Y. (2011). Visualizing proteins and macromolecular complexes by negative stain EM: from grid preparation to image acquisition. *Journal of Visualized Experiments : JoVE*, *58*, 1–8. doi: 10.3791/3227

Bowie, A., & O'Neill, L. A. J. (2000). The interleukin-1 receptor/Toll-like receptor superfamily: Signal generators for pro-inflammatory interleukins and microbial products. *Journal of Leukocyte Biology*, *67*(4), 508–514. doi: 10.1002/jlb.67.4.508

Boyce, B. F., Xiu, Y., Li, J., Xing, L., & Yao, Z. (2015). NF-κB-mediated regulation of osteoclastogenesis. *Endocrinology and Metabolism*, *30*(1), 35–44. doi: 10.3803/EnM.2015.30.1.35

Boyer, L., Magoc, L., Dejardin, S., Cappillino, M., Paquette, N., Hinault, C., Charriere, G. M., Ip, W. K. E., Fracchia, S., Hennessy, E., Erturk-Hasdemir, D., Reichhart, J. M., Silverman, N., Lacy-Hulbert, A., & Stuart, L. M. (2011). Pathogen-Derived Effectors Trigger Protective Immunity via Activation of the Rac2 Enzyme and the IMD or Rip Kinase Signaling Pathway. *Immunity*, *35*(4), 536–549. doi: 10.1016/j.immuni.2011.08.015

Buchon, N., Silverman, N., & Cherry, S. (2014). Immunity in Drosophila melanogaster-from microbial recognition to whole-organism physiology. *Nature Reviews Immunology*, *14*(12), 796–810. doi: 10.1038/nri3763

Bulet, P., Dimarcq, J. L., Hetru, C., Lagueux, M., Charlet, M., Hegy, G., Van Dorsselaer, A., & Hoffmann, J. A. (1993). A novel inducible antibacterial peptide of Drosophila carries an O-glycosylated substitution. *Journal of Biological Chemistry*, *268*(20), 14893–14897. doi: 10.1016/s0021-9258(18)82417-6

Bulet, P., Hetru, C., Dimarcq, J. L., & Hoffmann, D. (1999). Antibacterial peptides in insects; structure and function. *Dev Comp Immunol*, *23*, 329–344.

Cammue, B. P. A., De Bolle, M. F. C., Terras, F. R. G., Proost, P., Van Damme, J., Rees, S. B., Vanderleyden, J., & Broekaert, W. F. (1992). Isolation and characterization of a novel class of plant antimicrobial peptides from Mirabilis jalapa L. seeds. *Journal of Biological Chemistry*, *267*(4), 2228–2233. doi: 10.1016/s0021-9258(18)45866-8

Cantacuzène, J. (1923). Célébration du 75me Aniversaire de la Fondation de la Société de Biologie: 48.

Cardoso, M. A., Fontenele, M., Lim, B., Bisch, P. M., Shvartsman, S. Y., & Araujo, H. M. (2017). A novel function for the ικB inhibitor cactus in promoting dorsal nuclear localization and activity in the Drosophila embryo. *Development (Cambridge)*, *144*(16), 2907–2913. doi: 10.1242/dev.145557

Carton, Y., Frey, F., Stanley, D. W., Vass, E., & Nappi, A. J. (2002). Dexamethasone inhibition of the cellular immune response of Drosophila melanogaster against a parasitoid. *Journal of Parasitology*, *88*(2), 405–407. doi: 10.1645/0022-3395(2002)088[0405:diotci]2.0.co;2

Celniker, G., Nimrod, G., Ashkenazy, H., Glaser, F., Martz, E., Mayrose, I., Pupko, T., & Ben-Tal, N. (2013). ConSurf: Using evolutionary data to raise testable hypotheses about protein function. *Israel Journal of Chemistry*, *53*(3–4), 199–206. doi: 10.1002/ijch.201200096

Cha, G.-H., Cho, K. S., Lee, J. H., Kim, M., Kim, E., Park, J., Lee, S. B., & Chung, J. (2003). Discrete Functions of TRAF1 and TRAF2 in Drosophila melanogaster Mediated by c-Jun N-Terminal Kinase and NF-κB-Dependent Signaling Pathways . *Molecular and Cellular Biology*, *23*(22), 7982–7991. doi: 10.1128/mcb.23.22.7982-7991.2003

Chamy, L. El, Hetru, C., & Hoffmann, J. (2010). Invertebrate Innate Immune Defenses. In S. H. E. Kaufman, B. T. Rouse, & D. L. Sacks (Eds.), The Immune Response to Infection (pp. 5–20). doi: 10.1128/9781555816872.ch1

Chamy, L. El, Leclerc, V., Caldelari, I., & Reichhart, J. M. (2008). Sensing of “danger signals” and pathogen-associated molecular patterns defines binary signaling pathways “upstream” of Toll. *Nature Immunology*, *9*(10), 1165–1170. doi: 10.1038/ni.1643

Chang, C. I., Chelliah, Y., Borek, D., Mengin-Lecreulx, D., & Deisanhofer, J. (2006). Structure of tracheal cytotoxin in complex with a heterodimeric pattern-recognition receptor. *Science*, *311*(5768), 1761–1764. doi: 10.1126/science.1123056

Chang, C. I., Ihara, K., Chelliah, Y., Mengin-Lecreulx, D., Wakatsuki, S., & Deisenhofer, J. (2005). Structure of the ectodomain of Drosophila peptidoglycan-recognition protein LCa suggests a molecular mechanism for pattern recognition. *Proceedings of the National Academy of Sciences of the United States of America*, *102*(29), 10279–10284. doi: 10.1073/pnas.0504547102

Charlet, M., Lagueux, M., Reichhart, J. M., Hoffmann, D., Braun, A., & Meister, M. (1996). Cloning of the gene encoding the antibacterial peptide drosocin involved in Drosophila immunity. Expression studies during the immune response. *European Journal of Biochemistry*, *241*(3), 699–706. doi: 10.1111/j.1432-1033.1996.00699.x

Chen, L., Paquette, N., Mamoor, S., Rus, F., Nandy, A., Leszyk, J., Shaffer, S. A., & Silverman, N. (2017). Innate immune signaling in Drosophila is regulated by transforming growth factor β (TGFβ)-activated kinase (Tak1)-triggered ubiquitin editing. *Journal of Biological Chemistry*, *292*(21), 8738–8749. doi: 10.1074/jbc.M117.788158

Chen, Z. J., Parent, L., & Maniatis, T. (1996). Site-specific phosphorylation of IκBα by a novel ubiquitination- dependent protein kinase activity. *Cell*, *84*(6), 853–862. doi: 10.1016/S0092-8674(00)81064-8

Cho, Y. S., Stevens, L. M., & Stein, D. (2010). Pipe-dependent ventral processing of easter by snake is the defining step in drosophila embryo DV axis formation. *Current Biology*, *20*(12), 1133–1137. doi: 10.1016/j.cub.2010.04.056

Choe, K. M., Werner, T., Stöven, S., Hultmark, D., & Anderson, K. V. (2002). Requirement for a peptidoglycan recognition protein (PGRP) in relish activation and antibacterial immune responses in Drosophila. *Science*, *296*(5566), 359–362. doi: 10.1126/science.1070216

Clark, K., Nanda, S., & Cohen, P. (2013). Molecular control of the NEMO family of ubiquitin-binding proteins. *Nature Reviews Molecular Cell Biology*, *14*(10), 673–685. doi: 10.1038/nrm3644

Connelly, M. A., & Marcu, K. B. (1995). CHUK, a new member of the helix-loop-helix and leucine zipper families of interacting proteins, contains a serine-threonine kinase catalytic domain. *Cellular and Molecular Biology Research*, *41*(6), 537–549.

Daigneault, J., Klemetsaune, L., & Wasserman, S. A. (2013). *The IRAK Homolog Pelle Is the Functional Counterpart of I k B Kinase in the Drosophila Toll Pathway*. *8*(9), 1–6. doi: 10.1371/journal.pone.0075150

Delaney, J. R., Stöven, S., Uvell, H., Anderson, K. V., Engström, Y., & Mlodzik, M. (2006). Cooperative control of Drosophila immune responses by the JNK and NF-κB signaling pathways. *EMBO Journal*, *25*(13), 3068–3077. doi: 10.1038/sj.emboj.7601182

DiDonato, J. A., Hayakawa, M., Rothwarf, D. M., Zandi, E., & Karin, M. (1997). A cytokine-responsive IκB kinase that activates the transcription factor NF-κB. *Nature*, *388*(6642), 548–554. doi: 10.1038/41493

Dimarcq, J. -L, Hoffmann, D., Meister, M., Bulet, P., Lanot, R., Reichhart, J. -M, & Hoffmann, J. A. (1994). Characterization and transcriptional profiles of a Drosophila gene encoding an insect defensin: A study in insect immunity. *European Journal of Biochemistry*, *221*(1),

201–209. doi: 10.1111/j.1432-1033.1994.tb18730.x

Drew, D., Shimada, E., Huynh, K., Bergqvist, S., Talwar, R., Karin, M., & Ghosh, G. (2007). Inhibitor κB kinase β binding by inhibitor κB kinase γ. *Biochemistry*, *46*(43), 12482–12490. doi: 10.1021/bi701137a

Dudzic, J. P., Kondo, S., Ueda, R., Bergman, C. M., & Lemaitre, B. (2015). Drosophila innate immunity: Regional and functional specialization of prophenoloxidases. *BMC Biology*, *13*(1), 1–16. doi: 10.1186/s12915-015-0193-6

Dushay, M. S., Åsling, B., & Hultmark, D. (1996). Origins of immunity: Relish, a compound rel-like gene in the antibacterial defense of Drosophila. *Proceedings of the National Academy of Sciences of the United States of America*, *93*(19), 10343–10347. doi: 10.1073/pnas.93.19.10343

Dushay, M. S., Roethele, J. B., Chaverri, J. M., Dulek, D. E., Syed, S. K., Kitami, T., & Eldon, E. D. (2000). Two attacin antibacterial genes of Drosophila melanogaster. *Gene*, *246*(1–2), 49–57. doi: 10.1016/S0378-1119(00)00041-X

Dziarski, R. (2004). Peptidoglycan recognition proteins (PGRPs). *Molecular Immunology*, *40*(12), 877–886. doi: 10.1016/j.molimm.2003.10.011

Ea, C., Deng, L., Xia, Z., Pineda, G., & Chen, Z. J. (2006). *Activation of IKK by TNF a Requires Site-Specific Ubiquitination of RIP1 and Polyubiquitin Binding by NEMO*. 245–257. doi: 10.1016/j.molcel.2006.03.026

Ekengren, S., & Hultmark, D. (1999). Drosophila cecropin as an antifungal agent. *Insect Biochemistry and Molecular Biology*, *29*(11), 965–972. doi: 10.1016/S0965-1748(99)00071-5

Eleftherianos, I., & Revenis, C. (2011). Role and importance of phenoloxidase in insect hemostasis. *Journal of Innate Immunity*, *3*(1), 28–33. doi: 10.1159/000321931

Engström, Y., Kadalayil, L., Sun, S. C., Samakovlis, C., Hultmark, D., & Faye, I. (1993). κB-like motifs regulate the induction of immune genes in Drosophila. In Journal of Molecular Biology (Vol. 232, Issue 2, pp. 327–333). doi: 10.1006/jmbi.1993.1392

Erickson, H. P. (2009). Size and shape of protein molecules at the nanometer level determined by sedimentation, gel filtration, and electron microscopy. *Biological Procedures Online*, *11*(1), 32–51. doi: 10.1007/s12575-009-9008-x

Ertürk-Hasdemir, D., Broemer, M., Leulier, F., Lane, W. S., Paquette, N., Hwang, D., Kim, C., Stöven, S., Meier, P., & Silverman, N. (2009). Two roles for the Drosophila IKK complex in the activation of Relish and the induction of antimicrobial peptide genes. *Proceedings of the National Academy of Sciences of the United States of America*, *106*(24), 9779–9784. doi: 10.1073/pnas.0812022106

Fang, R., Wang, C., Jiang, Q., Lv, M., Gao, P., Yu, X., Mu, P., Zhang, R., Bi, S., Feng, J.-M., & Jiang, Z. (2017). NEMO–IKKβ Are Essential for IRF3 and NF-κB Activation in the cGAS–STING Pathway. *The Journal of Immunology*, *199*(9), 3222–3233. doi: 10.4049/jimmunol.1700699

Faye, I., & Lindberg, B. G. (2016). Towards a paradigm shift in innate immunity—seminal work by Hans G. Boman and co-workers. *Philosophical Transactions of the Royal Society B: Biological Sciences*, *371*(1695). doi: 10.1098/rstb.2015.0303

Fehlbaum, P., Bulet, P., Michaut, L., Lagueux, M., Broekaert, W. F., Hetru, C., & Hoffmann, J. A. (1994). Insect immunity: Septic injury of drosophila induces the synthesis of a potent antifungal peptide with sequence homology to plant antifungal peptides. *Journal of Biological Chemistry*, *269*(52), 33159–33163. doi: 10.1016/s0021-9258(20)30111-3

Ferrandon, D., Imler, J. L., Hetru, C., & Hoffmann, J. A. (2007). The Drosophila systemic immune response: Sensing and signalling during bacterial and fungal infections. In Nature Reviews Immunology (Vol. 7, Issue 11, pp. 862–874). doi: 10.1038/nri2194

Fujita, H., Rahighi, S., Akita, M., Kato, R., Sasaki, Y., Wakatsuki, S., & Iwai, K. (2014). *Mechanism Underlying IκB Kinase Activation Mediated by the Linear*. *34*(7), 1322–1335. doi: 10.1128/MCB.01538-13

Galko, M. J., & Krasnow, M. A. (2004). Cellular and genetic analysis of wound healing in Drosophila larvae. *PLoS Biology*, *2*(8). doi: 10.1371/journal.pbio.0020239

Gandhe, A. S., John, S. H., & Nagaraju, J. (2007). Noduler, A Novel Immune Up-Regulated Protein Mediates Nodulation Response in Insects. *The Journal of Immunology*, *179*(10), 6943–6951. doi: 10.4049/jimmunol.179.10.6943

Ganz, T. (2003). The role of antimicrobial peptides in innate immunity. *Integrative and Comparative Biology*, *43*(2), 300–304. doi: 10.1093/icb/43.2.300

Gay, N. J., & Keith, F. J. (1991). Drosophila Toll and Il-1 receptor. *Nature*, *351*, 355–356.

Ghosh, G., Wang, V. Y. F., Huang, D. Bin, & Fusco, A. (2012). NF-kB regulation: Lessons from structures. *Immunological Reviews*, *246*(1), 36–58. doi: 10.1111/j.1600-065X.2012.01097.x

Gilmore, T. D., & Wolenski, F. S. (2012). NF-kappaB: where did it come from and why? *Immunol Rev*, *246*(1), 14–35. doi: 10.1111/j.1600-065X.2012.01096.x

Glaser, F., Pupko, T., Paz, I., Bell, R. E., Bechor-Shental, D., Martz, E., & Ben-Tal, N. (2003). ConSurf: Identification of functional regions in proteins by surface-mapping of phylogenetic information. *Bioinformatics*, *19*(1), 163–164. doi: 10.1093/bioinformatics/19.1.163

Gobert, V., Gottar, M., Matskevich, A. A., Rutschmann, S., Royet, J., Belvin, M., Hoffmann, J. A., & Ferrandon, D. (2003). Dual Activation of the Drosophila Toll Pathway by Two Pattern Recognition Receptors. *Science*, *302*(5653), 2126–2130. doi: 10.1126/science.1085432

Goto, A., Kumagai, T., Kumagaie, C., Hirose, J., Narita, H., Hitoshi, M., Tatsuhiko, K., Beck, K., & Kitagawa, Y. (2001). A Drosophila haemocyte-specific protein, hemolectin, similar to human von Willebrand factor. *Biochemical Journal*, *359*, 99–108. doi: 10.1017/CBO9780511546198.103

Goto, A., Okado, K., Martins, N., Cai, H., Barbier, V., Lamiable, O., Troxler, L., Santiago, E., Kuhn, L., Paik, D., Silverman, N., Holleufer, A., Hartmann, R., Liu, J., Peng, T., Hoffmann,

J. A., Meignin, C., Daeffler, L., & Imler, J.-L. (2018). The Kinase IKKβ Regulates a STING- and NF-κB-Dependent Antiviral Response Pathway in Drosophila. *Immunity*, 225–234. doi: 10.1016/j.immuni.2018.07.013

Gottar, M., Gobert, V., Matskevich, A. A., Reichhart, J. M., Wang, C., Butt, T. M., Belvin, M., Hoffmann, J. A., & Ferrandon, D. (2006). Dual Detection of Fungal Infections in Drosophila via Recognition of Glucans and Sensing of Virulence Factors. *Cell*, *127*(7), 1425–1437. doi: 10.1016/j.cell.2006.10.046

Gregorio, E. De, Spellman, P. T., Tzou, P., Rubin, G. M., & Lemaitre, B. (2002). *The Toll and Imd pathways are the major regulators of the immune response in Drosophila*. *21*(11).

Gross, I., Georgel, P., Kappler, C., Reichhart, J. M., & Hoffmann, J. A. (1996). Drosophila immunity: A comparative analysis of the Rel proteins dorsal and Dif in the induction of the genes encoding diptericin and cecropin. *Nucleic Acids Research*, *24*(7), 1238–1245. doi: 10.1093/nar/24.7.1238

Hadian, K., Griesbach, R. a., Dornauer, S., Wanger, T. M., Nagel, D., Metlitzky, M., Beisker, W., Schmidt-Supprian, M., & Krappmann, D. (2011). NF-κB essential modulator (NEMO) interaction with linear and Lys-63 ubiquitin chains contributes to NF-κB activation. *Journal of Biological Chemistry*, *286*(29), 26107–26117. doi: 10.1074/jbc.M111.233163

Hanson, M. A., & Lemaitre, B. (2020). New insights on Drosophila antimicrobial peptide function in host defense and beyond. *Current Opinion in Immunology*, *62*, 22–30. doi: 10.1016/j.coi.2019.11.008

Hashimoto, C., Hudson, K. L., & Anderson, K. V. (1988). The Toll gene of drosophila, required for dorsal-ventral embryonic polarity, appears to encode a transmembrane protein. *Cell*, *52*(2), 269–279. doi: 10.1016/0092-8674(88)90516-8

Hatada, E. N., Nieters, A., Wulczyn, F. G., Naumann, M., Meyer, R., Nuciforat, G., Mckeithant, T. W., & Scheidereit, C. (1992). *The ankyrin repeat domains of the*. *89*(March), 2489–2493.

Hayden, M. S., & Ghosh, S. (2012). NF-κB, the first quarter-century: Remarkable progress and outstanding questions. *Genes and Development*, *26*(3), 203–234. doi: 10.1101/gad.183434.111

Hedengren, M., Åsling, B., Dushay, M. S., Ando, I., Ekengren, S., Wihlborg, M., & Hultmark, D. (1999). Relish, a central factor in the control of humoral but not cellular immunity in Drosophila. *Molecular Cell*, *4*(5), 827–837. doi: 10.1016/S1097-2765(00)80392-5

Hedges, S. B., Dudley, J., & Kumar, S. (2006). TimeTree: A public knowledge-base of divergence times among organisms. *Bioinformatics*, *22*(23), 2971–2972. doi: 10.1093/bioinformatics/btl505

Heil, M., & Land, W. G. (2014). Danger signals – Damaged-self recognition across the tree of life. *Frontiers in Plant Science*, *5*(October), 1–16. doi: 10.3389/fpls.2014.00578

Hillyer, J. F. (2016). Insect immunology and hematopoiesis. *Developmental and Comparative Immunology*, *58*(8), 102–118. doi: 10.1016/j.dci.2015.12.006

Hoffmann, D., Brehelin, M., & Hoffmann, J. A. (1974). Modifications of the hemogram and of the hemocytopoietic tissue of male adults of Locusta migratoria (Orthoptera) after injection of Bacillus thuringiensis. *Journal of Invertebrate Pathology*, *24*(2), 238–247. doi: 10.1016/0022-2011(74)90017-2

Hoffmann, J. (2011). *The Host Defense of Insects : A Paradigm*. 3–35.

Hoffmann, J. A., Kafatos, F. C., Janeway, C. A., & Ezekowitz, R. A. B. (1999). Phylogenetic perspectives in innate immunity. In Science (Vol. 284, Issue 5418, pp. 1313–1318). doi: 10.1126/science.284.5418.1313

Hoffmann, J. A., & Reichhart, J. (2002). Innate Immunity: an Evolutionary Perspective. *Molecular and Cellular Biology*, *3*(2), 121–126. Retrieved from https://vpn.rz.uni-kiel.de/proxy/313d9f69/https/www.nature.com/articles/ni0202-121.pdf

Honda, K., Takaoka, A., & Taniguchi, T. (2006). Type I Inteferon Gene Induction by the Interferon Regulatory Factor Family of Transcription Factors. *Immunity*, *25*(3), 349–360. doi: 10.1016/j.immuni.2006.08.009

Hu, S., & Yang, X. (2000). dFADD, A novel death domain-containing adapter protein for the Drosophila caspase DREDD. *Journal of Biological Chemistry*, *275*(40), 30761–30764. doi: 10.1074/jbc.C000341200

Hu, X., Yagi, Y., Tanji, T., Zhou, S., & Ip, Y. T. (2004). Multimerization interaction of Toll and Spätzle in Drosophila. *Proceedings of the National Academy of Sciences of the United States of America*, *101*(25), 9369–9374. doi: 10.1073/pnas.0307062101

Hultmark, D., Engström, A., Andersson, K., Steiner, H., Bennich, H., & Boman, H. G. (1983). Insect immunity. Attacins, a family of antibacterial proteins from Hyalophora cecropia. *The EMBO Journal*, *2*(4), 571–576. doi: 10.1002/j.1460-2075.1983.tb01465.x

Hultmark, Dan, Engström, Å., Bennich, H., Kapur, R., & Boman, H. G. (1982). Insect immunity: isolation and structure of cecropin D and four minor antibacterial components from Cecropia pupae. *Eur. J. Biochem.*, *127*, 207–217.

Huxford, T., & Ghosh, G. (2009). A structural guide to proteins of the NF-kappaB signaling module. In Cold Spring Harbor perspectives in biology (Vol. 1, Issue 3, pp. 1–17). doi: 10.1101/cshperspect.a000075

Imler, J. (2014). Overview of Drosophila immunity : A historical perspective. *Developmental and Comparative Immunology*, *42*(1), 3–15. doi: 10.1016/j.dci.2013.08.018

Imler, J. L., & Bulet, P. (2005). Antimicrobial peptides in Drosophila: Structures, activities and gene regulation. *Chemical Immunology and Allergy*, *86*(1), 1–21. doi: 10.1159/000086648

Imler, J. L., & Hoffmann, J. A. (2000). Signaling mechanisms in the antimicrobial host defense of Drosophila. *Current Opinion in Microbiology*, *3*(1), 16–22. doi: 10.1016/S1369-5274(99)00045-4

Ip, Y. T., Reach, M., Engstrom, Y., Gonzalez-crespo, S., & Tatei, K. (1993). *Dif , a dorsal-Related Gene That Mediates an Immune Response in Drosophila*. *75*(or dl), 753–763.

Irving, P., Troxler, L., Heuer, T. S., Belvin, M., Kopczynski, C., Reichhart, J. M., Hoffmann, J. A., & Hetru, C. (2001). A genome-wide analysis of immune responses in Drosophila. *Proceedings of the National Academy of Sciences of the United States of America*, *98*(26), 15119–15124. doi: 10.1073/pnas.261573998

Janeway, C. A. (1989). Approaching the asymptote? Evolution and revolution in immunology. *Cold Spring Harbor Symposia on Quantitative Biology*, *54*(1), 4475–4487. doi: 10.1101/sqb.1989.054.01.003

Ji, Y., Thomas, C., Tulin, N., Lodhi, N., Kolenko, V., Tulin, A. V, & Tulin, A. V. (2020). *Charon Mediates Immune Deficiency − Driven PARP-1 − Dependent Immune Responses in Drosophila*. doi: 10.4049/jimmunol.1600994

Jung, S. H., Evans, C. J., Uemura, C., & Banerjee, U. (2005). The Drosophila lymph gland as a developmental model of hematopoiesis. *Development*, *132*(11), 2521–2533. doi: 10.1242/dev.01837

Kambris, Z., Brun, S., Jang, I. H., Nam, H. J., Romeo, Y., Takahashi, K., Lee, W. J., Ueda, R., & Lemaitre, B. (2006). Drosophila Immunity: A Large-Scale In Vivo RNAi Screen Identifies Five Serine Proteases Required for Toll Activation. *Current Biology*, *16*(8), 808–813. doi: 10.1016/j.cub.2006.03.020

Kaneko, T., & Silverman, N. (2005). Bacterial recognition and signalling by the Drosophila IMD pathway. *Cellular Microbiology*, *7*(4), 461–469. doi: 10.1111/j.1462-5822.2005.00504.x

Kang, D., Liu, G., Lundström, A., Gelius, E., & Steiner, H. (1998). A peptidoglycan recognition protein in innate immunity conserved from insects to humans. *Proceedings of the National Academy of Sciences of the United States of America*, *95*(17), 10078–10082. doi: 10.1073/pnas.95.17.10078

Kappler, C., Meister, M., Lagueux, M., Gateff, E., Hoffmann, J. A., & Reichhart, J. M. (1993). Insect immunity: Two 17 bp repeats nesting a χB-related sequence confer inducibility to the diptericin gene and bind a polypeptide in bacteria-challenged Drosophila. *EMBO Journal*, *12*(4), 1561–1568. doi: 10.1002/j.1460-2075.1993.tb05800.x

Karin, M., & Delhase, M. (2000). The IκB kinase (IKK) and NF-κB: Key elements of proinflammatory signalling. *Seminars in Immunology*, *12*(1), 85–98. doi: 10.1006/smim.2000.0210

Karin, Michael. (1999). How NF-κB is activated: The role of the IκB kinase (IKK) complex. *Oncogene*, *18*(49), 6867–6874. doi: 10.1038/sj.onc.1203219

Karin, Michael, & Ben-neriah, Y. (2000). Phosphorylation meets ubiquitination: the control of NF-κB activity. *Annual Review of Immunology*, 621–663. doi: DOI: 10.1146/annurev.immunol.18.1.621

Kensche, T., Tokunaga, F., Ikeda, F., Goto, E., Iwai, K., & Dikic, I. (2012). Analysis of nuclear factor-κB (NF-κB) essential modulator (NEMO) binding to linear and lysine-linked ubiquitin chains and its role in the activation of NF-κB. *Journal of Biological Chemistry*, *287*(28), 23626–23634. doi: 10.1074/jbc.M112.347195

Kim, Y. S., Han, S. J., Ryu, J. H., Choi, K. H., Hong, Y. S., Chung, Y. H., Perrot, S., Raibaud, A., Brey, P. T., & Lee, W. J. (2000). Lipopolysaccharide-activated kinase, an essential component for the induction of the antimicrobial peptide genes in Drosophila melanogaster cells. *Journal of Biological Chemistry*, *275*(3), 2071–2079. doi: 10.1074/jbc.275.3.2071

Kishore, N., Khai Huynh, Q., Mathialagan, S., Hall, T., Rouw, S., Creely, D., Lange, G., Caroll, J., Reitz, B., Donnelly, A., Boddupalli, H., Combs, R. G., Kretzmer, K., & Tripp, C. S. (2002). IKK-i and TBK-1 are enzymatically distinct from the homologous enzyme IKK-2. Comparative analysis of recombinant human IKK-i, TBK-1, and IKK-2. *Journal of Biological Chemistry*, *277*(16), 13840–13847. doi: 10.1074/jbc.M110474200

Kleino, A., Ramia, N. F., Bozkurt, G., Shen, Y., Nailwal, H., Huang, J., Napetschnig, J., Gangloff, M., Chan, F. K. M., Wu, H., Li, J., & Silverman, N. (2017). Peptidoglycan-Sensing Receptors Trigger the Formation of Functional Amyloids of the Adaptor Protein Imd to Initiate Drosophila NF-κB Signaling. *Immunity*, *47*(4), 635-647.e6. doi: 10.1016/j.immuni.2017.09.011

Kleino, A., & Silverman, N. (2014). The Drosophila IMD pathway in the activation of the humoral immune response. *Developmental and Comparative Immunology*, *42*(1), 25–35. doi: 10.1016/j.dci.2013.05.014

Kleino, A., & Silverman, N. (2019). Regulation of the Drosophila Imd pathway by signaling amyloids. *Insect Biochemistry and Molecular Biology*, *108*(February), 16–23. doi: 10.1016/j.ibmb.2019.03.003

Kleino, A., Valanne, S., Ulvila, J., Kallio, J., Myllymäki, H., Enwald, H., Stöven, S., Poidevin, M., Ueda, R., Hultmark, D., Lemaitre, B., & Rämet, M. (2005). Inhibitor of apoptosis 2 and TAK1-binding protein are components of the Drosophila Imd pathway. *EMBO Journal*, *24*(19), 3423–3434. doi: 10.1038/sj.emboj.7600807

Ko, M. S., Biswas, T., Mulero, M. C., Bobkov, A. A., Ghosh, G., & Huxford, T. (2020). Structurally plastic NEMO and oligomerization prone IKK2 subunits define the behavior of human IKK2:NEMO complexes in solution. *Biochimica et Biophysica Acta - Proteins and Proteomics*, *1868*(12). doi: 10.1016/j.bbapap.2020.140526

Kobayashi, A., Matsui, M., Kubo, T., & Natori, S. (1993). Purification and characterization of a 59-kilodalton protein that specifically binds to NF-kappa B-binding motifs of the defense protein genes of Sarcophaga peregrina (the flesh fly). *Molecular and Cellular Biology*, *13*(7), 4049–4056. doi: 10.1128/mcb.13.7.4049

Komander, D., Reyes-Turcu, F., Licchesi, J. D. F., Odenwaelder, P., Wilkinson, K. D., & Barford, D. (2009). Molecular discrimination of structurally equivalent Lys 63-linked and linear polyubiquitin chains. *EMBO Reports*, *10*(5), 466–473. doi: 10.1038/embor.2009.55

Kumar, S., & Hedges, S. B. (2011). Timetree2: Species divergence times on the iPhone. *Bioinformatics*, *27*(14), 2023–2024. doi: 10.1093/bioinformatics/btr315

Kumar, S., Stecher, G., Suleski, M., & Hedges, S. B. (2017). TimeTree: A Resource for Timelines, Timetrees, and Divergence Times. *Molecular Biology and Evolution*, *34*(7), 1812–1819. doi: 10.1093/molbev/msx116

Kunji, E. R. S., Harding, M., Butler, P. J. G., & Akamine, P. (2008). Determination of the molecular mass and dimensions of membrane proteins by size exclusion chromatography. In Methods (Vol. 46, Issue 2, pp. 62–72). Elsevier Inc. doi: 10.1016/j.ymeth.2008.10.020

Kylsten, P., Samakovlis, C., & Hultmark, D. (1990). The cecropin locus in Drosophila; A compact gene cluster involved in the response to infection. *EMBO Journal*, *9*(1), 217–224. doi: 10.1002/j.1460-2075.1990.tb08098.x

Lagueux, M., Perrodou, E., Levashina, E. A., Capovilla, M., & Hoffmann, J. A. (2000). Constitutive expression of a complement-like protein in Toll and JAK gain-of-function mutants of Drosophila. *Proceedings of the National Academy of Sciences of the United States of America*, *97*(21), 11427–11432. doi: 10.1073/pnas.97.21.11427

Landau, M., Mayrose, I., Rosenberg, Y., Glaser, F., Martz, E., Pupko, T., & Ben-Tal, N. (2005). ConSurf 2005: The projection of evolutionary conservation scores of residues on protein structures. *Nucleic Acids Research*, *33*(SUPPL. 2), 299–302. doi: 10.1093/nar/gki370

Larabi, A., Devos, J. M., Ng, S., Nanao, M. H., Round, A., Maniatis, T., & Panne, D. (2013). Article Crystal Structure and Mechanism of Activation of TANK-Binding Kinase 1. *CellReports*, *3*(3), 734–746. doi: 10.1016/j.celrep.2013.01.034

Lemaitre, B. (2004). The road to Toll. *Nature Reviews Immunology*, *4*(7), 521–527. doi: 10.1038/nri1390

Lemaitre, B., & Hoffmann, J. (2007). The host defense of Drosophila melanogaster. In Annual Review of Immunology (Vol. 25, pp. 697–743). doi: 10.1146/annurev.immunol.25.022106.141615

Lemaitre, B., Kromer-metzger, E., Michaut, L., Nicolas, E., Meister, M., Georgel, P., Reichhart, J., & Hoffmann, J. A. (1995). *A recessive mutation , immune deficiency (imd), defines two distinct control pathways in the Drosophila host defense*. *92*(October), 9465–9469.

Lemaitre, B., Nicolas, E., Michaut, L., Reichhart, J. M., & Hoffmann, J. A. (1996). The dorsoventral regulatory gene cassette spatzle/Toll/Cactus controls the potent antifungal response in Drosophila adults. *Cell*, *86*(6), 973–983. doi: 10.1016/S0092-8674(00)80172-5

Leone, P., Bischoff, V., Kellenberger, C., Hetru, C., Royet, J., & Roussel, A. (2008). Crystal structure of Drosophila PGRP-SD suggests binding to DAP-type but not lysine-type peptidoglycan. *Molecular Immunology*, *45*(9), 2521–2530. doi: 10.1016/j.molimm.2008.01.015

Leulier, F., Rodriguez, A., Khush, R. S., Abrams, J. M., & Lemaitre, B. (2000). The Drosophila caspase Dredd is required to resist Gram-negative bacterial infection. *EMBO Reports*, *1*(4), 353–358. doi: 10.1093/embo-reports/kvd073

Levashina, E. A., Ohresser, S., Bulet, P., Reichhart, J. -M, Hetru, C., & Hoffmann, J. A. (1995). Metchnikowin, a Novel Immune-Inducible Proline-Rich Peptide from Drosophila with Antibacterial and Antifungal Properties. *European Journal of Biochemistry*, *233*(2), 694–700. doi: 10.1111/j.1432-1033.1995.694_2.x

Li, Q., Van Antwerp, D., Mercurio, F., Lee, K.-F., & Verma, I. M. (1999). Severe Liver Degeneration in Mice Lacking the IκB Kinase 2 Gene. *Science*, *284*(5412), 321–325. doi: 10.1126/science.284.5412.321

Li, X.-D., Wu, J., Gao, D., Wang, H., Sun, L., & Chen, Z. J. (2013). Pivotal Roles of cGAS-cGAMP Signaling in Antiviral Defense and Immune Adjuvant Effects. *Science*, *341*(6152), 1390–1394.

Li, Y., Kang, J., Friedman, J., Tarassishin, L., Ye, J., Kovalenko, A., Wallach, D., & Horwitz, M. S. (1999). Identification of a cell protein (FIP-3) as a modulator of NF-κB activity and as a target of an adenovirus inhibitor of tumor necrosis factor α-induced apoptosis. *Proceedings of the National Academy of Sciences of the United States of America*, *96*(3), 1042–1047. doi: 10.1073/pnas.96.3.1042

Li, Z. W., Chu, W., Hu, Y., Delhase, M., Deerinck, T., Ellisman, M., Johnson, R., & Karin, M. (1999). The IKKβ subunit of IκB kinase (IKK) is essential for nuclear factor κB activation and prevention of apoptosis. *Journal of Experimental Medicine*, *189*(11), 1839–1845. doi: 10.1084/jem.189.11.1839

Liang, C., Zhang, M., & Sun, S. C. (2006). β-TrCP binding and processing of NF-κB2/p100 involve its phosphorylation at serines 866 and 870. *Cellular Signalling*, *18*(8), 1309–1317. doi: 10.1016/j.cellsig.2005.10.011

Liu, S., Liu, H., Johnston, A., Hanna-Addams, S., Reynoso, E., Xiang, Y., & Wang, Z. (2017). MLKL forms disulfide bond-dependent amyloid-like polymers to induce necroptosis. *Proceedings of the National Academy of Sciences of the United States of America*, *114*(36), E7450–E7459. doi: 10.1073/pnas.1707531114

Liu, S., Misquitta, Y.R., Olland, A., Johnson, M.A., Kelleher, K.S., Kriz, R., Lin, L.L., Stahl, M. & Mosyak, L. (2013). Crystal structure of a human IκB kinase β asymmetric dimer. *Journal of Biological Chemistry*, *288*(31), 22758-22767. doi: 10.1074/jbc.M113.482596

Liu, T., Zhang, L., Joo, D., & Sun, S. C. (2017). NF-κB signaling in inflammation. In Signal Transduction and Targeted Therapy (Vol. 2, Issue April). doi: 10.1038/sigtrans.2017.23

Lo, Y., Lin, S., Rospigliosi, C. C., Conze, D. B., Wu, C., Ashwell, J. D., Eliezer, D., & Wu, H. (2009). Article Structural Basis for Recognition of Diubiquitins by NEMO. *Molecular Cell*, *33*(5), 602–615. doi: 10.1016/j.molcel.2009.01.012

Loof, T. G., Mörgelin, M., Johansson, L., Oehmcke, S., Olin, A. I., Dickneite, G., Norrby-Teglund, A., Theopold, U., & Herwald, H. (2011). Coagulation, an ancestral serine protease cascade, exerts a novel function in early immune defense. *Blood*, *118*(9), 2589–2598. doi: 10.1182/blood-2011-02-337568

Lopez, M. A., Meier, D., Wong, W. W. L., & Fontana, A. (2016). TNF induced inhibition of Cirbp expression depends on RelB NF-κB signalling pathway. *Biochemistry and Biophysics Reports*, *5*, 22–26. doi: 10.1016/j.bbrep.2015.11.007

Lorand, L., & Graham, R. M. (2003). Transglutaminases: Crosslinking enzymes with pleiotropic functions. *Nature Reviews Molecular Cell Biology*, *4*(2), 140–156. doi: 10.1038/nrm1014

Lu, Y., Wu, L. P., & Anderson, K. V. (2001). The antibacterial arm of the Drosophila innate immune response requires an IκB kinase. *Genes and Development*, *15*(1), 104–110. doi: 10.1101/gad.856901

Luo, C., Shen, B., Manley, J. L., & Zheng, L. (2001). Tehao functions in the Toll pathway in Drosophila melanogaster: Possible roles in development and innate immunity. *Insect Molecular Biology*, *10*(5), 457–464. doi: 10.1046/j.0962-1075.2001.00284.x

Maeda, S., Koehl, A., Matile, H., Hu, H., Hilger, D., Schertler, G. F. X., Manglik, A., Skiniotis, G., Dawson, R. J. P., & Kobilka, B. K. (2018). Development of an antibody fragment that stabilizes GPCR/G-protein complexes. *Nature Communications*, *9*(1), 1–9. doi: 10.1038/s41467-018-06002-w

Makris, C., Godfrey, V. L., Krähn-Senftleben, G., Takahashi, T., Roberts, J. L., Schwarz, T., Feng, L., Johnson, R. S., & Karin, M. (2000). Female mice heterozygous for IKKγ/NEMO deficiencies develop a dermatopathy similar to the human X-linked disorder incontinentia pigmenti. *Molecular Cell*, *5*(6), 969–979. doi: 10.1016/S1097-2765(00)80262-2

Manfruelli, P., Reichhart, J. M., Steward, R., Hoffmann, J. A., & Lemaitre, B. (1999). A mosaic analysis in Drosophila fat body cells of the control of antimicrobial peptide genes by the Rel proteins Dorsal and DIF. *EMBO Journal*, *18*(12), 3380–3391. doi: 10.1093/emboj/18.12.3380

Mapalo, M. A., Arakawa, K., Baker, C. M., Persson, D. K., Mirano-Bascos, D., & Giribet, G. (2020). The unique antimicrobial recognition and signaling pathways in tardigrades with a comparison across ecdysozoa. *G3: Genes, Genomes, Genetics*, *10*(3), 1137–1148. doi: 10.1534/g3.119.400734

Mathes, E., Wang, L., Komives, E., & Ghosh, G. (2010). Flexible regions within IκBα create the ubiquitin-independent degradation signal. *Journal of Biological Chemistry*, *285*(43), 32927–32936. doi: 10.1074/jbc.M110.107326

May, M. J., Marienfeld, R. B., & Ghosh, S. (2002). Characterization of the IκB-kinase NEMO binding domain. *Journal of Biological Chemistry*, *277*(48), 45992–46000. doi: 10.1074/jbc.M206494200

Medzhitov, R., Preston-Hurlburt, P., & Janeway, C. A. (1997). A human homologue of the Drosophila toll protein signals activation of adaptive immunity. *Nature*, *388*(6640), 394–397. doi: 10.1038/41131

Meinander, A., Runchel, C., Tenev, T., Chen, L., Kim, C. H., Ribeiro, P. S., Broemer, M., Leulier, F., Zvelebil, M., Silverman, N., & Meier, P. (2012). Ubiquitylation of the initiator caspase DREDD is required for innate immune signalling. *EMBO Journal*, *31*(12), 2770–2783. doi: 10.1038/emboj.2012.121

Meng, X., Khanuja, B. S., & Ip, Y. T. (1999). Toll receptor-mediated Drosophila immune response requires Dif, an NF- κB factor. *Genes and Development*, *13*(7), 792–797. doi: 10.1101/gad.13.7.792

Mercurio, F., Murray, B. W., Shevchenko, A., Bennett, B. L., Young, D. B., Li, J. W., Pascual, G., Motiwala, A., Zhu, H., Mann, M., & Manning, A. M. (1999). IκB Kinase (IKK)-Associated

Protein 1, a Common Component of the Heterogeneous IKK Complex. *Molecular and Cellular Biology*, *19*(2), 1526–1538. doi: 10.1128/mcb.19.2.1526

Mercurio, F., Zhu, H., Murray, B. W., Shevchenko, A., Bennett, B. L., Li, J. W., Young, D. B., Barbosa, M., Mann, M., Manning, A., & Rao, A. (1997). IKK-1 and IKK-2: Cytokine-activated IκB kinases essential for NF-κB activation. *Science*, *278*(5339), 860–866. doi: 10.1126/science.278.5339.860

Metalnikov, S. I. (1927). Infection microbienne et l'immunité chez la mite des abeilles Galleria mellonella. Monographie de l'Institut Pasteur. Editeur Masson, 8(139).

Michaut, L., Fehlbaum, P., Moniatte, M., Van Dorsselaer, A., Reichhart, J. M., & Bulet, P. (1996). Determination of the disulfide array of the first inducible antifungal peptide from insects: Drosomycin from Drosophila melanogaster. *FEBS Letters*, *395*(1), 6–10. doi: 10.1016/0014-5793(96)00992-1

Ming, M., Obata, F., Kuranaga, E., & Miura, M. (2014). Persephone/Spätzle pathogen sensors mediate the activation of toll receptor signaling in response to endogenous danger signals in apoptosis-deficient Drosophila. *Journal of Biological Chemistry*, *289*(11), 7558–7568. doi: 10.1074/jbc.M113.543884

Mishima, Y., Quintin, J., Aimanianda, V., Kellenberger, C., Coste, F., Clavaud, C., Hetru, C., Hoffmann, J. A., Latge, J. P., Ferrandon, D., & Roussel, A. (2009). The N-terminal domain of Drosophila gram-negative binding protein 3 (GNBP3) defines a novel family of fungal pattern recognition receptors. *Journal of Biological Chemistry*, *284*(42), 28687–28697. doi: 10.1074/jbc.M109.034587

Morris, O., Liu, X., Domingues, C., Pennetta, G., Buchon, N., Morris, O., Liu, X., Domingues, C., Runchel, C., Chai, A., Basith, S., & Tenev, T. (2016). Signal Integration by the I k B Protein Pickle Shapes Drosophila Innate Host Defense Article Signal Integration by the I k B Protein Pickle Shapes Drosophila Innate Host Defense. *Cell Host and Microbe*, *20*(3), 283–295. doi: 10.1016/j.chom.2016.08.003

Nakajima, Y., Qu, X. M., & Natori, S. (1987). Interaction between liposomes and sarcotoxin IA, a potent antibacterial protein of Sarcophaga peregrina (flesh fly). *Journal of Biological Chemistry*, *262*(4), 1665–1669. doi: 10.1016/s0021-9258(19)75688-9

Nakamoto, M., Moy, R. H., Xu, J., Bambina, S., Yasunaga, A., Shelly, S. S., Gold, B., & Cherry, S. (2012). Virus Recognition by Toll-7 Activates Antiviral Autophagy in Drosophila. *Immunity*, *36*(4), 658–667. doi: 10.1016/j.immuni.2012.03.003

Nakatsuji, T., & Gallo, R. L. (2012). Antimicrobial peptides: Old molecules with new ideas. *Journal of Investigative Dermatology*, *132*(3 PART 2), 887–895. doi: 10.1038/jid.2011.387

Nam, H. J., Jang, I. H., Asano, T., & Lee, W. J. (2008). Involvement of pro-phenoloxidase 3 in lamellocyte-meidated spontaneous melanization in Drosophila. *Molecules and Cells*, *26*(6), 606–610.

Nappi, A. J., Vass, E., Frey, F., & Carton, Y. (1995). Superoxide anion generation in Drosophila during melanotic encapsulation of parasites. *European Journal of Cell Biology*, *68*(4), 450–

456.

Neyen, C., Poidevin, M., Roussel, A., & Lemaitre, B. (2012). Tissue- and Ligand-Specific Sensing of Gram-Negative Infection in Drosophila by PGRP-LC Isoforms and PGRP-LE . *The Journal of Immunology*, *189*(4), 1886–1897. doi: 10.4049/jimmunol.1201022

Ooi, J. Y., Yagi, Y., Hu, X., & Ip, Y. T. (2002). The Drosophila Toll-9 activates a constitutive antimicrobial defense. *EMBO Reports*, *3*(1), 82–87. doi: 10.1093/embo-reports/kvf004

Pahl, H. L. (1999). Activators and target genes of Rel/NF-κB transcription factors. In Oncogene (Vol. 18, Issue 49, pp. 6853–6866). doi: 10.1038/sj.onc.1203239

Paquette, N., Broemer, M., Aggarwal, K., Chen, L., Husson, M., Ertürk-Hasdemir, D., Reichhart, J. M., Meier, P., & Silverman, N. (2010). Caspase-Mediated Cleavage, IAP Binding, and Ubiquitination: Linking Three Mechanisms Crucial for Drosophila NF-κB Signaling. *Molecular Cell*, *37*(2), 172–182. doi: 10.1016/j.molcel.2009.12.036

Parthier, C., Stelter, M., Ursel, C., Fandrich, U., Lilie, H., Breithaupt, C., & Stubbs, M. T. (2014). Structure of the Toll-Spätzle complex, a molecular hub in Drosophila development and innate immunity. *Proceedings of the National Academy of Sciences of the United States of America*, *111*(17), 6281–6286. doi: 10.1073/pnas.1320678111

Parvy, J. P., Yu, Y., Dostalova, A., Kondo, S., Kurjan, A., Bulet, P., Lemaître, B., Vidal, M., & Cordero, J. B. (2019). The antimicrobial peptide defensin cooperates with tumour necrosis factor to drive tumour cell death in Drosophila. *ELife*, *8*, 1–26. doi: 10.7554/eLife.45061

Peltzer, N., & Walczak, H. (2019). Cell Death and Inflammation – A Vital but Dangerous Liaison. In Trends in Immunology (Vol. 40, Issue 5, pp. 387–402). doi: 10.1016/j.it.2019.03.006

Petersen, U. M., Björklund, G., Tony Lp, Y., & Engström, Y. (1995). The dorsal-related immunity factor, Dif, is a sequence-specific trans-activator of Drosophila Cecropin gene expression. *EMBO Journal*, *14*(13), 3146–3158. doi: 10.1002/j.1460-2075.1995.tb07317.x

Poltorak, A., He, X., Smirnova, I., Liu, M. Y., Van Huffel, C., Du, X., Birdwell, D., Alejos, E., Silva, M., Galanos, C., Freudenberg, M., Ricciardi-Castagnoli, P., Layton, B., & Beutler, B. (1998). Defective LPS signaling in C3H/HeJ and C57BL/10ScCr mice: Mutations in Tlr4 gene. *Science*, *282*(5396), 2085–2088. doi: 10.1126/science.282.5396.2085

Porchet, B. (1928). La resistance aux infections chez les insectes. *Bull Soc Vaudoise Sci Natl*, *56*, 221.

Rahighi, S., Ikeda, F., Kawasaki, M., Akutsu, M., Suzuki, N., Kato, R., Kensche, T., Uejima, T., Bloor, S., Komander, D., Randow, F., Wakatsuki, S., & Dikic, I. (2009). Specific Recognition of Linear Ubiquitin Chains by NEMO Is Important for NF-kB Activation. *Cell*, *136*(6), 1098–1109. doi: 10.1016/j.cell.2009.03.007

Régnier, C. H., Song, H. Y., Gao, X., Goeddel, D. V., Cao, Z., & Rothe, M. (1997). Identification and characterization of an IκB kinase. *Cell*, *90*(2), 373–383. doi: 10.1016/S0092-8674(00)80344-X

Reichhart, J. M., Georgel, P., Meister, M., Lemaitre, B., Kappler, C., & Hoffmann, J. A. (1993). Expression and nuclear translocation of the rel/NF-κB-related morphogen dorsal during the

immune response of Drosophila. In Comptes Rendus de l'Academie des Sciences - Series III (Vol. 316, Issue 10, pp. 1218–1224).

Reichhart, J. M., Meister, M., Dimarcq, J. L., Zachary, D., Hoffmann, D., Ruiz, C., Richards, G., & Hoffmann, J. A. (1992). Insect immunity: Developmental and inducible activity of the Drosophila diptericin promoter. *EMBO Journal*, *11*(4), 1469–1477. doi: 10.1002/j.1460-2075.1992.tb05191.x

Rizki, T. M., Rizki, R. M., & Grell, E. H. (1980). A Mutant Affecting the Crystal Cells in Drosophila melanogaster. *Roux's Archives of Developmental Biology*, *99*.

Rothwarf, D. M., Zandi, E., Natoli, G., & Karin, M. (1998). IKK-γ is an essential regulatory subunit of the IκB kinase complex. *Nature*, *395*(6699), 297–300. doi: 10.1038/26261

Roy, S. S., Patra, M., Nandy, S. K., Banik, M., Dasgupta, R., & Basu, T. (2013). *In Vitro Holdase Activity of E . coli Small Heat-Shock Proteins IbpA , IbpB and IbpAB : A Biophysical Study with Some Unconventional Techniques In Vitro Holdase Activity of E . coli Small Heat-Shock Proteins IbpA , IbpB and IbpAB : A Biophysical Study wit*. *December*. doi: 10.2174/092986652166613122409440 8

Royet, J., & Dziarski, R. (2007). Peptidoglycan recognition proteins: Pleiotropic sensors and effectors of antimicrobial defences. *Nature Reviews Microbiology*, *5*(4), 264–277. doi: 10.1038/nrmicro1620

Rudolph, D., Yeh, W. C., Wakeham, A., Rudolph, B., Nallainathan, D., Potter, J., Elia, A. J., & Mak, T. W. (2000). Severe liver degeneration and lack of NF-κB activation in NEMO/IKK γ-deficient mice. *Genes and Development*, *14*(7), 854–862. doi: 10.1101/gad.14.7.854

Rushe, M., Silvian, L., Bixler, S., Chen, L. L., Cheung, A., Bowes, S., Cuervo, H., Berkowitz, S., Zheng, T., Guckian, K., Pellegrini, M., & Lugovskoy, A. (2008). *Article Structure of a NEMO / IKK-Associating Domain Reveals Architecture of the Interaction Site*. *May*, 798–808. doi: 10.1016/j.str.2008.02.012

Russo, J., Dupas, S., Frey, F., Carton, Y., & Brehélin, M. (1996). Insect immunity: Early events in the encapsulation process of parasitoid (Leptopilina boulardi) eggs in resistant and susceptible strains of Drosophila. *Parasitology*, *112*(1), 135–142. doi: 10.1017/s0031182000065173

Rutschmann, S., Jung, A. C., Zhou, R., Silverman, N., Hoffmann, J. A., & Ferrandon, D. (2000). Role of Drosophila IKKγ in a Toll-independent antibacterial immune response. *Nature Immunology*, *1*(4), 342–347. doi: 10.1038/79801

Sakurai, H., Suzuki, S., Kawasaki, N., Nakano, H., Okazaki, T., Chino, A., Doi, T., & Saiki, I. (2003). Tumor necrosis factor-α-induced IKK phosphorylation of NF-κB p65 on serine 536 is mediated through the TRAF2, TRAF5, and TAK1 signaling pathway. *Journal of Biological Chemistry*, *278*(38), 36916–36923. doi: 10.1074/jbc.M301598200

Samakovlis, C., Kimbrell, D. A., Kylsten, P., Engstrom, A., & Hultmark, D. (1990). The immune response in Drosophila: Pattern of cecropin expression and biological activity. *EMBO Journal*, *9*(9), 2969–2976. doi: 10.1002/j.1460-2075.1990.tb07489.x

Santamaria, P., & Nüsslein-Volhard, C. (1983). Partial rescue of dorsal , a maternal effect mutation affecting the dorso-ventral pattern of the Drosophila embryo, by the injection of wild-type cytoplasm . *The EMBO Journal*, *2*(10), 1695–1699. doi: 10.1002/j.1460-2075.1983.tb01644.x

Scarff, C. A., Fuller, M. J. G., Thompson, R. F., & Iadaza, M. G. (2018). Variations on negative stain electron microscopy methods: Tools for tackling challenging systems. *Journal of Visualized Experiments*, *2018*(132), 1–8. doi: 10.3791/57199

Scherfer, C., Karlsson, C., Loseva, O., Bidla, G., Goto, A., Havemann, J., Dushay, M. S., & Theopold, U. (2004). Isolation and characterization of hemolymph clotting factors in Drosophila melanogaster by a pullout method. *Current Biology*, *14*(7). doi: 10.1016/j.cub.2004.03.030

Schmidt-Supprian, M., Bloch, W., Courtois, G., Addicks, K., Israël, A., Rajewsky, K., & Pasparakis, M. (2000). NEMO/IKKγ-deficient mice model incontinentia pigmenti. *Molecular Cell*, *5*(6), 981–992. doi: 10.1016/S1097-2765(00)80263-4

Schröfelbauer, B., Polley, S., Behar, M., Ghosh, G., & Hoffmann, A. (2012). NEMO Ensures Signaling Specificity of the Pleiotropic IKKβ by Directing Its Kinase Activity toward IκBα. *Molecular Cell*, *47*(1), 111–121. doi: 10.1016/j.molcel.2012.04.020

Schupbach, T., & Wieschaus, E. (1989). *Female sterile mutations on the second chromosome of Drosophila melanogaster. I. Maternal effect mutations. 121*(1), 1–18.

Selsted, M. E., Szklarek, D., & Lehrer, R. I. (1984). Purification and Antibacterial Activity of Antimicrobial Peptides of Rabbit Granulocytes. *Microbiology*, *45*(1), 150–154.

Sen, R., & Baltimore, D. (1986). Inducibility of κ immunoglobulin enhancer-binding protein NF-κB by a posttranslational mechanism. *Cell*, *47*(6), 921–928. doi: 10.1016/0092-8674(86)90807-X

Shalini, S., Dorstyn, L., Dawar, S., & Kumar, S. (2015). Old, new and emerging functions of caspases. *Cell Death and Differentiation*, *22*(4), 526–539. doi: 10.1038/cdd.2014.216

Shapiro, R. S., & Anderson, K. V. (2006). Drosophila Ik2, a member of the IκB kinase family, is required for mRNA localization during oogenesis. *Development*, *133*(8), 1467–1475. doi: 10.1242/dev.02318

Sheehan, G., Garvey, A., Croke, M., & Kavanagh, K. (2018). Innate humoral immune defences in mammals and insects: The same, with differences? *Virulence*, *9*(1), 1625–1639. doi: 10.1080/21505594.2018.1526531

Shokal, U., & Eleftherianos, I. (2017). Evolution and function of thioester-containing proteins and the complement system in the innate immune response. *Frontiers in Immunology*, *8*(JUN), 1–9. doi: 10.3389/fimmu.2017.00759

Shrestha, S., Park, Y., Stanley, D., & Kim, Y. (2010). Genes encoding phospholipases A2 mediate insect nodulation reactions to bacterial challenge. *Journal of Insect Physiology*, *56*(3), 324–332. doi: 10.1016/j.jinsphys.2009.11.008

Silke, J., & Meier, P. (2013). Inhibitor of Apoptosis (IAP) Proteins-Modulators of Cell Death and Inflammation. *Cold Spring Harbor Laboratory Press*, *5*(2), 1–19.

Silverman, N., Zhou, R., Erlich, R. L., Hunter, M., Bernstein, E., Schneider, D., & Maniatis, T. (2003). Immune activation of NF-kappaB and JNK requires Drosophila TAK1. *The Journal of Biological Chemistry*, *278*(49), 48928–48934. doi: 10.1074/jbc.M304802200

Silverman, N., Zhou, R., Stöven, S., Pandey, N., Hultmark, D., & Maniatis, T. (2000). A Drosophila IκB kinase complex required for relish cleavage and antibacterial immunity. *Genes and Development*, *14*(19), 2461–2471. doi: 10.1101/gad.817800

Sims, J. E., March, C. J., Cosman, D., Widmer, M. B., Macdonald, H. R., Mcmahan, C. J., Grubin, C. E., Wignall, J. M., Jackson, J. L., Call, S. M., Friend, D., Alpert, A. R., Gillis, S., Urdal, D. L., & Dower, S. K. (1988). cDNA expression cloning of the IL-1 receptor, a member of the immunoglobulin superfamily. *Science*, *241*(4865), 585–589. doi: 10.1126/science.2969618

Skaug, B., Jiang, X., & Chen, Z. J. (2009). The role of ubiquitin in NF-κB regulatory pathways. *Annual Review of Biochemistry*, *78*, 769–796. doi: 10.1146/annurev.biochem.78.070907.102750

Smale, S. T. (2010). Selective Transcription in Response to an Inflammatory Stimulus. *Cell*, *140*(6), 833–844. doi: 10.1016/j.cell.2010.01.037

Smale, S. T. (2011). Hierarchies of NF-κB target-gene regulation. *Nature Immunology*, *12*(8), 689–694. doi: 10.1038/ni.2070

Spencer, E., Jiang, J., & Chen, Z. J. (1999). Signal-induced ubiquitination of IκBα by the F-box protein Slimb/β-TrCP. *Genes and Development*, *13*(3), 284–294. doi: 10.1101/gad.13.3.284

Stanley, D., Miller, J., & Tunaz, H. (2009). Eicosanoid actions in insect immunity. *Journal of Innate Immunity*, *1*(4), 282–290. doi: 10.1159/000210371

Stark, H. (2010). GraFix: Stabilization of fragile macromolecular complexes for single particle Cryo-EM. In Methods in Enzymology (Vol. 481, Issue C). Elsevier Masson SAS. doi: 10.1016/S0076-6879(10)81005-5

Steiner, H., Hultmark, D., Engström, Å., Bennich, H., & Boman, H. G. (1981). Sequence and specificity of two antibacterial proteins involved in insect immunity. *Nature*, *292*(5820), 246–248. doi: 10.1038/292246a0

Steiner, H., Hultmark, D., Rasmuson, T., & Boman, H. G. (1980). from Hemolymph of Immunized Pupae of Hyalophora cecropia. *European Journal of Biochemistry / FEBS*, *16*, 7–16.

Steward, R., Zusman, S. B., Huang, L. H., & Schedl, P. (1988). The dorsal protein is distributed in a gradient in early drosophila embryos. *Cell*, *55*(3), 487–495. doi: 10.1016/0092-8674(88)90035-9

Stöven, S., Ando, I., Kadalayil, L., Engström, Y., & Hultmark, D. (2000). Activation of the

Drosophila NF-κB factor Relish by rapid endoproteolytic cleavage. *EMBO Reports*, *1*(4), 347–352. doi: 10.1093/embo-reports/kvd072

Stöven, S., Silverman, N., Junell, A., Hedengren-olcott, M., Erturk, D., Engstro, Y., Maniatis, T., & Hultmark, D. (2003). *Caspase-mediated processing of the Drosophila NF-κB factor Relish*. *100*(10), 5991–5996.

Stroschein-Stevenson, S. L., Foley, E., O'Farrell, P. H., & Johnson, A. D. (2006). Identification of Drosophila gene products required for phagocytosis of Candida albicans. *PLoS Biology*, *4*(1), 0087–0099. doi: 10.1371/journal.pbio.0040004

Štulík, K., Pacáková, V., & Tichá, M. (2003). Some potentialities and drawbacks of contemporary size-exclusion chromatography. *Journal of Biochemical and Biophysical Methods*, *56*(1–3), 1–13. doi: 10.1016/S0165-022X(03)00053-8

Sun, S. C., Asling, B., & Faye, I. (1991). Organization and expression of the immunoresponsive lysozyme gene in the giant silk moth, Hyalophora cecropia. *Journal of Biological Chemistry*, *266*(10), 6644–6649. doi: 10.1016/s0021-9258(18)38165-1

Sun, Shao Cong. (2011). Non-canonical NF-κB signaling pathway. *Cell Research*, *21*(1), 71–85. doi: 10.1038/cr.2010.177

Sun, Shao Cong, & Faye, I. (1992). Affinity purification and characterization of CIF, an insect immunoresponsive factor with NF-κ-B-like properties. *Comparative Biochemistry and Physiology -- Part B: Biochemistry And*, *103*(1), 225–233. doi: 10.1016/0305-0491(92)90436-U

Takeda, K., & Akira, S. (2005). Toll-like receptors in innate immunity. *International Immunology*, *17*(1), 1–14. doi: 10.1093/intimm/dxh186

Takeda, K., Kaisho, T., & Akira, S. (2003). Toll-like receptors. *Annual Review of Immunology*, *21*(1), 335–376. doi: 10.1146/annurev.immunol.21.120601.141126

Tanaka, M., Fuentes, M. E., Yamaguchi, K., Durnin, M. H., Dalrymple, S. A., Hardy, K. L., & Goeddel, D. V. (1999). Embryonic lethality, liver degeneration, and impaired NF-κB activation in IKK-β-deficient mice. *Immunity*, *10*(4), 421–429. doi: 10.1016/S1074-7613(00)80042-4

Tang, D., Kang, R., Coyne, C. B., Zeh, H. J., & Lotze, M. T. (2012). PAMPs and DAMPs: Signal 0s that spur autophagy and immunity. *Immunological Reviews*, *249*(1), 158–175. doi: 10.1111/j.1600-065X.2012.01146.x

Tartey, S., Matsushita, K., Vandenbon, A., Ori, D., Imamura, T., Mino, T., Standley, D. M., Hoffmann, J. A., Reichhart, J., & Akira, S. (2014). *Akirin 2 is critical for inducing inflammatory genes by bridging I j B- f and the SWI / SNF complex*. *33*(20), 2332–2349.

Tartey, S., & Takeuchi, O. (2015). Chromatin Remodeling and Transcriptional Control in Innate Immunity: Emergence of Akirin2 as a Novel Player. *Biomolecules*, *5*(3), 1618–1633. doi: 10.3390/biom5031618

Tauszig, S., Jouanguy, E., Hoffmann, J. A., & Imler, J. L. (2000). Toll-related receptors and the

control of antimicrobial peptide expression in Drosophila. *Proceedings of the National Academy of Sciences of the United States of America*, *97*(19), 10520–10525. doi: 10.1073/pnas.180130797

Theopold, U., Krautz, R., & Dushay, M. S. (2014). The Drosophila clotting system and its messages for mammals. *Developmental and Comparative Immunology*, *42*(1), 42–46. doi: 10.1016/j.dci.2013.03.014

Tokunaga, F., Sakata, S., Saeki, Y., Satomi, Y., Kirisako, T., Kamei, K., Nakagawa, T., Kato, M., Murata, S., Yamaoka, S., Yamamoto, M., Akira, S., Takao, T., Tanaka, K., & Iwai, K. (2009). *Involvement of linear polyubiquitylation of NEMO in NF-κB activation*. *11*, 123. Retrieved from http://dx.doi.org/10.1038/ncb1821

Trinh, D. V, Zhu, N., Farhang, G., Kim, B. J., & Huxford, T. (2008). The nuclear I kappaB protein I kappaB zeta specifically binds NF-kappaB p50 homodimers and forms a ternary complex on kappaB DNA. *Journal of Molecular Biology*, *379*(1), 122–135. doi: 10.1016/j.jmb.2008.03.060

Tzou, P., Reichhart, J. M., & Lemaitre, B. (2002). Constitutive expression of a single antimicrobial peptide can restore wild-type resistance to infection in immunodeficient Drosophila mutants. *Proceedings of the National Academy of Sciences of the United States of America*, *99*(4), 2152–2157. doi: 10.1073/pnas.042411999

Vedadi, M., Niesen, F. H., Allali-Hassani, A., Fedorov, O. Y., Finerty, P. J., Wasney, G. A., Yeung, R., Arrowsmith, C., Ball, L. J., Berglund, H., Hui, R., Marsden, B. D., Nordlund, P., Sundstrom, M., Weigelt, J., & Edwards, A. M. (2006). Chemical screening methods to identify ligands that promote protein stability, protein crystallization, and structure determination. *Proceedings of the National Academy of Sciences of the United States of America*, *103*(43), 15835–15840. doi: 10.1073/pnas.0605224103

Vidai, S., Khush, R. S., Leulier, F., Tzou, P., Nakamura, M., & Lemaitre, B. (2001). Mutations in the Drosophila dTAK1 gene reveal a conserved function for MAPKKKs in the control of rel/NF-κB-dependent innate immune responses. *Genes and Development*, *15*(15), 1900–1912. doi: 10.1101/gad.203301

Vlahopoulos, S., & Zoumpourlis, V. C. (2004). JNK: A key modulator of intracellular signaling. *Biochemistry (Moscow)*, *69*(8), 844–854. doi: 10.1023/B:BIRY.0000040215.02460.45

Wang, Z., Wilhelmsson, C., Hyrsl, P., Loof, T. G., Dobes, P., Klupp, M., Loseva, O., Mörgelin, M., Iklé, J., Cripps, R. M., Herwald, H., & Theopold, U. (2010). Pathogen entrapment by transglutaminase - A conserved early innate immune mechanism. *PLoS Pathogens*, *6*(2). doi: 10.1371/journal.ppat.1000763

Weber, A. N. R., Tauszig-Delamasure, S., Hoffmann, J. A., Lelièvre, E., Gascan, H., Ray, K. P., Morse, M. A., Imler, J. L., & Gay, N. J. (2003). Binding of the Drosophila cytokine Spätzle to Toll is direct and establishes signaling. *Nature Immunology*, *4*(8), 794–800. doi: 10.1038/ni955

Werner, T., Borge-Renberg, K., Mellroth, P., Steiner, H., & Hultmark, D. (2003). Functional diversity of the Drosophila PGRP-LC gene cluster in the response to lipopolysaccharide and peptidoglycan. *Journal of Biological Chemistry*, *278*(29), 26319–26322. doi:

10.1074/jbc.C300184200

Wicker, C., Reichhart, J. M., Hoffmann, D., Hultmark, D., Samakovlis, C., & Hoffmann, J. A. (1990). Insect immunity. Characterization of a Drosophila cDNA encoding a novel member of the diptericin family of immune peptides. *Journal of Biological Chemistry*, *265*(36), 22493–22498. doi: 10.1016/s0021-9258(18)45732-8

Williams, L. M., & Gilmore, T. D. (2020). Looking Down on NF-κB. *Molecular and Cellular Biology*, *40*(15). doi: 10.1128/mcb.00104-20

Williams, L. M., Sridhar, S., Samaroo, J., Adindu, E. K., Addanki, A., Molecular, B. B., Carrión, P. J. A., Dirusso, C. J., Rodriguez-sastre, N., Siggers, T., Thomas, D., Calikyan, A., Chen, Y., Coia, A. B., Cutillo, D., Breanna, R., Jiang, W., Kreber, I. C., Kurak, E. B., … Masoudi, P. (2021). *Diversification of Transcription Factor NF- κB in Protists*. 1–39.

Wilson, E. O. (1987). The Little Things That Run the World (The Importance and Conservation of Invertebrates) Author (s): Edward O . Wilson Published by : Blackwell Publishing for Society for Conservation Biology Stable URL : http://www.jstor.org/stable/2386020. *Blackwell Publishing for Society for Conservation Biology*, *1*(4), 344–346.

Woronicz, J. D., Gao, X., Cao, Z., Rothe, M., & Goeddel, D. V. (1997). IκB kinase-β: NF-κB activation and complex formation with IκB kinase-α and NIK. *Science*, *278*(5339), 866–869. doi: 10.1126/science.278.5339.866

Wu, S., Avila-Sakar, A., Kim, J., Booth, D. S., Greenberg, C. H., Rossi, A., Liao, M., Li, X., Alian, A., Griner, S. L., Juge, N., Yu, Y., Mergel, C. M., Chaparro-Riggers, J., Strop, P., Tampé, R., Edwards, R. H., Stroud, R. M., Craik, C. S., & Cheng, Y. (2012). Fabs enable single particle cryoEM studies of small proteins. *Structure*, *20*(4), 582–592. doi: 10.1016/j.str.2012.02.017

Xia, Z., Sun, L., Chen, X., Pineda, G., Jiang, X., Adhikari, A., Zeng, W., & Chen, Z. J. (2009). Direct activation of protein kinases by unanchored polyubiquitin chains. *Nature*, *461*(7260), 114–119. doi: 10.1038/nature08247

Xiao, G., Fong, A., & Sun, S. C. (2004). Induction of p100 processing by NF-κB-inducing kinase involves docking IκB kinase α (IKKα) to p100 and IKKα-mediated phosphorylation. *Journal of Biological Chemistry*, *279*(29), 30099–30105. doi: 10.1074/jbc.M401428200

Xu, G., Lo, Y.C., Li, Q., Napolitano, G., Wu, X., Jiang, X., Dreano, M., Karin, M. & Wu, H., (2011). Crystal structure of inhibitor of κB kinase β. *Nature*, *472*(7343), 325-330. doi: 10.1038/nature09853

Yamamoto, M., Yamazaki, S., Uematsu, S., Sato, S., Hemmi, H., Hoshino, K., Kaisho, T., Kuwata, H., Takeuchi, O., Takeshige, K., Saitoh, T., Yamaoka, S., Yamamoto, N., Yamamoto, S., Muta, T., Takeda, K., & Akira, S. (2004). Regulation of Toll/IL-1-receptor-mediated gene expression by the inducible nuclear protein IkappaBzeta. *Nature*, *430*(6996), 218–222. doi: 10.1038/nature02738

Yamaoka, S., Courtois, G., Bessia, C., Whiteside, S. T., Weil, R., Agou, F., Kirk, H. E., Kay, R. J., & Israël, A. (1998). Complementation cloning of NEMO, a component of the IκB kinase complex essential for NF-κB activation. *Cell*, *93*(7), 1231–1240. doi: 10.1016/S0092-

8674(00)81466-X

Yamazaki, S., Muta, T., & Takeshige, K. (2001). A Novel IκB Protein, IκB-ζ, Induced by Proinflammatory Stimuli, Negatively Regulates Nuclear Factor-κB in the Nuclei. *Journal of Biological Chemistry*, *276*(29), 27657–27662. doi: 10.1074/jbc.M103426200

Yang, F., Tang, E., Guan, K., & Wang, C.-Y. (2003). IKKβ Plays an Essential Role in the Phosphorylation of RelA/p65 on Serine 536 Induced by Lipopolysaccharide. *The Journal of Immunology*, *170*(11), 5630–5635. doi: 10.4049/jimmunol.170.11.5630

Yang, X. D., & Sun, S. C. (2015). Targeting signaling factors for degradation, an emerging mechanism for TRAF functions. *Immunological Reviews*, *266*(1), 56–71. doi: 10.1111/imr.12311

Yi, H. Y., Chowdhury, M., Huang, Y. D., & Yu, X. Q. (2014). Insect antimicrobial peptides and their applications. *Applied Microbiology and Biotechnology*, *98*(13), 5807–5822. doi: 10.1007/s00253-014-5792-6

Yoshikawa, A., Sato, Y., Yamashita, M., Mimura, H., Yamagata, A. and Fukai, S. (2009). Crystal structure of the NEMO ubiquitin-binding domain in complex with Lys 63-linked di-ubiquitin. *FEBS letters*, *583*(20), 3317-3322. doi: 10.1016/j.febslet.2009.09.028

Zandi, E. (1998). Direct Phosphorylation of IkB by IKK and IKK: Discrimination Between Free and NF-B-Bound Substrate. *Science*, *281*(5381), 1360–1363. doi: 10.1126/science.281.5381.1360

Zandi, E., Rothwarf, D. M., Delhase, M., Hayakawa, M., & Karin, M. (1997). The IκB kinase complex (IKK) contains two kinase subunits, IKKα and IKKβ, necessary for Iκb phosphorylation and NF-κB activation. *Cell*, *91*(2), 243–252. doi: 10.1016/S0092-8674(00)80406-7

Zapata, J. M., Matsuzawa, S. I., Godzik, A., Leo, E., Wasserman, S. A., & Reed, J. C. (2000). The Drosophila tumor necrosis factor receptor-associated factor-1 (DTRAF1) interacts with pelle and regulates NFκB activity. *Journal of Biological Chemistry*, *275*(16), 12102–12107. doi: 10.1074/jbc.275.16.12102

Zhang, J., Clark, K., Lawrence, T., Peggie, M. W., & Cohen, P. (2014). An unexpected twist to the activation of IKKβ: TAK1 primes IKKβ for activation by autophosphorylation. *The Biochemical Journal*, *461*(3), 531–537. doi: 10.1042/BJ20140444